

GRADUATE SCHOOL

APTAMER SELECTION USING CAPILLARY ELECTROPHORESIS SELEX

A THESIS SUBMITTED TO THE FACULTY OF THE GRADUATE SCHOOL OF
THE UNIVERSITY OF MINNESOTA
BY

Renee Karen Mosing

IN PARTIAL FULFILLMENT OF THE
REQUIREMENTS FOR THE DEGREE OF
DOCTOR OF PHILOSOPHY

Michael T. Bowser, Adviser

October, 2008

© Renee Karen Mosing 2008

Acknowledgements

Thank you to Dr. Shaun Mendonsa who trained me in many of the techniques implemented in this thesis. He gave me very patient and thoughtful advice throughout the completion of this project.

Thank you to Dr. Karin Musier-Forsyth for our many conversations about my project. Her advice was immensely useful. Her willingness to teach me techniques outside my discipline was invaluable, and helped take this research to a level that may not have otherwise been possible.

Thank you to Dr. Edgar Arriaga who was always willing to share his experience with me. His thoughtful advice helped determine how to analyze the bacteria and mitochondria experiments. Without his expertise these experiments would not have gotten as far.

Thank you to Dr. Robert Gorelik for allowing me to tour his HIV facilities at the Frederick Institute and for providing me with reverse transcriptase samples. My experience at the Institute with Robert was invaluable.

I would like to give a heartfelt thank you to Dr. Mike Bowser, my graduate advisor for creating an academic environment where I was never limited. He always supported and guided me while I followed my own path. He created opportunities for me which made this graduate experience irreplaceable.

Many thanks to my dear friend and co graduate student Ryan Turgeon, who kept me sane during my project and the formatting of this thesis.

I would like to thank my husband Curtis Cline who was always patient, understanding, and supportive of my educational goals. His countless hours of encouragement kept me focused on achieving my dreams.

Finally, I would like to thank my parents who knew I would achieve much farther than my own expectations. Without their unconditional support throughout this research and my entire life, none of this would have been possible.

Dedication

To my parents,
who always supported my education.

Abstract

SELEX is a method used for the combinatorial selection of aptamers, or single stranded nucleic acid sequences that bind with high affinity and specificity to target molecules. Although successful, SELEX is a very time consuming, laborious process. We introduced a modification to this process called capillary electrophoresis-SELEX. This protocol proved to be significantly more efficient, which greatly decreased the time requirement of the process from weeks to days. This improvement was observed despite the lower loading capacity and resolution limited injections on CE which introduced approximately 10^{13} sequences to the separation instead of the 10^{15} sequences introduced in more traditional selections protocols. In fact, ssDNA aptamers with picomolar affinity for HIV-1 RT were identified in 4 rounds. Further sequence/structure characterization of these sequences demonstrated no homology, indicating that several sequences can bind with high affinity to the target. Interestingly, the aptamers were 10 fold more selective for the original target (HIV-1 RT) than other reverse transcriptases. Despite this result, the aptamers did not demonstrate inhibition of reverse transcriptase activity. The success of these collections prompted investigation of more challenging targets such as mitochondria and bacteria. These targets are difficult to purify and have surface chemistries that are constantly changing. Aptamers for these targets must identify a feature on the surface that is consistent in order to be conserved throughout the process. Our experiments indicated that the aptamers may have bound to features on the surface that are not very abundant, making affinity characterization cumbersome. Future experiments aim to determine if the aptamers are becoming more refined for specific

features rather than just focusing on increase in affinity. Finally, initial experiments were performed for a model that will drive selections toward a specific binding site on the surface of the HIV assembly protein, capsid. Further experiments are proposed to allow aptamer binding to specific sites, and for aptamer characterization.

Table of Contents

Acknowledgements.....	i
Dedication.....	iii
Abstract.....	iv
List of Figures.....	ix
List of Tables.....	xii
Chapter 1: Introduction.....	1
1.1 Aptamers.....	2
1.2 Aptamer History.....	3
1.3 SELEX.....	4
1.3.1 Conventional Protocols.....	4
1.3.2 SELEX Modifications.....	6
1.4 Electrophoresis.....	7
1.5 Capillary Electrophoresis.....	8
1.5.1 Background.....	8
1.5.2 Electroosmotic Flow.....	9
1.5.3 Electrophoretic Mobility, Analyte Velocity, and Resolution.....	10
1.6 CE and Binding Separations.....	11
1.7 CE-SELEX.....	15
1.7.1 Initial Experiments.....	15
1.7.2 Defining the Collection Window.....	16
1.7.3 Dissociation Constant Estimation.....	18
1.7.4 Cloning and Sequencing.....	19
1.7.5 Final Characterization.....	19
1.7.6 Advantages of CE-SELEX.....	22
1.8 Aptamer Applications.....	25
1.9 SELEX Automation.....	30
1.10 Scope of Thesis.....	31
Chapter 2: Capillary Electrophoresis-SELEX Selection of Aptamers with Affinity for HIV-1 Reverse Transcriptase.....	33

2.1 Abstract.....	34
2.2 Introduction.....	35
2.3 Experimental Section.....	37
2.3.1 Materials	37
2.3.2 Capillary Electrophoresis Selection.....	37
2.3.3 PCR Amplification.....	38
2.3.4 Cloning and Sequencing	40
2.3.5 Dissociation Constant Measurements	40
2.4 Results and Discussion	41
2.5 Concluding Remarks.....	46
Chapter 3: Characterization of HIVRT binding ssDNA Aptamers Identified using CE-SELEX..	49
3.2 Introduction.....	51
3.3 Experimental Section.....	53
3.3.1 Materials	53
3.3.2 ³² P DNA Labeling.....	54
3.3.3 Ultrafiltration Assays	55
3.3.4 RNA Template Preparation.....	56
3.3.5 Inhibition Experiments.....	56
3.3.6 Polyacrylamide Gel Shift Assay	57
3.4 Results and Discussion	58
3.5 Concluding Remarks.....	62
Chapter 4: CE-SELEX Identification of Aptamers that Bind Complex Targets	64
4.2 Introduction.....	66
4.2.1 Bacteria Surface Chemistry	66
4.2.2 Mitochondria Surface Chemistry	69
4.2.3 CE and Bacteria Separations.....	71
4.2.4 CE and Mitochondria Separations	72
4.2.5 CE-SELEX Selections of Bacteria and Mitochondria	73
4.2.6 Aptamers for Bacteria and Mitochondria.....	74
4.3 Experimental Section.....	75

4.3.1 Materials	75
4.3.2 <i>Escherichia coli</i> and <i>Bacillus subtilis</i> Culturing.....	75
4.3.3 Bacteria Viability.....	76
4.3.4 Nuclease Activity Determination.....	77
4.3.5 Mitochondria Isolation.....	77
4.3.6 Capillary Electrophoresis Selection.....	78
4.3.7 Centrifugal Selection	79
4.3.8 PCR Amplification.....	79
4.3.9 Purification.....	80
4.3.10 <i>E. coli</i> and <i>B. subtilis</i> Binding Measurements	80
4.3.11 Mitochondria Binding Measurements.....	81
4.4 Results and Discussion	82
4.4.1 Bacteria	82
4.4.2 Mitochondria.....	88
4.5 Concluding Remarks.....	91
Chapter 5: Significance and Future Directions.....	93
5.1 Summary of Research.....	94
5.2 Future Directions	95
5.2.1 Aptamers for Specific Binding Regions	95
5.2.2 Negative Selections.....	97
5.2.3 The Model.....	98
5.2.4 Preliminary Results.....	99
5.2.5 Preliminary Results and Discussion.....	102
5.3 Future Experiments.....	104
5.3.1 Further Capsid Experiments	104
5.3.2 Selection Optimization.....	104
5.4 Conclusions.....	107
References.....	108

List of Figures

Figure 1.1: Example of an aptamer. The unique structure of this sequence facilitates binding to the target. Tighter binding is generally associated with more contact between the aptamer and the target.....2

Figure 1.2: Schematic of the SELEX process. A library of random nucleic acid sequences is incubated with the target. Binding sequences are separated from nonbinding sequences via nitrocellulose filtration. The binding sequences are PCR amplified, purified, and made single stranded. This process is continued until no further enrichment in affinity is observed.....5

Figure 1.3: Schematic of CE-SELEX. The target and single stranded nucleic acid library are incubated in free solution. The mixture is injected on capillary electrophoresis and separated under high voltage. Unbound sequences are discarded. Bound sequences are collected, PCR amplified, purified, and made single stranded. The process is continued until there is no further increase in affinity.....15

Figure 1.4: Schematic of selection procedure. (left) When using an uncoated capillary that generates EOF the aptamer-target complex will migrate earlier than the unbound ssDNA. Equation 1.6 should be used to calculate the time required for an analyte that reached the detection window 1-2 minutes before the leading edge of the unbound ssDNA peak to reach the outlet of the separation capillary. (b) When using a coated capillary that does not generate EOF the aptamer-target complex will migrate after the unbound ssDNA. Equation 1.6 should be used to calculate the time required for an analyte that reached the detection 1-2 minutes after the trailing edge of the unbound ssDNA peak to reach the outlet of the separation capillary.....17

Figure 1.5: Schematic of dissociation constant estimation via nitrocellulose filters. Samples are introduced to a 96 well plate and pushed through nitrocellulose and nylon filters via vacuum (left). Each filter is dried and exposed to a phosphor screen. The amount of radioactively labeled DNA on each filter is counted using a phosphorimager (right). Bound counts remain on the nitrocellulose filter and unbound sequences are retained by the nylon filter.....20

Figure 2.1: Effect of injection size on peak shape of a 2.5 mM ssDNA library separated using CE. Injection parameters: 1 psi, 5 seconds, 1 psi, 3 seconds, and 0.5 psi, 3 seconds. 1.8×10^{13} sequences were loaded onto the capillary in the 1 psi, 3 second injection. The arrow shows the position on the electropherogram where collection of binding sequences was stopped. CE conditions: TGK buffer, pH 8.3; UV detection at 254 nm; 50.2 cm, 50 μm i.d., 360 μm o.d. capillary; 30 kV separation voltage.....41

Figure 2.2: Affinity of the ssDNA pool for HIVRT after 2-4 rounds of selection. K_d 's were measured by fluorescently labeling an aliquot of the ssDNA pool followed by

affinity capillary electrophoresis analysis. Error bars are the 95% confidence intervals.....	42
Figure 2.3: Binding curves of (A) clone 4.3 (see Table 2.1) and (B) the unselected library. Ultrafiltration was used to separate bound from free ³² P labeled ssDNA in the presence of increasing concentrations of HIVRT. Strong binding affinity was observed for clone 4.3 ($K_d = 190 \pm 70$ pM). The affinity of the unselected library was significantly lower ($K_d > 1$ μ M).....	46
Figure 3.1: Gel images of clone 4.3 (left) and 4.5 (right). Aptamer concentrations increased from left to right. The product band is shown on the top, the mid band is the primer, and the last band is ³² P label. The RT ⁻ lane indicated the reaction in the absence of HIVRT. This control exhibited no product formation as expected. Gel conditions: 16% 19:1 acrylamide:bisacrylamide 10 cm x 10 cm gel, 100 V, 3 hours. Gel was immediately exposed to a phosphor screen.....	61
Figure 3.2: Graphical representation of the inhibition experiment. The fraction of product formation is plotted against the aptamer concentration. As the concentration of aptamer increases, there is no observable change in product formation, indicating the aptamer does not interfere with reverse transcriptase activity.....	61
Figure 4.1: Depiction of gram positive (A) and gram negative (B) bacterial cell walls.....	82
Figure 4.2: Schematic of homebuilt CE instrument with dual wavelength detection. Image adopted from Vratilov Kostal and Edgar Arriaga, University of Minnesota.....	82
Figure 4.3: Dissociation constants of library for <i>E. coli</i> (left) and <i>B. subtilis</i> (right) measured using flow cytometry. A constant library concentration was titrated with increasing concentrations of cells. The bound fraction was identified by the detection of fluorescence where the cells scatter.....	83
Figure 4.4: Gel image describing nuclease activity of <i>E. coli</i> and <i>B. subtilis</i> . Lane 1-8 were <i>E. coli</i> controls, lane 8 and 18 were a 25 bp DNA ladder, and lane 9-17 were the <i>B. subtilis</i> controls. Length of incubation time increased from left to right.....	84
Figure 4.5: Electropherogram demonstrating separation of <i>E. coli</i> . Separation conditions: 50.2 cm, 75 μ m i.d., 350 μ m o.d. bare fused silica capillary, 1 psi, 4 second injection, 30 KV separation normal polarity. Cell aggregates could be observed which was minimized by sonicating the cells prior to separation.....	85
Figure 4.6: Histograms of <i>B. subtilis</i> binding using flow cytometry. Left: Bacteria control (red) and 25 nM library (blue). Right: After collection 7 bacteria control (red), 25 nM collection #7 (blue), and 25 nM library (green). The significant shift for the library indicated initial affinity that was not observed after collections.....	87

Figure 4.7: Electropherograms of mitochondria and DNA migration under selection conditions. Top trace is DNA only, middle trace is untreated mitochondria and bottom trace is trypsin treated mitochondria. Selection conditions: 50.2 cm 50 μm i.d., 360 μm o.d. N-CHO coated capillary, 15 kV separation reverse polarity, 1 psi, 4 second injection.....88

Figure 4.8: Example electropherograms of dual detection capillary electrophoresis. A) sample in the absence of DNA. B) sample with mitochondria and 2 nM DNA. C) sample with mitochondria and 20 nM DNA. Top (green) trace is the ssDNA and the bottom trace (red) is the mitochondria. Spikes that appeared in both channels were attributed to bound DNA. CE conditions: 15 kV reverse polarity separation, 15 kV, 5 second electrokinetic injection, 30 cm AAP coated capillary. Post column detection with dual PMT boxes for mitochondria ($\lambda_{\text{ex}} = 543 \text{ nm}$, $\lambda_{\text{em}} = 560 \text{ nm}$) and carboxyfluorescein labeled DNA ($\lambda_{\text{ex}} = 488 \text{ nm}$, $\lambda_{\text{em}} = 520 \text{ nm}$).....90

Figure 5.1: Selection procedure for driving the selection toward a binding pocket. A) Overall outcome of first doing a positive selection to obtain all aptamers and then do a negative selection to eliminate sequences that do not bind to the desired location. B) Selection schematic of blocking all of the regions on the target except the desired binding region.....97

Figure 5.2: Schematic of a negative selection: A refined library from a positive selection is incubated with the modified target that you do not desire affinity to. The bound and free fractions are separated using capillary electrophoresis. The unbound fraction is collected, PCR amplified, made single stranded, and purified. The result is a refined library that can be used in the next positive selection.....98

Figure 5.3: Migration time of 22 μm capsid confirmed by varying the injection volume. (top) 3 psi, 5 sec, (middle) 2 psi, 5 sec, (bottom) 1 psi, 5 sec. Selection conditions: TGK separation buffer, 50.2 cm, 50 μm i.d., 360 μm o.d. bare fused silica capillary, 30 KV separation, 200 nm UV detection. The ssDNA library migrates at approximately 5 minutes indicated by the arrow.....103

List of Tables

Table 1.1: The efficiency of different portioning methods for SELEX. NR indicates data that was not reported.....	6
Table 1.2: Comparison of aptamers identified using SELEX and CE-SELEX.....	23
Table 2.1: Sequences of the clones obtained from the ssDNA pool after four rounds of CE-SELEX selection against HIVRT.....	44
Table 2.2: Dissociation constants of sequences chosen at random from Table 2.1. The confidence limit of the average value is the standard deviation. All other error limits are the 95% confidence intervals.....	45
Table 3.1: Aptamer affinity for HIVRT in different buffer compositions. Error indicates the 95% confidence interval. * indicates that the dissociation constant was determined using APCE described in Chapter 1.5. CE conditions: 30 kV normal polarity separation, 1 psi, 4 sec injection, 50 μm i.d., 360 μm o.d., 50.2 cm capillary, TKG separation buffer and specified incubation buffer.....	58
Table 3.2: Binding specificity of HIVRT aptamers. Original target was HIV-1 RT. Error indicates the 95% confidence interval.....	59
Table 4.1: Flow cytometry parameters.....	80
Table 4.2: Number of events from each channel and coincident events.....	91
Table 5.1: Affinity of library for capsid after each collection cycle. Affinity measured by % bound at 22 μM . CE conditions: 30 kV normal polarity separation, 1 psi, 4 sec injection, 50 μm i.d., 360 μm o.d., 50.2 cm capillary, TKG separation buffer, 1/5 PBS incubation buffer.....	103

List of Abbreviations

AIDS	Acquired immune deficiency syndrome
ACE	Affinity Capillary Electrophoresis
AMV RT	Avian Myeloblastosis Virus Reverse Transcriptase
APCE	Affinity Probe Capillary Electrophoresis
APS	Ammonium persulfate
AZT	3'-azido-2',3'-dideoxythymidine
BrU	5-bromo-2'-deoxythymidine
BSA	Bovine Serum Albumin
CE	Capillary Electrophoresis
CEC	Capillary electrochromatography
CEMSA	Capillary electrophoresis mobility shift assay
CE-SELEX	Capillary Electrophoresis-Systematic Evolution of Ligands by Exponential enrichment
DDC	2',3'-dideoxycytidine
DDI	2',3'-dideoxyinosine
DNA	Deoxyribose nucleic acid
dsDNA	Double stranded DNA
ECEEM	Equilibrium capillary electrophoresis of equilibrium mixtures
EOF	Electroosmotic Flow
FIV RT	Feline Immunodeficiency Virus Reverse

	Transcriptase
HIV	Human Immunodeficiency Virus
HIVRT	HIV-Reverse Transcriptase
I.D.	Inner Diameter
KCE	Kinetic capillary electrophoresis
K_d	Dissociation Constant
kDa	kilodalton
LIF	Laser Induced Fluorescence
LOD	Limit of Detection
MW	Molecular Weight
MWCO	Molecular weight cutoff
M-MuLV RT	Moloney Murine Leukemia Virus Reverse Transcriptase
NECEEM	Non equilibrium capillary electrophoresis of equilibrium mixtures
NPY	Neuropeptide Y
O.D.	Outer Diameter
PAH	Poly aromatic hydrocarbon
PCR	Polymerase Chain Reaction
PFTase	Protein farnesyltransferase
RNA	Ribose nucleic acid
RNase H	Ribonuclease H
RT-PCR	Real time polymerase chain reaction
SELEX	Systematic Evolution of Ligands by

SPR	EXponential enrichment
ssDNA	Surface Plasmon Resonance
0.5 X TBE	Single stranded deoxyribonucleic acid
TEMED	45 mM tris, 45 mM borate, 2.5 mM EDTA, pH 8.3
TGK	Tetramethylethylenediamine
	25 mM Tris, 192 mM glycine, 5 mM KH ₂ PO ₄ , pH 8.3

Preface

Chapters 1 and 2 were reproduced in part with permission from:

1. Renee K. Mosing and Michael T. Bowser. “CE-SELEX: Isolating Aptamers using Capillary Electrophoresis” in *Handbook of Capillary Electrophoresis and Associated Microchip Based Analysis*, James Landers Ed., CRC Press, 2007.

Copyright 2007 CRC Press

2. Renee K. Mosing and Michael T Bowser. “Microfluidic Selection and Applications of Aptamers” *Journal of Separation Science*, **30**, 1420-1426 (2007).

Copyright 2007 American Chemical Society

3. Renee K. Mosing, Shaun D. Mendonsa, and Michael T. Bowser. “Capillary Electrophoresis-SELEX Selection of Aptamers with Affinity for HIV-1 Reverse Transcriptase”, *Analytical Chemistry*, **77**, 6107-6112 (2005).

Copyright 2007 American Chemical Society

Chapter 1: Introduction

1.1 Aptamers

Aptamers are single stranded deoxyribonucleic acid (ssDNA) or ribonucleic acid (RNA) sequences that fold into unique secondary and tertiary structures that allow them to bind to target molecules with high affinity and selectivity (Figure 1.1). Although the work leading up to aptamers has been ongoing for decades, the term “aptamer” from the Latin root “aptus” meaning “to fit” was only recently coined¹. Modern libraries are 70-120 bases long with a 30-80 base random region flanked by two primer regions to facilitate polymerase chain reaction (PCR) amplification². Preferably, library random regions should be at least 30 bases in length to facilitate folding of all possible structural motifs such as hairpins, bulges, pseudoknots, and g-quartets. Larger random regions add diversity because it increases the number of possible sequences and the positions along the nucleic acid where these motifs can be located³. The result is a nucleic acid library that contains many sequences and structures. Ideally, some of these sequences will have the right structure to “fit” into binding pockets on the target molecule.

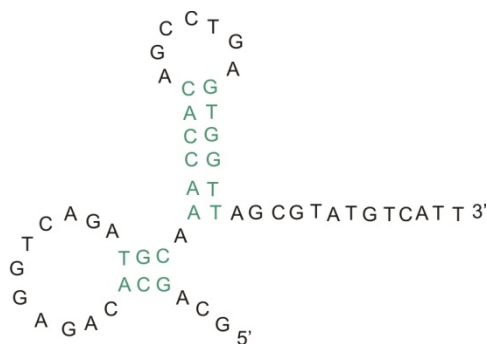


Figure 1.1: Example of an aptamer. The unique structure of this sequence facilitates binding to the target⁴. Tighter binding is generally associated with more contact between the aptamer and the target.⁵

1.2 Aptamer History

The idea of using nucleic acids to perform a desired function has become widespread. There are several categories of nucleic acid research including ribozymes⁶, zinc fingers⁷, RNAi⁸ etc. One of the subdivisions of nucleic acid research is aptamer technology.

The concept of nucleic acid manipulation was first developed in the 1960s by Sol Spiegelman who discovered that amplification, mutation, and selection were the fundamental properties of Darwinian Evolution⁹. This in mind, he devised a set of experiments in which he could perform this evolution *in vitro* to identify the best RNA template for the QB bacteriophage RNA polymerase. This polymerase, like many polymerases, makes mistakes along the template it is replicating. These mistaken sequences served as the randomization of the oligonucleotide pool. Spiegelman then studied the efficiency of replication of these mistaken sequences. It is not surprising that after several rounds of amplification by the enzyme and (and inadvertent mutation) the final sequences that remained were truncated variants of the original naturally occurring template. However, these variants proved to undergo replication more efficiently by the enzyme than the original template^{10, 11}.

The quest to understand and use the unique properties of nucleic acids didn't stop there. Later in the 1980s Cech, Altman, and Pace discovered that the *Tetrahymena thermophila* group I intron catalyzed a transesterification reaction¹². Subsequent works indicated that RNase P was necessary in the hydrolysis of the correct phosphodiester bond of its pre-tRNA substrates¹³. These experiments demonstrated that naturally

occurring RNA could catalyze at least 2 kinds of chemical reactions thus giving rise to the study of catalytic RNA¹⁴. Once these original models were understood, Been *et al.* successfully manipulated the *Tetrahymena thermophila* group I intron to achieve primer extension¹⁵. Waugh *et al.* also studied the effects of oligonucleotide manipulation by minimizing the RNase P subunit using phylogenetic analysis¹⁶. Both of these works were highly successful and increased interest in using the unique properties of nucleic acids to perform a desired function.

1.3 SELEX

1.3.1 Conventional Protocols

In 1990 Gold *et al.*, Joyce *et al.*, and Szostak *et al.* independently developed a process to identify aptamers from large combinatorial nucleic acid libraries. This process has been coined Systematic Evolution of Ligands by EXponential enrichment (SELEX)¹⁷, sometimes called *in vitro* selection¹ or *in vitro* evolution¹⁸ (Figure 1.2). The SELEX process has been described in a number of reviews¹⁹⁻²³. In the first SELEX reports, nitrocellulose filters were used as the partitioning method between binding and nonbinding sequences. Since most proteins have affinity for nitrocellulose, the protein and the binding sequences will be retained by the filter. These sequences are collected, PCR amplified, purified, and made single stranded. The resulting refined pool is used for further selection rounds.

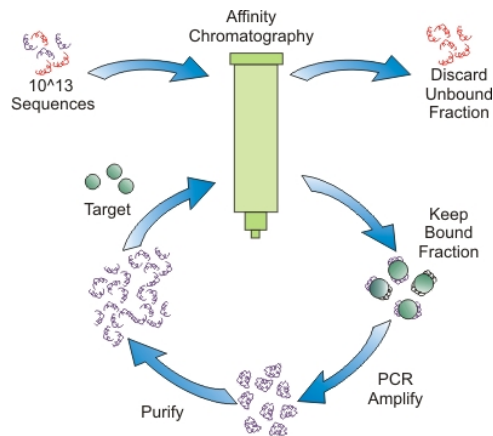


Figure 1.2: Schematic of the SELEX process. A library of random nucleic acid sequences is incubated with the target. Binding sequences are separated from nonbinding sequences via nitrocellulose filtration. The binding sequences are PCR amplified, purified, and made single stranded. This process is continued until no further enrichment in affinity is observed.

Tuerk and Gold demonstrated nitrocellulose partitioning for the original aptamers¹⁷. After several selection rounds, the first aptamer, an RNA aptamer for T4 DNA polymerase was identified. The initial library consisted of an 8 base randomized region of the mRNA hairpin within the naturally occurring translational operator. After four selection rounds the 2 dominant sequences were observed. Both sequences in the final pool bound with similar affinities. One sequence demonstrated complete conservation of the naturally occurring 8-base region while the other dominant sequence had only 4 of these bases conserved. This method of partitioning was received well and is still being used today^{24, 25}. However, these experiments used a region of a nucleic acid that was known to bind the target. Further SELEX experiments aimed to determine if a nucleic acid could be found for a target in which a nucleic acid binding sequence was

unknown. In these cases, the SELEX process has taken significantly longer (8-12 cycles) which can take months to complete.

1.3.2 SELEX Modifications

In a similar technique to the nitrocellulose based partitioning, Eulberg *et al.* used a microwell titer plate (Xenobind)^{25,26}. These plates have surfaces that interact with molecules much like the nitrocellulose filters. A myriad of other partitioning methods followed including centrifugation²⁷⁻²⁹, flow cytometry³⁰, surface plasmon resonance (SPR)^{31,32}, agarose and polyacrylamide gels³³⁻³⁵, magnetic beads³⁶, SP sepharose³⁷, magnets³⁸, and GST fusion³⁹⁻⁴¹, and capillary electrophoresis⁴²⁻⁴⁴. Although these

Target	Method	Aptamer	# of Cycles	K _d	Reference
African Trypanosomes	Centrifugation	RNA	13	60 ± 17 nM	²⁷
Rat Brain Tumor Microvessels	Flow cytometry	ssDNA	8	NR	³⁰
AtSPL14	SPR	dsDNA	20	NR	³²
Human Neutrophil Elastase	Gels	RNA	10	NR	³³
Anthrax Spores	Ligands	ssDNA	4	No binding detected	³⁶
Substance P	SP sepharose	RNA	12	190 nM	³⁷
Streptavidin	Magnets	DNA	13	56.7 ± 8.2 nM	³⁸
Human Polyadenylation Factor CstF	GST Fusion	RNA	7	1.5 nM	⁴¹
HIVRT	Capillary Electrophoresis	ssDNA	4	180 ± 70 pM	⁴⁵

Table 1.1: The efficiency of different portioning methods for SELEX. NR indicates data that was not reported.

methods have reduced the number of biases in the selection process, the protocols remain labor and time intensive. These methods are described in Table 1.1.

In addition to partitioning methods, other modifications to the SELEX process have become prevalent. These aim to make aptamers more stable for biological applications and/or to tweak the process in the search of the highest affinity aptamer possible. These modern processes include the identification of biostable mirror image aptamers called speigelmers⁴⁶, photoSELEX⁴⁷ which identifies aptamers that covalently bond with their target, refining selections² by randomizing the best binder and continuing the process, and conditional SELEX² which is performing the selection in the presence of a regulator molecule.

These partitioning methods suffer from a number of biases including poor elution kinetics of tight binding aptamers, dependence on linker molecules which change the target and create the opportunity of enrichment of aptamers for the linker molecule, dependence on negative selections against filters etc. which may exclude high affinity aptamers, inadequate resolution of bound and free fractions, and non specific binding to surfaces etc. Clearly there is still a need for a partitioning method that can efficiently separate the bound and free fractions without biasing the collection pool.

1.4 Electrophoresis

Electrophoresis was defined by Michaelis in 1909 as the difference in mobility of analytes in an electrical field⁴⁸. This change in mobility is usually a result of the size and charge ratio of the analyte as it passes through a slab gel or nongel media such as paper or

cellulose which acts as a molecular sieve. Electrophoresis has become widespread for biological applications. In fact, Arne Tiselius was awarded a nobel prize in 1948 for his work on serum protein separations using electrophoresis⁴⁹.

At a glance it appears as though electrophoresis would be an ideal mode of separation in SELEX selections. Although electrophoresis is a very straightforward, robust method for the separation of charged analytes, there are some considerations when using it for SELEX applications. The sieves are not inert and may interact with the library which would add additional bias to the selection process. Traditional electrophoresis is plagued by Joule heating which limits the upper limits of voltages possible, ultimately leading to limited resolution. Additionally, electrophoresis requires staining for detection which makes quantitation implausible due to analyte specific staining efficiencies. Perhaps the most limiting feature of traditional electrophoresis when thinking about SELEX experiments is the instability of complexes over the course of the separation^{50, 51}.

1.5 Capillary Electrophoresis

1.5.1 Background

The more modern type of electrophoresis called capillary electrophoresis (CE) is an electrophoretic separation technique in which the separation happens in thin (20-100 μm) capillaries⁴⁹. These thin capillaries minimize Joule heating by introducing a large surface area in which heat can be quickly dissipated. Ultimately, higher voltages can be used, minimizing sample separation time to only a few minutes⁵⁰. CE is a high resolution alternative to traditional methods. A further property of CE is that noncovalent

complexes are mostly preserved over the course of the separation⁴⁹. Furthermore, quantitation of analytes does not suffer from irreproducibility due to loading error, staining efficiency, or dispersion.

Capillary electrophoresis is an ideal separation technique for SELEX selections. There are no molecular sieves in CE allowing the separation to completely happen in free solution without bias. The higher voltages promote high resolution between bound and free fractions. Finally, complex dissociation is minimal compared to more conventional electrophoresis methods.

1.5.2 Electroosmotic Flow

First identified by Helmholtz in the 1800s, EOF is a unique component of electrophoresis that causes the bulk movement of the buffer in one direction⁵². It is caused by an electrical double layer that forms at the negatively charged glass capillary surface. Depending on buffer pH, the silanol groups on the glass capillary surface commonly used in CE are negatively charged. The positively charged buffer components are attracted to this negative charge, forming a double layer. This double layer only happens close to the capillary surface in the “Stern” layer also called the “diffuse” layer because the charge density drops off exponentially with distance from the surface. When an electric potential is applied, the cations outside the “Stern” layer (farther away from the capillary surface) will migrate toward the cathode. The strong hydrogen bonding properties of water drag the rest of the bulk solution with them.

The presence of EOF is ideal for SELEX selections and further characterization of aptamers because it minimizes separation time which can lead to band broadening⁵³,⁵⁴ and dissociation of complexes⁵⁵.

1.5.3 Electrophoretic Mobility, Analyte Velocity, and Resolution

A number of factors influence the rate and direction of analytes including pH, capillary coatings, applied voltage, and buffer viscosity. Unlike conventional chromatography, only one phase is involved in electrophoretic separations. With the exception of neutral coated capillaries, CE has EOF force which often acts against the normal migration of the analyte. The mobility of an analyte is defined by⁴⁹

$$\mu = \mu_{ep} + \mu_{eo} \quad \text{Equation 1.1}$$

Where μ is the actual mobility of the analyte, μ_{ep} ($\text{cm}^2\text{V}^{-1}\text{s}^{-1}$) is the apparent mobility of the analyte, and μ_{eo} is the electroosmotic mobility. The electrophoretic mobility is directly proportional to the ionic charge of the sample and inversely proportional to the frictional forces from resulting from buffer viscosity and analyte size/shape as described in equation 1.2 at a given pH.

$$\mu = \frac{z}{6\pi\eta r} \quad \text{Equation 1.2}$$

Where z is the net charge of the analyte, η is the viscosity, and r is the Stokes radius defined by the equation below

$$r = \frac{k_B T}{6\pi\eta D} \quad \text{Equation 1.3}$$

Where k_B is the Boltzmann constant, T is the temperature, and D is the diffusion coefficient.

The migration velocity of an analyte moving through the capillary is dependent on the electric field strength. This field strength is the result of the applied potential over the capillary and is described by equation 1.3⁴⁹.

$$v = \mu_{EP} \left(\frac{V}{L} \right) \quad \text{Equation 1.4}$$

Where V is the applied voltage (V) and L is the length of the capillary (cm). This equation illustrates that in high electric fields promote rapid migration and separation times. The speed of separation is limited by resolution which is defined by

$$R_s = \frac{1}{4} \left(\frac{\Delta \mu \sqrt{N}}{\mu + \mu_{EP}} \right) \quad \text{Equation 1.5}$$

Where N is the number of theoretical plates at a given voltage and capillary length is defined by

$$N = \frac{\mu_{EP} V}{2D} \quad \text{Equation 1.6}$$

indicating that higher resolution is achieved by lower velocities and longer migration times.

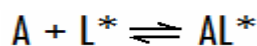
1.6 CE and Binding Separations

The first reports of studying binding interactions using capillary electrophoresis date back to the early 1990s⁵⁶⁻⁵⁹. Since then binding on CE has been well characterized and described in a number of excellent reviews⁶⁰⁻⁶³. CE has been used to study a myriad

of binding systems including peptide-ligands⁶⁴, metal ion-protein binding^{65, 66}, antigen-antibody interactions⁵⁷, and other protein-ligand interactions with a variety of affinities (fM-M) for their targets.

Muncha *et al* demonstrated a technique utilizing the mobility shift of bound molecules called capillary electrophoresis mobility shift assays (CEMSA) for dissociation constant estimation of low affinity ligands.⁶⁷ In these experiments, the target concentration is held constant and titrated with increasing concentrations of ligand in the separation buffer. Rather than direct detection and quantitation of the ligand peak, CEMSA relies on the change in peak shape or migration time of the free analyte as a function of ligand added. Often with weak binders, affinity is determined by minor distortions of the free analyte and ligand peaks. The original paper discussed the interaction between RNA and several peptides with dissociation constants in the micromolar range. This method has been used successfully for the characterization of protein-DNA interactions^{68, 69} and peptide-protein interactions⁷⁰.

Binding analytes with higher affinity (pM-nM) can be characterized by affinity capillary electrophoresis (ACE)⁵⁶. These methods can be broken down into two separate strategies which are called competitive or non competitive assays^{71, 72}. In competitive assays, labeled ligand (L*) and unlabeled ligand (L) compete for a limited amount of binding sites on the analyte (A). Upon CE separation, 2 distinct quantifiable peaks which represent L* and A-L*, the labeled bound and free fractions are formed (Equation 1.4).



Equation 1.4

Competitive assays yield information about the original concentration of the unlabeled ligand. Noncompetitive assays are more advantageous because of an increased linear dynamic range, lower detection limits, the ability to distinguish between cross reactivity with other species in complicated matrices, and the ability to detect multiple compounds that have affinity for the ligand⁷¹. In these assays, the concentration of the analyte is held constant and titrated with increasing concentrations of ligand. In these assays, the labeled analyte (A*) is added in excess to a solution containing only the ligand (Equation 1.5) and separated using CE. The result is 2 defined peaks which correspond to LA* and A*.



The first demonstration of APCE was by German *et al*⁷³. In these experiments, non competitive APCE were developed for both IgE and thrombin aptamers. These experiments were highly successful, yielding an impressive 26 pM LOD and five order of magnitude linear range. The highly selective nature of aptamers allowed successful APCE to be carried out even in complicated matrices such as serum. The selectivity of aptamers were later used by Haes *et al* who demonstrated an aptamer based APCE assay for ricin in the presence of BSA and casein, interfering proteins. Despite the addition of these interfering proteins, as little as 500 pM or 7.1 amol of ricin could be detected⁷⁴. These experiments demonstrated high selectivity in cases where unrelated proteins were introduced. However, Pavski and Le continued this work by developing an APCE assay for HIV-reverse transcriptase in the presence of other reverse transcriptases and

denatured HIVRT. Although the cell culture media did cause some interference, this could be eliminated by diluting the media with buffer. Ultimately the HIVRT aptamer used in these assays showed no cross reactivity with these proteins⁷⁵.

In a related assay, Zhang *et al.* have developed a novel affinity PCR approach to detecting low abundance proteins⁷⁶. This assay is similar to noncompetitive APCE the probe is incubated with the analyte and separated on CE. However, in lieu of fluorescent detection, fractions are collected in a similar method to the fraction collection described for CE-SELEX previously. The collected aptamer probes are PCR amplified using a quantitative method. The amount of analyte can be determined indirectly using this approach. As few as 180 HIVRT molecules (30 fm) could be detected using this strategy.

Krylov *et al.* have combined the two ideas of migration shift assay and ACE to make what they call non equilibrium capillary electrophoresis of equilibrium mixtures (NECEEM)⁷⁷. NECEEM is a kind of kinetic capillary electrophoresis (KCE) in which a dissociation constant and rate constant can be calculated from a single electropherogram⁷⁸. This is mathematically derived from the exponential decay on either side of the complex from the dissociation of the ligand and analyte from each other. In mixtures where ligand affinity varies, NECEEM can conceivably be used to characterize the abundance and strength of binding ligands. NECEEM has been very accurate in determining kinetic parameters for a number of binding analytes including many DNA-protein complexes⁷⁹, aptamer-target complexes^{80, 81}, and peptide-peptide interactions⁸².

1.7 CE-SELEX

This thesis describes the use of Capillary Electrophoresis-SELEX (CE-SELEX) for the selection of ssDNA aptamers^{42-44, 83} (Figure 1.3). This process relies on the high resolving power of capillary electrophoresis as the partitioning method of bound and free fractions. Capillary electrophoresis allows for a free solution separation which eliminates biases present in traditional SELEX methods. In this procedure, the target is incubated with the library in free solution. A few nanoliters are injected on the capillary and separated under high voltage. The bound fraction is separated from the free due to an observed mobility shift based on size and charge. The bound sequences are collected, PCR amplified, and purified. The refined pool is suitable for further rounds of enrichment. The process is continued until there is no observed increase in affinity.

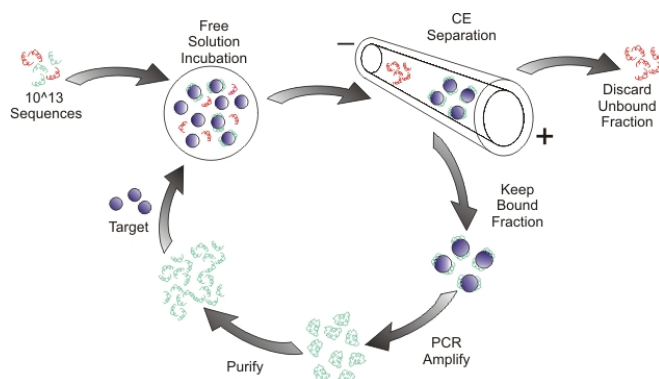


Figure 1.3: Schematic of CE-SELEX. The target and single stranded nucleic acid library are incubated in free solution. The mixture is injected on capillary electrophoresis and separated under high voltage. Unbound sequences are discarded. Bound sequences are collected, PCR amplified, purified, and made single stranded. The process is continued until there is no further increase in affinity.

1.7.1 Initial Experiments

CE-SELEX relies on an adequate separation between the bound and free DNA sequences. Initial experiments involve defining the migration of the ssDNA library and

the target separately. In most cases the bound fraction will migrate between the free DNA and free target peaks. Large targets tend to dominate the migration of the complex causing the bound fraction to migrate closer to the target and vice versa. Additionally, few targets will have a more negative charge density than ssDNA which means the mobility of the target will be less negative. However, this is only an educated assumption since the low concentration of the target and high concentration of the library make the detection of the complex during a selection impossible.

Once an acceptable separation is achieved, the library is heated to 72°C and cooled to room temperature to allow stable room temperature conformations to be formed. A large amount of library (100 µM) is incubated with a minimal amount of target (50-500 pM). Having excess library creates competition for binding sites and increases the chances that a high affinity binder will be in the collection fraction. A few nanoliters are injected on capillary electrophoresis and the bound is separated from the free under high voltage. The bound fraction is collected as described below.

1.7.2 Defining the Collection Window

The collection strategy is defined in Figure 1.4. Figure 1.4a demonstrates a typical selection in the presence of electro osmotic flow (described previously). Since few molecules are more negative than DNA, the complex should migrate off the capillary first into a collection vial containing ~50 µL buffer.

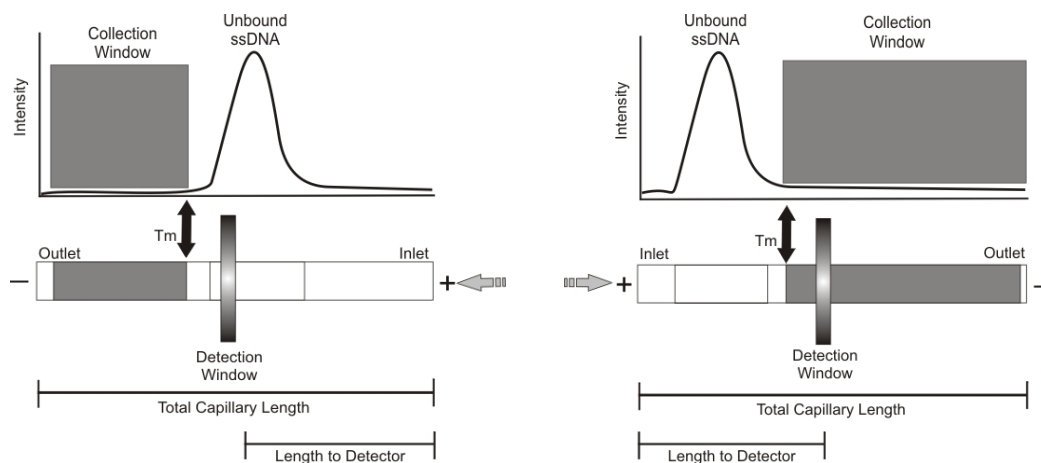


Figure 1.4: Schematic illustrating the selection procedure for CE-SELEX. (left) When using an uncoated capillary that generates EOF the aptamer-target complex will migrate earlier than the unbound ssDNA. Equation 1.6 should be used to calculate the time required for an analyte that reached the detection window 1-2 minutes before the leading edge of the unbound ssDNA peak to reach the outlet of the separation capillary. (b) When using a coated capillary that does not generate EOF the aptamer-target complex will migrate after the unbound ssDNA. Equation 1.6 should be used to calculate the time required for an analyte that reached the detection 1-2 minutes after the trailing edge of the unbound ssDNA peak to reach the outlet of the separation capillary.

To account for variable migration times between runs, the collection window must be defined while the run is in progress. This is easily determined since CE utilizes on column detection. To calculate when the visualized sample is actually exiting the capillary (t_{out}) is given by

$$t_{out} = \frac{L_T}{L_D} t_{det} \quad \text{Equation 1.6}$$

Where t_{det} is the time required for the analyte to reach the detector, L_T is the total length of the capillary, and L_D is the capillary length to the detector. Once the library hits the detector, 1-2 minutes are subtracted from the time to ensure we cut out sequences that are unbound, but under the LOD of the detector. This time is used as t_{det} . At this calculated

time the separation is stopped and the outlet vial containing the bound fraction is removed and distributed for PCR amplification. The remaining unbound sequences on the capillary are washed to waste using a pressure rinse.

Figure 1.4b describes the selection strategy in the absence of EOF. In the absence of EOF the library migrates toward the anode, so the separation order is reversed. Again the complex is less negative than the library so in these cases the unbound library will migrate off the capillary first. Equation 1.6 is used to determine when the unbound library fraction has migrated off the capillary. At this point the separation is stopped. The outlet vial containing the unbound sequences is discarded. The bound fraction is rinsed off the capillary into a clean collection vial. These samples are distributed for PCR amplification.

1.7.3 Dissociation Constant Estimation

After each cycle, “bulk” dissociation constants, which are an average weighted representation of all sequences in the pool are determined by non competitive ACE (previously described). Aptamers make ideal probes because they are easy to label with a fluorescent tag. The fluorescently labeled ssDNA collection pool is titrated with increasing concentrations of target. As more target is added, the free DNA peak decreases. The bound fraction is calculated from the free ssDNA and a dissociation constant (K_d) is calculated using the following equation

$$\frac{I_0 - I}{I_0} = \frac{c}{K_d + [\text{target}]} \quad \text{Equation 1.7}$$

Where I_0 is the peak height of the library in the absence of target, I is the peak height of the unbound library peak in the presence of target, c is a constant, and 84 is the concentration of the target.

1.7.4 Cloning and Sequencing

Once the bulk dissociation constants reach a plateau the final pool is sent for cloning and sequencing so that individual sequences can be characterized. To prepare for final cloning, the pool is PCR amplified for 8 cycles to ensure all of the sequences are double stranded. Primers should not be labeled at either end so that the DNA will be easily ligated into the cloning vector. dsDNA is ligated into a pGEM vector and transfected into DH5 *Escherichia coli* and colonies are raised. Plasmids from at least 30 colonies are chosen at random and the sequences of individual clones are determined using the T7 promoter sequence.

1.7.5 Final Characterization

1.7.5.1 Dissociation Constants

After the sequences of individual aptamers are obtained, it is relatively inexpensive to have sufficient quantities for further characterization synthesized. Generally, more accurate dissociation constants are obtained. There are countless methods for obtaining dissociation constants including anisotropy, panning separations, flow cytometry etc. Two specific methods utilizing the low detection limits of radioactivity were primarily used in this research. In each of these experiments, the 5' end of the DNA is labeled with a ^{32}P label. These sequences are kept at a constant concentration and titrated with increasing concentrations of the target. The bound free

fractions can be detected using either ultrafiltration or a dot blot assay. In ultrafiltration, the unbound fraction is filtered through a MWCO filter in which the target is retained. The filtrate containing the unbound fraction is collected and quantitated on a scintillation counter. The resulting counts are fit to equation 1.7. The dot blot assay is similar except the bound and free fractions can both be quantitated (Figure 1.5). The samples are passed through a nitrocellulose filter which binds proteins and the bound fraction. They then pass through a nylon filter which collects the unbound DNA. Both filters are exposed to a radioactive screen and are quantitated using a phosphorimager. The results are fit to the following equation to determine a K_d

$$\frac{I_B}{I_B + I_U} = \frac{c}{K_d + [\text{target}]} \quad \text{Equation 1.8}$$

Where I_B is the radioactive counts of the bound (nitrocellulose) filter, and I_U is the radioactive counts of the unbound (nylon) filter.

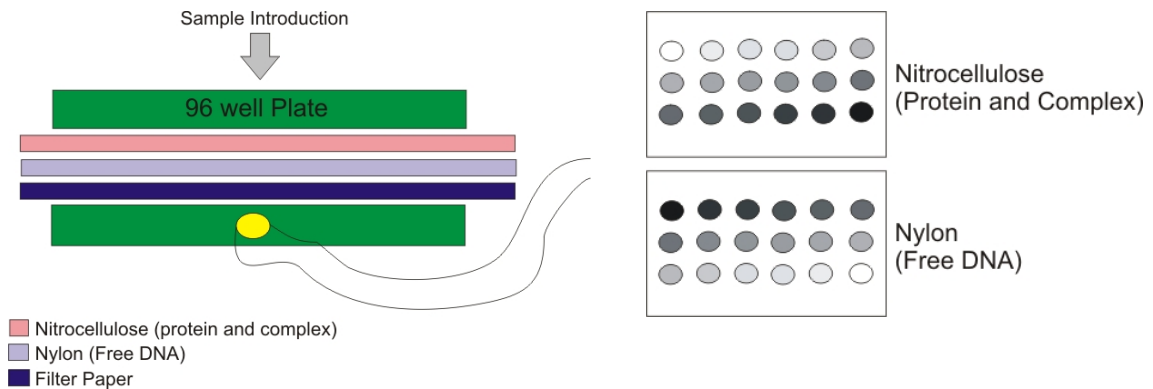


Figure 1.5: Schematic of dissociation constant estimation via nitrocellulose filters. Samples are introduced to a 96 well plate and pushed through nitrocellulose and nylon filters via vacuum (left). Each filter is dried and exposed to a phosphor screen. The amount of radioactively labeled DNA on each filter is counted using a phosphorimager (right). Bound counts remain on the nitrocellulose filter and unbound sequences are retained by the nylon filter.

1.7.5.2 Structure and Sequence Motifs

In conventional selections, sequence patterns or motifs are commonly observed in the aptamers recovered from cloning. This suggests that the selection has converged on certain sequence elements that are important for binding the target. Software programs such as ClustalW are readily available for identifying these motifs in large numbers of sequences⁸⁵. Only the random region of the sequences is generally entered into the analysis to avoid the homology of the primer region dominating the analysis. Contrary to conventional selections, sequence motifs are rare in aptamers selected using CE-SELEX. This suggests that the heterogeneity of the pool remains high even after the selection has converged on a collection of high affinity aptamers.

Common structural elements can be identified using mFold, a program that predicts secondary structure of ssDNA or RNA⁸⁶. For this analysis, the primer regions since are generally included because they most likely contribute to the overall structure of the nucleic acid. This analysis is useful in identifying common structural elements in aptamers even if they are generated by differing sequences.

1.7.5.3 Application Specific Characterization

Final characterization depends what the aptamer was designed to do. Sequencing and synthesis allow the affinities of individual aptamers to be determined. Affinities of the aptamers are compared with that of the unselected library or a nonsensical sequence such as polyT as a control experiment. Selectivity is assessed by measuring the affinity of the aptamer and in the presence of potential interferents depending on whether the

aptamer is to be used as a therapeutic or diagnostic agent. Selectivity and affinities can also be determined in various buffer, pH, or temperature conditions to determine the effectiveness on a DNA microarray chip. Further experiments such as binding studies on truncated regions of the aptamer help determine how the nucleic acid is interacting with the target. Finally, activity assays can be performed if the aptamer was designed to inhibit the function of the target to determine if the aptamer interferes with the active site (Chapter 3).

1.7.6 Advantages of CE-SELEX

CE-SELEX provides a number of benefits over traditional SELEX methods. First, since the partitioning method is a free solution separation, non specific binding to surfaces and unfavorable elution kinetics are eliminated. This in combination with the high resolution property of CE make CE-SELEX an extremely efficient process requiring only 2-4 selection rounds in comparison to the 8-12 rounds required for conventional techniques. This reduces the time requirement of the process from weeks to days (Table 1). Aptamers for IgE were obtained in as little as 2 selection rounds⁴³. Krylov and coworkers used CE-SELEX to identify aptamers for PFTase⁸⁷ and MutS⁸⁸. Interestingly, aptamers with sub nanomolar affinity were obtained for PFTase after a single selection round, demonstrating the separation power of the technique.

Target	CE-SELEX		SELEX		Reference
	# of Rounds	K _d (nM)	# of Rounds	K _d (nM)	
IgE	4	23 ± 12	15	6	43, 89
HIVRT	4	0.18 ± 0.07	12	1	45, 90
NPY	4	300 ± 200	12	370	44, 91
PFTase	1	0.5	-	n/a	87
mutS	3	3.6 ± 0.5	-	n/a	92
Kinase C-δ	9	122	-	n/a	93
Ricin	4	58 ± 19	9	105 ± 41	94
Histone H-4 Peptide	4	5 ± 2	-	n/a	95

Table 1.2: Comparison of aptamers identified using SELEX and CE-SELEX

CE-SELEX has been adopted by a number of groups. Aptamers with low nanomolar to picomolar dissociation constants have been identified, in line with traditional protocols. A notable exception is the aptamer selected for HIV-reverse transcriptase. These selections yielded an average picomolar affinity of 340 ± 160 . The lowest K_d in this pool was an impressive 180 ± 70 pM⁴⁵ (See Chapter 2).

In a direct comparison, Tang *et al* were able to isolate aptamers with similar affinities for ricin using CE-SELEX and conventional SELEX protocols⁹⁶. It was noted that 87.2% of the pool demonstrated affinity for ricin after four cycles of CE-SELEX selection while only 38.5% of the pool demonstrated affinity for ricin after 9 selection rounds of conventional SELEX techniques. This is not uncommon, since traditional SELEX protocols requires several more cycles than CE-SELEX. This allows the pool to

converge into specific groups based on the structure/sequence motifs. Some of these specific groups do not have affinity for the target, but rather linker molecules, filters etc. The lack of a structure or sequence motif in CE-SELEX pools suggests that numerous sequences can bind the target with high affinity.

The small sample volume required for CE-SELEX selections allows additional modifications to the process. Berezovski *et al.* have taken advantage of the low mass requirements of CE to develop a protocol that eliminates PCR from the process. Using this method, they were able to identify aptamers for h-RAS using three selection rounds without PCR amplification. Removing PCR from the process further reduces the time requirement of the process since it is the most time consuming step of CE-SELEX selections. They refer to their method as “Non-SELEX”⁹⁷.

There are a number of less obvious advantages to CE-SELEX. After 8-12 rounds of conventional protocols several sequence motifs often dominate the nucleic acid pool. These motifs are not observed after CE-SELEX selection, indicating that the heterogeneity of the pool remains high even after selection⁴²⁻⁴⁵. This suggests that CE-SELEX provides a larger number of independent, high affinity aptamers than conventional selections. For example, after four rounds of CE-SELEX selection the weakest aptamer out of six selected at random still bound HIV reverse transcriptase with an impressive 500 pM dissociation constant⁴⁵. An additional advantage is that CE-SELEX is compatible with DNA modifications such as non natural bases since the

hydrophobic nature of non natural bases do not have the opportunity to interact with filter materials or stationary phases.

Finally, target size is not a limiting factor of CE-SELEX. Traditional selections of smaller molecules involves attaching the target to a stationary surface and using affinity chromatography as the partitioning method which biases the selection for nucleic acids that bind the target when it is adhered to a stationary surface. To test size limitations on CE-SELEX, selections were performed using neuropeptide Y (NPY), a 36 amino acid as the target⁴². The molecular weight (MW) of NPY is 4 KDa, approximately 4 times less than that of the library (~25 KDa). Aptamers as low as 300 nM were obtained after 4 selection rounds. This was significant since it showed that CE-SELEX could be used to selection aptamers for molecules smaller than the nucleic acid library without attaching the target to a stationary phase or “haptan” tag as is common in conventional selections.

1.8 Aptamer Applications

Aptamers have been isolated for a large number of targets including small molecules^{21, 98}, peptides, proteins^{22, 99}, and even entire cells^{100, 101}. Aptamers hold significant therapeutic¹⁰²⁻¹⁰⁴ and diagnostic potential¹⁰⁵⁻¹⁰⁷. The specificity and tight binding properties of aptamers allows them to rival antibodies for therapeutic and diagnostic applications. However, aptamers address many of the limitations of antibodies¹⁰⁵. They are cheaply and reproducibly synthesized even with modifications. They are small in size which makes crossing the tissue barrier less challenging. The small size also accommodates higher loading capacities for diagnostic applications

because they can be tightly packed together. They do not require an animal host so they can be found for virtually any target including those that are toxic or those that do not stimulate an immune response. Additionally, they are not restricted to use in physiological conditions and are easily regenerated after use in pH and heat extremes.

These benefits over antibodies have given aptamers increased attention. In fact, the first aptamer drug was approved by the FDA and is commercially available. The drug, Macugen consists of an aptamer for the VEGF protein which is responsible for age related wet macular degeneration. Once bound, the aptamer effectively treats the disease¹⁰⁸. There are a number of other aptamer based medications following Macugen in clinical trials¹⁰⁹.

Diagnostic applications of aptamers are even more diverse^{105-107, 110}. Aptamers are ideal candidates for probes in applications where selective detection and quantitation of a specific analyte is required. Methods such as affinity probe capillary electrophoresis (described later) allow one analyte to be thoroughly characterized (K_d , concentration, etc.) The recent addition of DNA microarrays has taken probe studies one step farther by allowing multiple targets to be studied simultaneously. In these experiments, specific DNA sequences are attached to a known position on a microarray using photolithographic or inkjet technologies. This methodology has a great impact in genomics since fluorescently labeled aptamers with some complimentary structure of those on the microarray will adhere when only microliter volume samples are introduced to the microarray. Obviously sequences with higher complementarity will bind more

strongly than those with only portions of complementarity. Fluorescence imaging can identify specific locations on the plate that have a signal. These microarrays can be used for expression profiling, mRNA profiling, pathogen detection, genotyping, or protein-DNA interaction discovery. Ellington and coworkers have described aptamer microarrays extensively^{111, 112}. They have used RNA aptamers for lysozyme and ricin as well as DNA aptamers for IgE and thrombin. These were easily attached on the microarray by biotinylating the nucleic acid and spotting it on a streptavidin slide. Using several aptamers simultaneously can be challenging because each aptamer is selected in a different buffer. Because of this, a universal buffer, or buffer in which all aptamers still possess affinity for their target needs to be selected. Despite modifying the buffer, an LOD for Cy3 and Cy5 labeled lysozyme was 1 pg/mL.

Aptamer microarrays were further enhanced by Gold *et al.* who incorporated aptamers selected using PhotoSELEX to improve specificity¹¹³⁻¹¹⁵. In PhotoSELEX selections, irreversible covalent binding is made possible by replacing thymidine bases with 5-bromo-2'-deoxythymidine (BrU). Upon excitation with a 308 nm laser, BrU will form a covalent bond with aromatic and sulfur containing amino acids. This is a distance related reaction so only residues on the DNA that bound with the proper shape to fit closely into binding pockets on the protein form these bonds. This is beneficial in microarrays because the crosslinking reaction can be used to adhere the aptamers to the microarray. Additionally, once the protein is bound the plate can simply be exposed to UV light to crosslink the protein to the plate. Highly stringent washing conditions can be

used to eliminate proteins that are nonspecifically bound. Gold *et al.* used this technique to obtain LOD's from 6 fM to 31 pM.

In addition to specific aptamer-target complex detection, a number of techniques have been developed to use aptamers as stationary phases for the separation of a wide range of analytes that possess similar structural features¹¹⁶⁻¹¹⁸. Aptamers have many characteristics that make them ideal stationary phases. Because nucleic acids are well characterized, immobilization of aptamers on stationary surfaces is rudimentary. The small size of aptamers allows them to be packed closely together which increases the surface area and loading capacity of these stationary phases. The retention of analytes is easily modified by buffer, pH, and/or temperature gradients^{117, 118}.

Michaud *et al.* used target specific aptamers to separate enantiomeric peptide and amino acid derivative pairs in packed microbore columns^{119, 120}. The aptamer stationary phase selectively retained the target while the enantiomer generally eluted with the dead volume. More recently, HPLC phases incorporating L-RNA aptamers have been demonstrated^{121, 122}. L-RNA aptamers were much more stable since they are more RNase resistant than naturally occurring D-nucleic acids.

Aptamers have also been used as stationary phases for non target compounds. Kotia *et al.* have shown DNA sequences that form G-quartets, the functional structure of the thrombin aptamer, are useful CEC stationary phases¹¹⁶. These phases were used to separate enantiomers, amino acids, polyacrylic aromatic hydrocarbons (PAH), dipeptides^{117, 123}, and proteins^{118, 124, 125}. The key to these separations was that the

aptamers did not have specific affinity for the targets. Instead, g-quartets were examined as a unique structure capable of forming weak interactions with the analytes. These weaker, non specific interactions allow a range of analytes to be analyzed simultaneously without inducing the peak broadening characteristic of slow mass transfer kinetics at the stationary phase surface. G-quartets are also interesting due to a dependence on a potassium ion concentration for proper folding. This suggests that elution can be easily controlled using potassium gradients. More recently, Connor *et al.* have used a stationary phase containing a 2-repeat sequence of the insulin linked polymorphic region of the human insulin gene reporter region to test the hypothesis that the formation of G-quartet structures is critical for insulin binding¹²⁶.

Deng *et al.* have achieved separations of a group of structurally similar small molecules using aptamers selected to bind adenosine and ATP as a stationary phase in a packed capillary chromatography column¹²⁷. Resolution was achieved for cyclic-AMP, NAD⁺, AMP, ADP and ATP. Frontal chromatography was used to demonstrate that the aptamer had different affinity for each analyte, making separation of the complex mixture possible. Retention times could easily be manipulated by altering the pH, buffer composition, and Mg⁺² concentration. This separation was used to quantify adenosine in microdialysis fractions collected from the rat somatosensory cortex¹²⁸. Significant preconcentration could be achieved using gradients of metal ion concentration and pH. Detection limits as low as 30 nM could be obtained using the concentration step. Notably, the columns were robust with over 200 injections being performed without noticeable degradation of the column¹²⁸.

Indeed aptamers have demonstrated promising results in therapeutics and diagnostics. The high affinity and specific binding properties of aptamers make them ideal recognition and affinity agents. It is not surprising that they have been put to good use in a range of applications. The incorporation of aptamers into many techniques has mirrored earlier antibody applications. In many cases, the smaller size, well defined chemistry, robustness, and simple synthesis of aptamers make them a preferable option to antibodies. This is particularly true for aptamer based stationary phase chromatography and microarrays. The limiting factor in widespread adaptation of aptamer technology is the speed in which it takes aptamers to be identified. Certainly the most important question is how to efficiently screen a combinatorial oligonucleotide library with an overwhelming number of sequence possibilities for binding sequences.

1.9 SELEX Automation

Although CE-SELEX has significantly reduced the time requirement of the process, it is still labor intensive. However, the microfluidic nature of the process makes it highly compatible with automation. Automation is desired because it increases the throughput and reliability of the process. Cox *et al.* have created a robotic workstation to isolate RNA aptamers^{129, 130}. While CE-SELEX reduced the time requirement of the process to days, this robotic workstation was capable of performing 6 cycles per day. Additionally, multiplexing allowed aptamers to be selected for as many as eight targets simultaneously.

More recently, Hybarger *et al* introduced a microfluidic prototype which relied on pressure gradients to load and move reagents through microlines¹³¹. This prototype

consisted of pressure loaded sample injection port, microlines for reagent storage, a pressurized reagent delivery module, PCR thermocycler, and valves for the selection and sample routing. Modules for each SELEX step are easily removed and modified. Once the sample was manually injected into the prototype, dye sensing valves were used to move the sample automatically, completely alleviating the laborious nature of the process. The prototype was capable of transcription, selection, reverse transcription, and PCR amplification. To demonstrate the utility of the process, RNA selections using SELEX and the prototype separately were performed for lysosyme. Interestingly, the end result was identical aptamers which validated the microfluidic technique.

1.10 Scope of Thesis

The recent addition of CE-SELEX to the analytical field has allowed widespread adaptation of aptamer technology. Although this technology is taking off exponentially, the CE-SELEX process to identify aptamers is still not well characterized. Mendonsa *et al.* began this work by trying to identify the lower size limitation of targets in CE-SELEX with NPY experiments. However, there are several other questions that need to be addressed. Chapter 2 of this thesis describes the selection of aptamers for HIV-reverse transcriptase. This demonstrated a proof of concept for the process. Chapter 3 describes further characterization of the inherent properties of these aptamers. Chapter 4 discusses the selection of more challenging targets such as bacteria and the sub cellular component mitochondria. Many protein samples are commercially available with a high level of purity. However, in some cases it is beneficial to obtain an aptamer for a target that is not very pure, or one in which the surface chemistry is always changing. To address this

issue, selections were performed against representative targets (*E. coli*, *B. subtilis* and mitochondria). The selections and results are described.

**Chapter 2: Capillary Electrophoresis-SELEX
Selection of Aptamers with Affinity for HIV-1
Reverse Transcriptase**

2.1 Abstract

Capillary electrophoresis-SELEX (CE-SELEX) was used to select ssDNA aptamers with affinity for HIV reverse transcriptase (HIVRT). A library of ssDNA was incubated with HIVRT. Sequences bound to HIVRT were isolated using CE, PCR amplified, and purified, yielding an enriched ssDNA pool suitable for further rounds of selection. Aptamers with dissociation constants as low as 180 pM were isolated after four rounds of selection. This is the first report of aptamers isolated by CE-SELEX with higher affinity than those obtained for the same target using conventional selection techniques. No sequence motifs were identified in the 27 clones sequenced, suggesting that there are many sequences that can bind HIVRT with low picomolar dissociation constants.

2.2 Introduction

Human immunodeficiency virus (HIV) is the pathogen that causes acquired immune deficiency syndrome (AIDS). HIV is a retrovirus that relies on a viral encoded reverse transcriptase (HIVRT) to convert viral RNA into double stranded DNA, which is then incorporated in the host genome for replication¹³²⁻¹³⁴. HIVRT exhibits RNA- and DNA-dependent polymerase as well as ribonuclease H (RNase H) activity. HIVRT is a heterodimer composed of p66 and p51 kDa polypeptide chain subunits. The p51 subunit is generated via proteolytic cleavage of the p66 subunit C-terminal domain resulting in high sequence homology between the two subunits. The secondary structures of the p66 and p51 subunits are different despite this sequence homology, giving rise to an asymmetric heterodimer.¹³²⁻¹³⁴

In the early 1990s, SELEX (Systematic Evolution of Ligands by EXponential enrichment) was used to identify DNA and RNA aptamers with high affinity and specificity for HIVRT^{90, 135}. SELEX is a process for selecting nucleic acids with high affinity and specificity for target molecules out of large random sequence libraries.^{1, 17, 18} SELEX has been thoroughly described in a number of reviews and in Chapter 1.^{21, 22, 136, 137} Briefly, an RNA or DNA library containing 10^{14} - 10^{15} random sequences is generated. Sequences with affinity for the target are selected from the pool using nitrocellulose filtration, affinity chromatography, or panning separations. These sequences are amplified using PCR to give a new nucleic acid pool suitable for further rounds of selection. Aptamers with low nanomolar dissociation constants are typically obtained after 8-12 rounds of selection. Aptamers are gaining increased attention for their potential as therapeutic¹³⁸⁻¹⁴⁰ and diagnostic agents.^{94, 141}

The highest affinity RNA aptamers for HIVRT identified by Tuerk *et al.* bind with a dissociation constant of 40 pM.¹³⁵ Nine rounds of selection were necessary to isolate these sequences. The best ssDNA aptamers for HIVRT bound significantly weaker ($K_d = 1$ nM) even though 12 rounds of selection were performed.⁹⁰ This is not surprising considering HIVRT is by nature an RNA binding enzyme. It was hoped that these aptamers would prevent viral replication and therefore be useful in treating AIDS. This work is described in Chapter 3.

Chapter 1 described the use of capillary electrophoresis as an alternative to SELEX selection procedure (CE-SELEX). Briefly, the random nucleic acid library is incubated with the target in free solution. The incubation mixture is then injected onto a CE capillary and separated under high voltage. Nucleic acids that bind the target migrate with a mobility different from that of unbound sequences, allowing them to be collected as different fractions. Bound sequences are then amplified and purified for further rounds of selection as in conventional SELEX. CE-SELEX has been used for a number of selections (See Table 1.1). These results indicate that CE-SELEX is a superior method, requiring fewer cycles to isolate aptamers comparable and sometimes better affinity than those selected using traditional methods.

In the current chapter, we have used CE-SELEX to obtain high affinity ssDNA aptamers for HIVRT. The number of cases of HIV worldwide continues to increase at an alarming rate. Aptamers with picomolar affinity may provide the sensitivity necessary to develop an affinity based diagnostic assay for HIV infection.

2.3 Experimental Section

2.3.1 Materials

Unless otherwise noted, all samples and buffers were prepared in deionized water obtained from a Milli-Q water purification system (Millipore Corp., Bedford, MA). The ssDNA library consisted of a 40 base random region flanked by two 20 base primer regions (5'-AGC AGC ACA GAG GTC AGA TG (40 random bases) TTC AGC GTA GCA CGC ATA GG-3'). All DNA libraries, PCR primers, and aptamers were obtained from Integrated DNA Technologies, Inc (Coralville, IA). HIVRT was obtained from Worthington Biochemical (Lakewood, NJ). All other chemicals were obtained from Sigma-Aldrich (St. Louis, MO) and were the best grade available. CE separation buffer consisted of 25 mM tris, 192 mM glycine, and 5 mM KH₂PO₄ (TGK) at pH 8.3.

2.3.2 Capillary Electrophoresis Selection

Prior to the selection the library was diluted in separation buffer, heated to 72°C and cooled to room temperature. HIVRT was spiked into the library to give a final concentration of 2.5 mM ssDNA library and 500 pM HIVRT. This mixture was incubated at room temperature prior to CE selection.

Capillary electrophoresis separations were performed on a P/ACE MDQ capillary electrophoresis system (Beckman Coulter, Inc., Fullerton, CA). A 50.2 cm long, 50 μm inner diameter, 360 μm outer diameter uncoated fused silica separation capillary (Polymicro Technologies, Phoenix, AZ) was used. The capillary was rinsed with separation buffer for 10 minutes at the start of the day and for 2 minutes between separations. Samples were injected using 1 psi pressure for 3 seconds. Approximately 1.8×10^{13} sequences were introduced into the capillary in the first round of selection. The separation was performed under the following conditions: 30 kV voltage (normal

polarity), UV detection at 254 nm, and ambient temperature. All sequences migrating more than 30 seconds earlier than the unbound sequences were collected into 48 μ L of separation buffer at the capillary outlet. The exact time that the unbound sequences would reach the outlet of the capillary would be calculated on the fly for each separation since detection takes place 10 cm from the end of the capillary. After the bound fraction migrated off the capillary, the separation voltage was turned off and the unbound sequences remaining on the capillary were flushed to waste using a high pressure rinse.

2.3.3 PCR Amplification

The 48 μ L fraction containing the bound sequences obtained using CE selection was divided into 8 x 6 μ L aliquots. PCR buffer was added to these fractions so that the final concentrations were as follows: 1.5 μ M forward primer (5'-AGC AGC ACA GAG GTC AGA TG-3'), 1.5 μ M reverse primer (5'-/biotin/-TTC ACG GTA GCA CGC ATA GG-3'), 0.15 unit/ μ L taq polymerase, and 7.5 mM MgCl₂. The final volume in each PCR tube was 20 μ L. The above samples and a control with no added DNA were placed in a thermal cycler and heated to 94°C for 5 minutes to ensure complete denaturation and dissociation of bound sequences from HIVRT. A total of 18 cycles of denaturing, annealing, and extension were then carried out for 30 seconds at 94°C, 30 seconds at 53°C, and 20 seconds at 72°C, respectively. At completion, a final 5 minute extension was carried out at 72°C. The presence of DNA following PCR was confirmed by electrophoresis on a 2% agarose gel (40 minutes at 120 V with ethidium bromide staining).

The double stranded PCR products were purified and made single stranded using a streptavidin agarose column (Pierce Biotechnology, Rockford, IL). The column was washed with streptavidin binding buffer (10 mM tris, 50 mM NaCl, and 1 mM EDTA,

pH 7.5) for 5 minutes. A 500 μL sample of streptavidin buffer was then added to the column with the amplified PCR products and allowed to incubate with periodic shaking for 30 minutes. The column was then washed 10 times with streptavidin binding buffer, removing extra PCR components. dsDNA was retained via the strong interaction between the streptavidin column and the biotinylated complementary sequence. A total of 200 μL of 0.15 M NaOH was added to the column at 37°C to disrupt the hydrogen bonds between the DNA sequences. Complementary sequences remained bound to the column through biotin-streptavidin interaction while the desired single stranded sequences were eluted from the column. The eluted ssDNA was concentrated by ethanol precipitation and redissolved in 20 μL of separation buffer, providing a new nucleic acid pool for further rounds of CE selection. To perform subsequent rounds of selection, a 1.1 μL of HIVRT was added to the 10 μL of the purified ssDNA pool to give a solution containing 500 pM HIVRT. This solution was incubated and selected using the procedures described above.

The affinity of the ssDNA pool was assessed after every round using affinity capillary electrophoresis^{61, 62} to monitor the progress of the selection. A 0.5 μL aliquot of the ssDNA pool was PCR amplified using the conditions listed above for five cycles in the presence of 5',6-carboxyfluorescein labeled forward primer to fluorescently label the sequences. Sequences were made single stranded using the procedure described above. Aliquots of the fluorescently labeled ssDNA pool were incubated with increasing concentrations of HIVRT and analyzed using CE. CE conditions were the same as those used for selection except that laser induced fluorescence (LIF) was used for detection ($\lambda_{\text{ex}} = 488 \text{ nm}$, $\lambda_{\text{em}} = 520 \text{ nm}$). The peak height of the free aptamer was fit to the following equation to estimate the dissociation constant:

$$\frac{I_0 - I}{I_c} = \frac{\text{Constant}}{K_d + [\text{HIVRT}]}$$

Equation 2.1

Where I is the peak height of the unbound DNA and I_0 is the peak height of the unbound DNA in the absence of HIVRT.

2.3.4 Cloning and Sequencing

After four rounds of selection, an aliquot of the nucleic acid pool was PCR amplified for eight cycles using the conditions listed above with the exceptions that the reverse primer was not biotinylated and the final extension was carried out for 10 minutes. ssDNA from this pool were cloned and sequenced at the Biotechnology Resource Center at the University of Minnesota (St. Paul, MN). Briefly, 50 μ L of the PCR amplified DNA was purified using a QIAquick PCR purification kit (Qiagen, Valencia, CA) and ligated into a pGEM vector (Promega, Madison, WI). This vector was then transfected into DH5 Escherichia coli. A total of 27 individual colonies were chosen at random and sequenced using the T7 promoter sequence.

2.3.5 Dissociation Constant Measurements

A random number generator was used to choose 6 sequences from the 27 clones sequenced after the fourth round of selection. These sequences were synthesized, and their dissociation constants were measured using an ultrafiltration assay. Sequences were radioactively labeled with ^{32}P using a 5' end labeling kit (Amersham Biosciences, Piscataway, NJ). Aliquots of each radiolabeled ssDNA sequence (25 pM) were incubated with increasing concentrations of HIVRT (0-50 nM) at room temperature. Samples were placed in a 100,000 MWCO microcon centrifuge filter (Millipore Corp.) and centrifuged

for 18 minutes at 500 RCF at 20 °C. The filtrate containing the unbound sequences was collected, mixed with 5 mL scintillation fluid, and assayed on a scintillation counter for 2 minutes. The dissociation constant was estimated by fitting the observed counts to Equation 2.1 where I is the measured counts for the unbound aptamer, and I_o is the measured counts for the aptamer in the absence of HIVRT.

2.4 Results and Discussion

A potential shortcoming of CE-SELEX is the limited number of sequences that can be injected onto the separation capillary. Libraries containing 10^{14} - 10^{15} sequences are common in conventional selections. It is desirable to keep the number of sequences high to increase the probability that the library contains high affinity aptamers. Typical CE injection volumes range from 5 to 50 nL. A 50 nL injection of a 2.5 mM ssDNA library will load $\sim 10^{14}$ sequences onto the separation capillary.

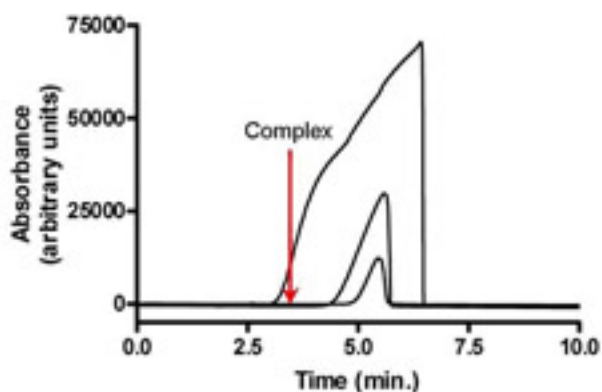


Figure 2.1: Effect of injection size on peak shape of a 2.5 mM ssDNA library separated using CE. Injection parameters: 1 psi, 5 seconds, 1 psi, 3 seconds, and 0.5 psi, 3 seconds. 1.8×10^{13} sequences were loaded onto the capillary in the 1 psi, 3 second injection. The arrow shows the position on the electropherogram where collection of binding sequences was stopped. CE conditions: TKG buffer, pH 8.3; UV detection at 254 nm; 50.2 cm, 50 μ m i.d., 360 μ m o.d. capillary; 30 kV separation voltage.

As shown in Figure 2.1, the injection severely overloads the capillary, giving rise to broad asymmetric peaks. This peak broadening makes the separation between the unbound and bound sequences more challenging. As shown in Figure 2.1, there is no resolution between the unbound sequences and the expected migration of the complex when large injections are used. Decreasing the size of the injection greatly improves the peak shape of the unbound DNA, facilitating collection of the bound sequences. In the current work, an injection of 1.8×10^{13} sequences (2.5 mM library, 3 seconds at 1 psi, 50 μm i.d. capillary) was chosen as a compromise between the injection size and resolution. Note that the number of sequences injected in subsequent rounds will be lower since PCR amplification plateaus at concentrations well below 2.5 mM. This is not as critical to the selection since the abundance of high affinity sequences will be much higher in later rounds than it was in the library used in the first round of selection.

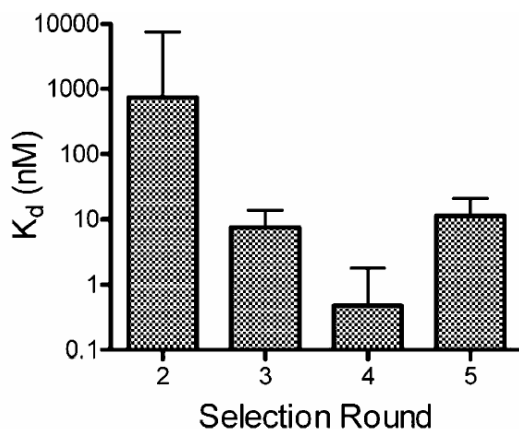


Figure 2.2: Affinity of the ssDNA pool for HIVRT after 2-4 rounds of selection. K_d 's were measured by fluorescently labeling an aliquot of the ssDNA pool followed by affinity capillary electrophoresis analysis. Error bars are the 95% confidence intervals.

The affinity of the nucleic acid pool for HIVRT was assessed at every round of selection using affinity capillary electrophoresis. An aliquot of the nucleic acid pool was

fluorescently labeled with a 5',6' carboxyfluorescein tag, making LIF detection possible. Although the addition of the label may have affected the conformation of the aptamer, this was still a good measure of the progress of the selection. As shown in Figure 2.2, exponential improvement in binding was observed in rounds 2-4. After round 4, the DNA pool exhibited an impressive 0.5 nM dissociation constant. Inexplicably, affinity worsened with further rounds of selection. This is not the first time this trend has been observed. Statistical fluctuations, contamination of the HIVRT target, or experimenter error are all possible contributors to this decrease in affinity.

Clones of the DNA pool after the fourth round of selection were prepared and sequenced. Table 2.1 lists the sequences of these clones. No sequence homology within these sequences or HIVRT aptamers previously described in literature were observed. This suggests that significant heterogeneity remains in the pool even though strong affinity for HIVRT is observed. The abundance of sequences with high affinity for HIVRT must therefore be high. This observed heterogeneity of DNA pools after CE-SELEX selection is a major departure from conventional selections. Several binding motifs generally dominate after 8-12 rounds of conventional SELEX selection. The heterogeneity of the sequences after CE-SELEX selection provides a larger number of high affinity sequences than traditional selection strategies.

Table 1. Sequences of the Clones Obtained from the ssDNA Pool after Four Rounds of CE-SELEX Selection against HIVRT^a

Clone	Sequence (5' → 3')
4.1.	AGCAGCACAGAGGTCAGAT GTATCGAATCCGATTGTTACGTGCGCCTTGGGGGTAAGGCGCCTATGCGTGTACCCTGAA
4.2.	AGCAGCACAGAGGTCAGAT GCCATAGGTGCCTGAATTGTCCCAAACATTGCGATGATCGACCTATGCGTGTACCCTGAA
4.3.	AGCAGCACAGAGGTCAGAT GGCAGGTTTCGACGTACAATGCTATGGAGGCTTTATGATCGCCTATGCGTGTACCCTGAA
4.4.	AGCAGCACAGAGGTCAGAT CCCCAAGTCAGACATTACCATGTTGGCCGCTGATCTCAGTTCCTATGCGTGTACCCTGAA
4.5.	AGCAGCACAGAGGTCAGAT GTCGGTCTTGTGTATACATACCCGTGTGTTTTTCATCTCAGGCTATGCGTGTACCCTGAA
4.6.	AGCAGCACAGAGGTCAGAT GTCAGGTCACAGCCTATGAATGAAGTGTTTTAAGAGACTATAACCTATGCGTGTACCCTGAA
4.7.	AGCAGCACAGAGGTCAGAT GACCGGCTCTTTCGATCTTACGATAAGGTCGGGCTAACACCTATGCGTGTACCCTGAA
4.8.	AGCAGCACAGAGGTCAGAT GACCGGTCAGAGGTTACACCCGTCGAGGCGCGCCTAAGCTTGCCACCCCTATGCGTGTACCCTGAA
4.9.	AGCAGCACAGAGGTCAGAT GCGACTTTTACGTTCTGCGGGTCCGTTGGGTGCAGCCGCTTCTATGCGTGTACCCTGAA
4.10.	AGCAGCACAGAGGTCAGAT GAGGGTAAAATTTTATATACTAGGAGCATCCTCTTTTAGTGCCTATGCGTGTACCCTGAA
4.11.	AGCAGCACAGAGGTCAGAT GCGTCTAAGTTCTCAGTATGTAGATCACTCATAACTGACACCCCTATGCGTGTACCCTGAA
4.12.	AGCAGCACAGAGGTCAGAT GAGGTTTACACCCGTCGAGGCGCGCCTAAGCTTGCCACCCCTATGCGTGTACCCTGAA
4.13.	AGCAGCACAGAGGTCAGAT GACTCGACGGTTCCTCAGCGATCAGTCTTCTTATGCTCCTATGCGTGTACCCTGAA
4.14.	AGCAGCACAGAGGTCAGAT GAGGACTGTCGATAAGTATAATGGCAAGTAGCTCGATACATCCTATGCGTGTACCCTGAA
4.15.	AGCAGCACAGAGGTCAGAT GTTATCCATGCGTTATGGACTACATATGTTTCTGAAATGTCCTATGCGTGTACCCTGAA
4.16.	AGCAGCACAGAGGTCAGAT GAGCAGGTTGTAAGAATTGGGACGCCCTTTGTTTGGGGAGCCCTATGCGTGTACCCTGAA
4.17.	AGCAGCACAGAGGTCAGAT GACGCGAGCAGGAGTAGGAAAGTAACTCTTCGATGCTCCTATGCGTGTACCCTGAA
4.18.	AGCAGCACAGAGGTCAGAT GTTATGACGGGCTGTTTATCGGTGAGGATTGGTAGAACTCCTATGCGTGTACCCTGAA
4.19.	AGCAGCACAGAGGTCAGAT GATGGTACATTGAGCGAGCTAAACTAGGATTAAGCTCACCCCTATGCGTGTACCCTGAA
4.20.	AGCAGCACAGAGGTCAGAT GACATGATGTTGCGACACGTAAGGAATAGAAAGCCCTCACCCCTATGCGTGTACCCTGAA
4.21.	AGCAGCACAGAGGTCAGAT GTCATCAGCCTTGTCAATGGTATTTTCTTCCAGTCACGTACCTATGCGTGTACCCTGAA
4.22.	AGCAGCACAGAGGTCAGAT GAATAATTATTTTCTATGCTTTTCTCCCTTAAGAGACCGCCCTATGCGTGTACCCTGAA
4.23.	AGCAGCACAGAGGTCAGAT GGTGCTATATCTGAGTACCGTTATTACCATTGTGTACATGGCCTATGCGTGTACCCTGAA
4.24.	AGCAGCACAGAGGTCAGAT GGCATAAGCTCACATAACGGTCATTAACCTTATCGACCTGGCCTATGCGTGTACCCTGAA
4.25.	AGCAGCACAGAGGTCAGAT GCGGTATGCTGGGTGATCTAACTGGGGATATTCTGATATTGCTATGCGTGTACCCTGAA
4.26.	AGCAGCACAGAGGTCAGAT GATGTAGCAGTTCGGTCATGCCTATCTACGGCAATCCACACCTATGCGTGTACCCTGAA
4.27.	AGCAGCACAGAGGTCAGAT GACTGGCAGATCGAACTGCCCGATGCTTCGTGGTAGCCATCCTATGCGTGTACCCTGAA

^a Primer sequences are shown in boldface type.

Table 2.1: Sequences of the clones obtained from the ssDNA pool after four rounds of CE-SELEX selection against HIVRT

Six of the sequences shown in table 2.1 were chosen at random and synthesized for further characterization. Affinity capillary electrophoresis was used in an attempt to measure the dissociation constants of the aptamer-HIVRT complexes. It was found that the aptamers bound HIVRT so strongly that LIF was not sensitive enough to detect the low concentrations necessary to give an accurate representation of the binding curve. Sequences were re synthesized without the addition of the 5',6' carboxyfluorescein label. These sequences were 32P labeled, and their affinities were measured using an ultrafiltration assay to separate bound from free sequences at varying concentrations of

HIVRT. As shown in Figure 2.3A, the radioactively labeled sequences provided sufficient sensitivity to measure the extent of binding at low picomolar concentrations.

Table 2.2 lists the dissociation constants of the aptamer-HIVRT complexes.

Sequence	K_d (pM)
4.3	190 ± 70
4.5	500 ± 400
4.14	500 ± 400
4.19	230 ± 150
4.20	180 ± 70
4.25	380 ± 180
average	340 ± 160
Unselected library	$>1 \mu\text{M}$

Table 2.2: Dissociation constants of sequences chosen at random from Table 2.1. The confidence limit of the average value is the standard deviation. All other error limits are the 95% confidence intervals.

Significant improvement in affinity was observed after four rounds of selection. Figure 2.3 B shows a binding curve of the ssDNA library before enrichment. Little binding was observed at HIVRT concentrations as high as $1 \mu\text{M}$, suggesting an even higher dissociation constant. The 180 pM K_d measured for clone 4.20 is five fold better than the strongest ssDNA HIVRT binding aptamer previously reported. Because the sequences listed in table 2.2 were chosen at random, this represents a true statistical sampling of the entire population as a whole. A sequence chosen from the pool at random will on average have a K_d of $340 \pm 160 \text{ pM}$. Note that the average sequence drawn from this pool will have a K_d three times better than the best ssDNA aptamer isolated in previous

selections. None of the aptamers assessed had a dissociation constant higher than 500 pM.

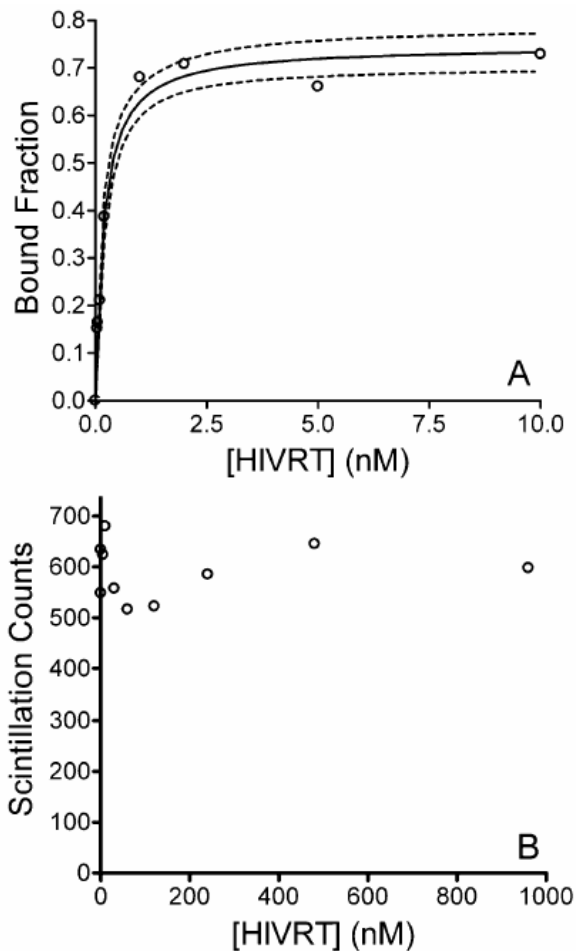


Figure 2.3: Binding curves of (A) clone 4.3 (see Table 2.1) and (B) the unselected library. Ultrafiltration was used to separate bound from free ^{32}P labeled ssDNA in the presence of increasing concentrations of HIVRT. Strong binding affinity was observed for clone 4.3 ($K_d = 190 \pm 70$ pM). The affinity of the unselected library was significantly lower ($K_d > 1$ μM)

2.5 Concluding Remarks

CE-SELEX was successfully used to isolate aptamers with high affinity for HIVRT. These aptamers were obtained after only 4 rounds of selection, significantly faster than the 9 rounds and 12 rounds used in previous ssDNA and RNA selections for

HIVRT, respectively. The increased rate of enrichment observed can be attributed to the higher separation power of CE and the decrease in surfaces where background interactions can occur. The low picomolar dissociation constants observed here are the strongest binding aptamers isolated using CE-SELEX to date. The affinity of the aptamers was significantly better than the pre-existing ssDNA aptamers for HIVRT, demonstrating for the first time that CE-SELEX can obtain aptamers with higher affinities than those isolated using conventional selection procedures. The 180 pM K_d for clone 4.20 is even approaching the 40 pM K_d of the strongest reported RNA aptamer for HIVRT. This is impressive considering that HIVRT is by nature an RNA binding protein. The heterogeneity of the pool at the completion of the selection should not be overlooked. The fact that no sequence motifs were observed suggests that there are many sequences that can bind HIVRT with dissociation constants in the low picomolar range. This contrasts conventional selections, which usually only yield a handful of binding motifs. The combination of strong binding interactions and heterogeneity suggests that CE-SELEX is more successful at retaining very strong binders while eliminating weak binders. The explanation for this could be as simple as the efficiency of the CE-SELEX selections. Sequences are lost during every round of selection. Isolating strong binders in relatively few rounds of selection could result in higher heterogeneity of the final nucleic acid pool. Another explanation could be the negative selections. Negative selections are common in conventional techniques although they do eliminate sequences from the pool. Nonspecific background interactions do not appear to be significant in

CE-SELEX, eliminating the need for these negative selections, which have the potential to reduce the heterogeneity of the pool.

Chapter 3: Characterization of HIVRT binding ssDNA Aptamers Identified using CE-SELEX

3.1 Abstract

The addition of CE-SELEX as an option to identify aptamers has significantly decreased the laborious, time consuming procedure to obtain aptamers. The ability to easily obtain aptamers has led to widespread adaptation of aptamer technologies. The utility of the HIVRT binding aptamers selected in Chapter 2 as diagnostic and therapeutic agents was tested. The aptamers bound in a variety of buffer conditions, suggesting they are universal and can be used for a variety of buffers for diagnostic applications. Additionally, the HIVRT aptamers had 10 fold more selectivity for the original target (HIV-1 RT) than other reverse transcriptases. This was significant since no added selection procedures were implemented to increase selectivity. This suggested the selection protocol identifies aptamers that are inherently selective. Inhibition experiments of the DNA primed reverse transcriptase reaction yielded no noticeable inhibition, indicating the aptamers bind in an area separate than the reverse transcriptase binding region.

3.2 Introduction

Detection of HIV continues to be a worldwide concern. Early detection is essential to both start treatment and prevent passing on the disease¹⁴². Initial detection methods dating back to 1985 relied on an assay to detect antibodies to viral proteins. However, it takes several months for the body to create enough antibodies for detection which limits early diagnosis. Despite ambitious efforts to advance HIV detection technologies, current detection methods still rely on antibody assays. The reliability of HIV testing has increased by identifying antibodies with more specific affinity for the virus. This has decreased the incidence of false negatives. However, the 3-6 month time requirement for detection and sensitivity has remained the same. Additionally, the ELISA technique is still labor intensive.^{142, 143}

In addition to initial detection, further viral quantification or viral load testing is part of routine HIV management to monitor the effectiveness of treatment. This routine testing is generally done through branched DNA (bDNA) technology which is performed by a series of hybridization reactions or real time PCR (RT-PCR) assays that measure HIVRT conversion of viral RNA to viral DNA¹⁴⁴. These assays have been used for decades as HIV diagnostic tools, however; they are limited by a number of factors. RT-PCR is easily contaminated. Additionally, since the starting template concentration is unknown, it is difficult to determine the amount of amplification necessary to be in a linear quantitation range. bDNA assays are favorable to RT-PCR assays because they are more sensitive and easily automated. However, nonspecific hybridization to nontarget

sequences often leads to excessive signal. Inaccuracy in these testing methods often leads to miscalculation of the necessary drug concentrations. Over medication of HIV patients leads to more side effects and a decrease in the effective lifetime of medications due to viral mutation and resistance. The need for better HIV detection strategies is hard to ignore.

In addition to detection, treatment of HIV is also unsatisfactory. Unlike many other regions of the virus, the reverse transcriptase and protease functional domains are largely conserved which makes them ideal targets for anti-AIDS drugs. HIVRT is targeted by three groups of antiretroviral drugs. The nucleoside inhibitors (NRTI), non nucleoside inhibitors (NNRTI), and pyrophosphate analogs¹⁴⁵. These medications inhibit the virus by halting the reverse transcriptase reaction, but do not interfere with the function of the enzyme^{146, 147}. Protease inhibitors such as saquinavir, ritonavir, indinavir, and nelfinavir inhibit protease activity and protein packaging which is essential for viral replication^{146, 148, 149}. Although these medications are effective, they target downstream functions of the virus and cause debilitating side effects. Newer medications prevent infection altogether by inhibiting target attachment of the virus to cells bearing CD4 cells on their surface. These are called 5-Helix¹⁵⁰ and T-20¹⁵¹. However, because the HIV virus rapidly mutates, these medications are only effective for a short period of time¹⁵².

Aptamer technologies are attractive alternatives to the traditional antibody testing. Diagnostic assays utilizing aptamers have demonstrated picomolar to femtomolar detection limits even in complicated matrices or in the presence of interfering

molecules^{73, 153}. These assays were simple to perform, and only require a few minutes to complete. Additionally, they are easily automated which reduces the laborious nature of current HIV testing. The combination of aptamer specificity and current aptamer diagnostic techniques may lead to earlier detection and more precise monitoring of HIV infection.

The tight, specific binding properties of aptamers make them ideal candidates for the treatment of HIV. These properties would result in the confident detection of minimal concentrations, allowing earlier diagnosis and treatment. In addition, the specific nature of aptamers minimizes the possibility of aptamer treatment adversely affecting normal body functions. The tight binding properties of aptamers promote low dosage requirements for effective treatment. Ultimately this would lead to longer effectiveness and fewer side effects.

This chapter discusses the characterization of the HIV-1 reverse transcriptase aptamers identified using CE-SELEX in Chapter 2. Aptamers with high specificity and picomolar affinity may provide the sensitivity necessary to develop more sensitive diagnostic assays for HIV infection. In addition, aptamer characteristics may make them ideal candidates for drug therapy.

3.3 Experimental Section

3.3.1 Materials

Unless otherwise noted, all samples and buffers were prepared in deionized water obtained from a Milli-Q water purification system (Millipore Corp., Bedford, MA). All

chemicals were obtained from Sigma-Aldrich (St. Louis, MO) and were the best grade available. All ssDNA primers and aptamers were obtained from Integrated DNA Technologies, Inc (Coralville, IA). RNA template (5'-CAG UGU GGA AAA UCU CUA GCA GUG GCG CCC GAA CAG GGA C-3') was obtained from Dharmacon RNA Technologies (Lafayette, CO). A ssDNA 5' end ³²P labeling kit was obtained from Amersham Biosciences (Piscataway, NJ). Microcon centrifugal filters MWCO 100,000 were obtained from Millipore (Bedford, MA). HIVRT was obtained from Worthington Biochemical (Lakewood, NJ). All other reverse transcriptases were the kind gift of Dr. Robert Gorelick (Frederick Institute, MD). Binding and inhibition experiments were carried out in 25 mM tris, 192 mM glycine, and 5 mM KH₂PO₄ (TGK) at pH 8.3. Universal binding assays were carried out in the following buffers: Bis-Tris (500 mM Bis Tris pH 8.0), 1/5 PBS (1X buffer includes 164 mM Na₂HPO₄, 34 mM NaH₂PO₄, 137 mM NaCl, 2.7 mM KCl, pH 7.2), and HEPES (250 mM sucrose, 10 mM HEPES, pH 5.0 adjusted with KOH).

3.3.2 ³²P DNA Labeling

ssDNA aptamers and the DNA inhibition template were labeled with a ³²P label at the 5' end according to the suggested protocol from Amersham Biosciences. This kit utilizes T4 polynucleotide kinase (PNK) which catalyzes the transfer of the terminal [γ -³²P]dATP phosphate of ATP to the 5' hydroxyl terminus of the DNA molecule. Briefly, 49 μ L of the provided exchange buffer containing T4 polynucleotide kinase and 100 pM DNA was added to a 0.5 mL microcentrifuge tube. A 1 μ L aliquot of [γ -³²P]dATP (20 μ Ci) was added and the reaction mixture was incubated at 37°C for 20 minutes. 5 μ L of

0.2 M EDTA was added to stop the reaction. Excess reagents were removed via ethanol precipitation. Following purification, the concentration of the labeled ssDNA was determined by absorbance at 254 nm.

3.3.3 Ultrafiltration Assays

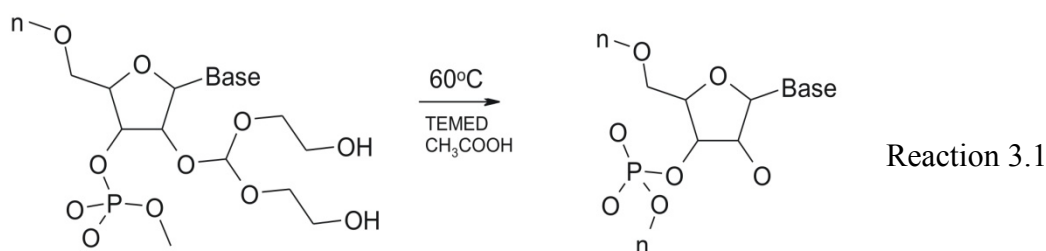
Table 3.1 describes the affinity of aptamers for the original target the Human Immunodeficiency Virus strain 1 (HIV-1 RT) as well as the reverse transcriptases of other retroviruses including the Human Immunodeficiency Virus strain 2 (HIV-2 RT), Feline Immunodeficiency Virus Reverse Transcriptase (FIV-RT), Moloney Murine Leukemia Virus Reverse Transcriptase (M-uLV RT), and Avian Myeloblastosis Reverse Transcriptase (AMV-RT). All dissociation constants were determined in triplicate. The ³²P labeled ssDNA aptamers were heated to 72°C for 2 minutes and allowed to cool to room temperature to ensure that the sequences were in their stable room temperature conformations. 25 pM aptamer was titrated with increasing concentrations (0-50 nM) of reverse transcriptase. These samples incubated for 20 minutes at room temperature to allow binding. Bound and free fractions were separated by spinning a 100,000 MWCO microcon centrifugal filter at 500 RCF for 20 minutes at ambient temperature. The free fraction was transferred into 5 mL scintillation fluid and counted on a scintillation counter for 2 minutes. The bound fraction was calculated and fit to Equation 3.1.

$$\frac{I_b}{I_b + I_f} = \frac{\text{Constant}}{K_d + [RT]} \quad \text{Equation 3.1}$$

Where I_o is the unbound counts in the absence of reverse transcriptase, I is the unbound counts in the presence of reverse transcriptase, and $[RT]$ is the concentration of the reverse transcriptase.

3.3.4 RNA Template Preparation

All RNA buffers, stock solutions, and chemicals were prepared in nuclease free water from Invitrogen (Carlsbad, CA). 2'-ACE protected RNA was deprotected according to Reaction 3.1.



The RNA in both stock tubes was completely dissolved in 400 μ L deprotection buffer (100 mM acetic acid, pH 8.3 adjusted with TEMED). Once dissolved, these samples were incubated at 60° for 30 minutes to allow the deprotection reaction to occur. The deprotected RNA was put back in pellet form by drying in a SpeedVac for 60°C for 1 hour. The RNA was diluted to a concentration of 90 nM in nuclease free TGK buffer.

3.3.5 Inhibition Experiments

The ability of the aptamers to inhibit DNA dependent RNA polymerase was determined using a DNA primed reverse transcriptase reaction. To help the primer anneal to the RNA template, the 32 P labeled DNA primer (5' - 32 P-GTC CCT GTT CGG GCG CCA CT-3') was incubated with RNA template and heated to 90°C for 90 seconds and allowed to cool to room temperature at 2°C/min. RNasin was added once the

temperature reached 40°C to prevent nuclease degradation. This mixture was distributed evenly into 9 vials and the following was added: dNTP's, aptamer (0-100 nM) and nuclease free TGK buffer. 1 µL HIVRT was added simultaneously to each tube except the control. Upon addition of the HIVRT the final volume in each reaction was 100 µL, yielding 45 nM RNA, 30 nM DNA primer, 0.02 mM dNTP's, 40 u/µL RNasin, and aptamer (0-100 nM). The samples were immediately incubated at 37°C for 15 minutes. 100 µL of 50 mM EDTA in 95% formamide was added to each sample simultaneously to quench the reaction. Samples were heated to 90°C to denature the HIVRT protein. Each sample was characterized on a polyacrylamide gel.

3.3.6 Polyacrylamide Gel Shift Assay

Each sample was run in a 16% 19:1 acrylamide:bisacrylamide denaturing gel with 7 M urea. The 10 cm x 10 cm gel was prepared by fixing spacers between the plates and sealing the edges with 1% agarose gel. 10 mL 16% 19:1 acrylamide:bisacrylamide, 7 M urea is prepared in 0.5 X TBE buffer (0.045 M tris, 0.045 M borate, 0.001 M EDTA. pH 8.3). The crosslinking reaction is activated by the addition of 0.2% (V,V) tetramethylethylenediamine (TEMED) and catalyzed by the addition of 10% (W,V) ammonium persulfate (APS). Crosslinking occurred overnight at 4°C.

5 µL of each reverse transcription sample was added to 8 µL loading dye which consists of 30% (V,V) glycerol, 0.25% (W,V) bromophenol blue, and 0.25% (W,V) xylene cyanol FF. The samples were loaded, and the gel was run for 3 hours at 100 V. The gel was exposed to a phosphor screen for several hours. The amount of product was quantitated using a phosphorimager.

3.4 Results and Discussion

The ability of aptamers to bind in conditions different from the selection criteria determines the flexibility of aptamers for a variety of applications. Several parameters may need to be adjusted to use an aptamer for a desired application. These include changing buffers, labels, substitutions, and aptamer length. Arguably, buffer selection is the most critical change for diagnostic strategies because salt components and concentrations can change the folding of the ssDNA. For example, potassium is required for G-quartet formation and Mg^{+2} is favorable for the thermodynamic stabilization of some structures. To test the universality of the HIVRT aptamers, dissociation constants for clone 4.3 were determined in several different buffers (Table 3.1). As demonstrated in the table, the aptamer 4.3 bound with picomolar affinity in all the buffers tested. In fact, the 95% confidence interval indicated that the affinity of the aptamer for HIVRT in each of these buffers was the same. This suggests the aptamers may be used in a variety of applications in which a buffer change is desired. This is particularly important for microarray based detection methods where a universal buffer must be selected for several aptamers.

Aptamer	TGK K_d (pM)	Bis-Tris K_d (pM)	PBS K_d (pM)*	HEPES K_d (pM)*
4.3	190 ± 70	355 ± 161	135 ± 148	151 ± 64

Table 3.1: Aptamer affinity for HIVRT in different buffer compositions. Error indicates the 95% confidence interval. * indicates that the dissociation constant was determined using ACE described in Chapter 1.5. CE conditions: 30 kV normal polarity separation, 1 psi, 4 sec injection, 50 μ m i.d., 360 μ m o.d., 50.2 cm capillary, TGK separation buffer and specified incubation buffer.

The utility of the HIVRT aptamers was further characterized by determining the specificity of binding. To answer this question, the affinity of the aptamers for other retroviral reverse transcriptases was studied. It was assumed that the aptamers would be more likely to bind to proteins that had high structure or sequence conservation to the original target. Each of the reverse transcriptases studied have function, structure, and/or sequence conservation with the original HIV-1 RT target. As demonstrated in Table 3.2, the aptamer sequences bound, on average, with 10 fold more sensitivity for the original target than for other reverse transcriptases. This was surprising because there were no additional precautions taken during the HIVRT selections to avoid affinity for molecules possessing similar features and/or functions. These precautions may have included negative selections which would eliminate sequences that had affinity for other reverse transcriptases.

Clone	HIV-1 RT (nM)	HIV-2 RT (nM)	FIV-RT (nM)	MuLV-RT (nM)	AMV-RT (nM)
4.3	0.190 ± 0.07	3.8 ± 4	1.3 ± 0.8	> 1 μM	> 1 μM
4.5	0.500 ± 0.4	5.0 ± 3	6.3 ± 5	> 1 μM	5.3 ± 5
4.14	0.500 ± 0.4	14 ± 10	1.5 ± 2	> 1 μM	4.0 ± 6
4.19	0.230 ± 0.2	25 ± 40	2.2 ± 1	> 1 μM	5.8 ± 7
4.20	0.180 ± 0.07	15 ± 20	4.5 ± 5	0.22 ± 0.3	4.4 ± 7
4.25	0.380 ± 0.2	12 ± 20	3.0 ± 3	0.20 ± 3	4.3 ± 6
Average	0.340 ± 0.2	12 ± 20	3.1 ± 3	3.69 ± 20	4.7 ± 6

Table 3.2: Binding specificity of HIVRT aptamers. Original target was HIV-1 RT. Error indicates the 95% confidence interval.

A notable exception is that 4 out of 6 clones had no affinity for MuLV-RT up to a concentration of 1 μM . Similar structure between reverse transcriptases has suggested a common catalytic mechanism exists between them^{154, 155}. However, despite highly conserved topology, MuLV-RT is known to deviate functionally from other reverse transcriptases. In fact, MuLV-RT incorporates dideoxynucleotides considerably less readily than HIV-1 RT^{156, 157}. Further studies have shown that a single residue difference (lysine in the K152 position of MuLV-RT and glycine in the HIV-1 RT equivalent position G112) alone participates in maintaining the integrity of the active site in MuLV-RT. Substitution of this residue has had little effect on the performance of HIV-RT, but has shown significant retardation of MuLV enzyme activity¹⁵⁸. These results indicate apparent differences between the two enzymes which may explain why aptamers may bind to HIV-1 RT but not MuLV-RT. Another possibility is that the aptamers bind to a region of HIV-1 RT that is not conserved in MuLV-RT.

In addition to binding specificity, the therapeutic potential of the aptamers was studied by testing the effect of the aptamers on the reverse transcription activity of the enzyme. In these experiments, a ³²P labeled DNA primer initiated a reverse transcriptase reaction. The reaction was allowed to proceed for 3 minutes in the presence of various aptamer concentrations (0-100 nM). The final product and the primer, each containing the radioactive tag were separated on a polyacrylamide gel. After exposure to a phosphor screen, the amount of product and unreacted primer was quantitated using a phosphorimager (Figure 3.1). The fraction of product was then calculated and plotted (Figure 3.2).

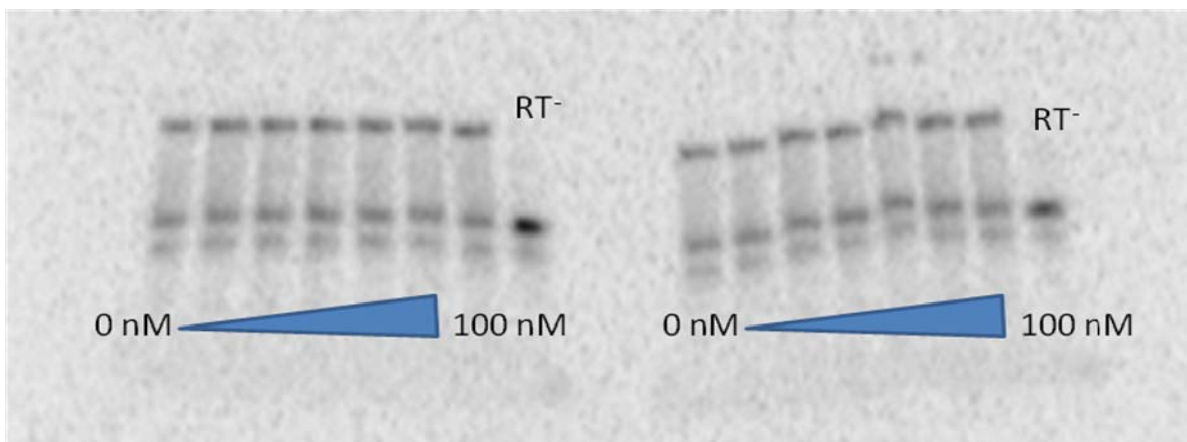


Figure 3.1: Gel images of clone 4.3 (left) and 4.5 (right). Aptamer concentrations increased from left to right. The product band is shown on the top, the mid band is the primer, and the last band is ^{32}P label. The RT⁻ lane indicated the reaction in the absence of HIVRT. This control exhibited no product formation as expected. Gel conditions: 16% 19:1 acrylamide:bisacrylamide 10 cm x 10 cm gel, 100 V, 3 hours. Gel was immediately exposed to a phosphor screen.

It was expected that less product would be formed as the concentration of aptamer increased. Surprisingly, product formation was not dependant on aptamer concentration.

This suggested that the aptamers did not inhibit reverse transcriptase activity.

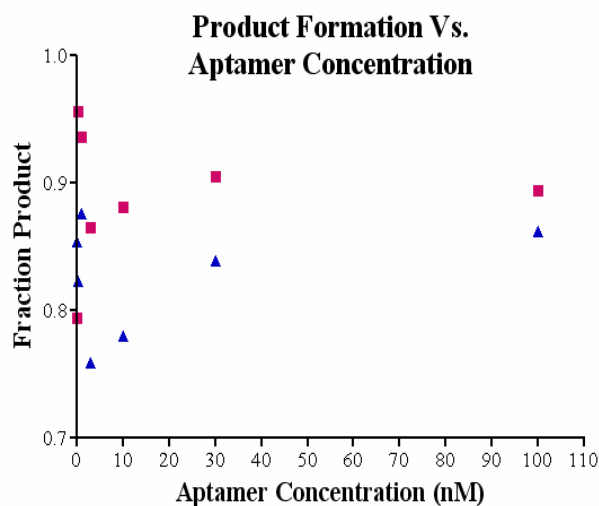


Figure 3.2: Graphical representation of the inhibition experiment. The fraction of product formation is plotted against the aptamer concentration. As the concentration of aptamer increases, there is no observable change in product formation, indicating the aptamer does not interfere with reverse transcriptase activity.

There are a number of reasons inhibition may not have been observed. HIVRT is a heterodimer which can carry out RNA-dependent and DNA-dependant polymerase as well as ribonuclease H activity. Interestingly, polymerase and RNase H activity occurs at opposing ends of the protein. It is feasible that the aptamers have affinity for the RNase H domain of the enzyme which may interfere with RNase H activity. This; however, was never studied. Another possible explanation is that the aptamers bind to a place on the HIVRT molecule that does not have any function. This is a reasonable explanation since the aptamers identified using CE-SELEX do not have sequence or structural motifs which may indicate that they have affinities for different areas on the surface of the protein.

3.5 Concluding Remarks

Aptamers for HIVRT selected using CE-SELEX have promising characteristics that make them suitable diagnostic agents. Picomolar binding was achieved not only in the selection buffer, but also 3 other buffers ranging in pH from 5.0-8.3. This is impressive because proper ssDNA folding is highly dependent on buffer composition and concentration. Furthermore, protein folding and ionic charge is dependent on a number of factors including buffer composition and concentration, temperature, and pH. Affinity in many buffers demonstrates the universal nature of the HIVRT aptamers for applications in which a different buffer is desired. The specificity of the aptamers was tested to determine the practicality of using aptamers to test for HIV levels in complicated matrices or in the presence of interfering molecules. Surprisingly, the aptamers had a 10 fold greater affinity for the original target (HIV-1 RT) than other

retroviral reverse transcriptases. Further specificity could have been obtained by performing negative selections in which sequences that have affinity for similar targets are discarded. The 10 fold decrease in affinity for other reverse transcriptases when negative selections were not performed demonstrates the inherent ability of CE-SELEX to identify highly specific aptamers in only 4 selection rounds. Despite the tight and specific binding properties, these aptamers did not interfere with reverse transcriptase activity. An explanation for this is the dual nature of the enzyme to carry out reverse transcriptase functions as well as RNase H activity. It is feasible that the aptamers bind to the RNase H domain or a region on the enzyme in which there is no function.

Chapter 4: CE-SELEX Identification of Aptamers that Bind Complex Targets

4.1 Abstract

Capillary Electrophoresis-SELEX (CE-SELEX) was used to perform selections against the non uniform targets mitochondria, *E. coli*, and *B. subtilis*. These selections presented additional challenges than with normal selections because aptamers had to bind to a feature on the surface of the target that is consistent in order to be conserved throughout the process. Additionally, these large heterogeneous samples demonstrated broad migration times that overlapped with the library, limiting resolution and making the separation of the bound and unbound fractions cumbersome. Although no increase in affinity was observed after several selection rounds for these targets, data suggests that ssDNA binding became more selective for specific features on the surface of the target.

4.2 Introduction

Aptamers have been identified for a number of proteins^{2, 43, 45}, peptides⁴⁴, bacterial spores³⁶, viruses^{159, 160}, and even whole mammalian cells^{95, 161}. Many of these samples do not experience lot variance, and are available in high purity making specificity easy to achieve. However, little work has been done on aptamer identification of targets that have different features based on the lot or targets where pure analyte is not available¹⁶². Bacteria and mitochondria are two good targets which experience non uniformity. In addition to non uniformity, the large size of bacteria and mitochondria increases the many structural and chemical features on the surface which can serve as viable binding sites. This means there are several places on one target where aptamers could bind specifically and/or non specifically. Because of these reasons, there is a great analytical need for better diagnostics of large non uniform samples such as bacteria and mitochondria.

4.2.1 Bacteria Surface Chemistry

The outer surface layers of bacteria have been well defined¹⁶³⁻¹⁶⁵. Despite the wide knowledge regarding bacteria surfaces, specific bacterium identification is still challenging because some bacterial surface features are largely conserved throughout subgroups and even different species^{165, 166}. This surface chemistry is very complex comprising of proteins, polysaccharides, lipids, and amphiphiles¹⁶⁷. The density of surface features and the charge distribution across the cell surface fluctuates daily based on pH, oxygen, temperature and nutrient levels^{163, 164}. In addition, bacteria adapt and mutate rapidly causing different proteins to be expressed altogether. Because the surface is constantly changing, aptamers must identify a part of the bacterial surface that is

conserved under all environmental conditions and during mutation. An additional challenge is aptamer specificity since many species of bacterium possess matching features.

4.2.1.1 Bacteria Classification

In bacteria, the cell wall forms a rigid structure of uniform thickness around the cell which is responsible for its characteristic (rod, coccus, or spiral) shape. Just inside the cell wall, or rigid peptidoglycan layer, are the cytoplasmic membrane and cell components¹⁶⁸. The peptidoglycan layer is what differentiates bacteria into Gram positive or Gram negative subsets (Figure 4.1). The peptidoglycan layer of Gram positive bacteria is very thick (20-80 nm)¹⁶⁹ compared to that of gram negative bacteria (10-50 nm)¹⁶⁸. Both organisms will uptake the crystal violet (Gram) dye. However, upon stringent ethanol washing only the Gram positive bacteria will retain the crystal violet dye. Though developed back in the 1800s, this is still the current method used for bacteria classification and identification.¹⁷⁰ Although this is sufficient for medication selection for patients with bacterial infection, more specific detection of bacterial type and strain is becoming increasingly important as bacterial resistance escalates.

More sophisticated techniques for the rapid, sensitive, and specific detection of bacteria strains have only recently begun to emerge. Multiplex PCR assays have allowed sensitive determination of up to 6 bacteria genomes simultaneously. DNA microarrays have the capacity to detect numerous samples concurrently; however, they often create a signal too weak for direct detection and require additional laborious enzymatic steps for signal amplification¹⁷¹. Surface Plasmon Resonance (SPR) has been

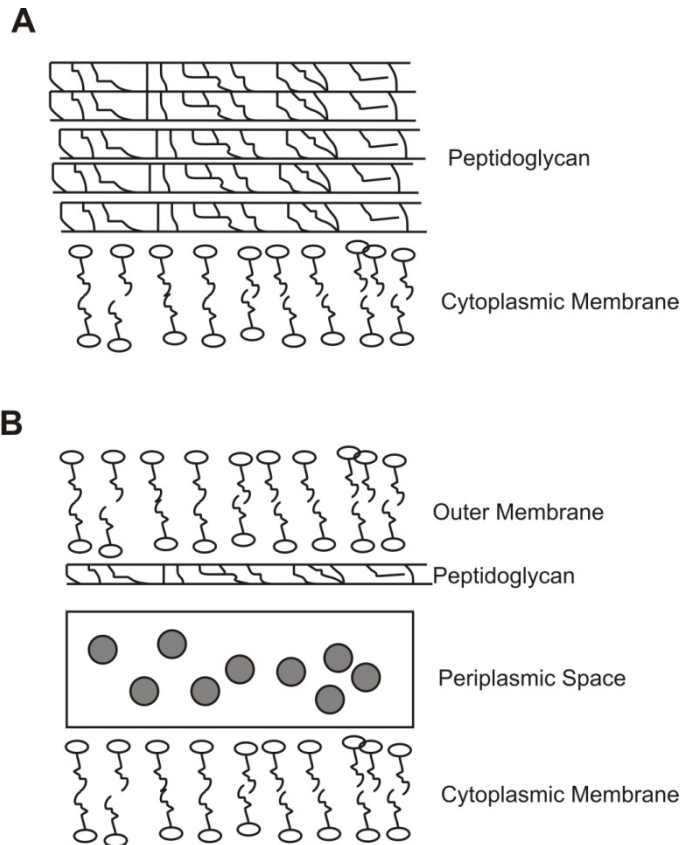


Figure 4.1: Depiction of gram positive (A) and gram negative (B) bacterial cell walls.

used to determine how each bacterial strain adheres to surfaces, a property unique to each bacterium¹⁷². Biosensor protocols can offer reliable sensitive detection but can lack specificity and mass production capabilities¹⁷³. More recently, mass spectrometry has been used for microbial studies. Finally, PCR protocols offer sensitive detection of different bacteria types¹⁷⁴. Although successful, all of these techniques require prior knowledge (i.e. DNA genome, surface adhesion properties etc.) about the bacteria and is not feasible for their quickly changing and adapting surfaces. Most approaches do not analyze intact cells which increases the long, laborious procedure. Ultimately this makes

quick detection unlikely. Furthermore these methods can only identify the bacterium type but they hold no therapeutic advantages. Ideally, a protocol for the quick detection, identification, and inactivation of bacteria would emerge.

4.2.2 Mitochondria Surface Chemistry

Mitochondrial surfaces are also plagued by inconsistencies which make aptamer identification challenging. Much like bacteria, mitochondria has a myriad of surface features including proteins, phospholipids, glycoproteins and cytoskeletal material¹⁷⁵. The surface chemistry of mitochondria fluctuates with age, disease, nutrient levels, and the type of skeletal muscle fiber the mitochondria was isolated from¹⁷⁶.

An additional obstacle is that it is difficult to obtain pure mitochondria samples. Isolation of mitochondria from cells is generally done by gradient density centrifugation¹⁷⁷⁻¹⁷⁹. However, this technique is inadequate because many organelles have overlapping densities and sedimentation rates. This results in a mitochondria sample that can contain lysozymes, denatured mitochondria, and other cellular components.

4.2.2.1 Mitochondria Classification

Mitochondria can have different morphologies and functions. These morphologies and functions are highly important and include apoptosis^{180, 181}, calcium homeostasis^{182, 183}, and oxidative phosphorylation^{184, 185}. The inability of mitochondria to properly carry out its tasks often leads to disease^{186, 187}. Diagnosis of mitochondrial diseases generally involves a complex myriad of muscle biopsies, histology, enzymology,

genetic analysis and exercise testing¹⁸⁸. Undoubtedly quicker, more direct methods for diagnosis of mitochondrial diseases is desired.

Recent advances in microscopy methods have introduced more direct approaches to determine mitochondrial properties while the mitochondrion is still in the cell. These techniques include electron and confocal microscopy which yields information about membrane structure membrane potential, and calcium parameters^{189, 190}. X-ray microanalysis has accurately defined cation levels¹⁹¹⁻¹⁹³. Optical trapping has been used to determine the force generated by mitochondria transport¹⁹⁴. Finally, patch clamp assays provide information about membrane conductivity¹⁹⁵.

Other methods for defining the properties of mitochondria that have been released from cells include patch clamp assays for information regarding permeability transition pore (PTP) activity¹⁹⁶, flow cytometry for information about membrane potential¹⁹⁷, and capillary electrophoresis (see below) which provides describes mitochondrial abundance, electrophoretic mobility¹⁹⁸.

Each of these techniques provides specific information about mitochondria and its function. However, quick techniques which yield information of the overall function and structure as a whole is desired. This would provide the ability to sort mitochondria with specific properties for further testing. Ultimately, quick identification of diseased mitochondria could be performed alleviating time consuming tests. Since mitochondria malfunction is a significant cause of disease, non invasive techniques to identify the properties of mitochondria are also desired.

4.2.3 CE and Bacteria Separations

The first CE experiment involving microbes was described by Hjertan *et al.* in 1987¹⁹⁹. These initial experiments involved *Lactobacillus casei* and tobacco mosaic virus (TMV). Although the two microorganisms could not be separated, Hjertan *et al.* demonstrated that CE could be used to move microorganisms through a capillary with an applied electric field. These experiments were highly successful. In fact, both microorganisms migrated in very sharp peaks in under 4 minutes when analyzed separately.

Subsequent work expanded CE experiments to erythrocytes²⁰⁰. In this report, Zhu and Chen were able to correlate peak height and the number of cells injected. Additionally, they were the first to identify extraneous peaks as cell aggregates. Migration of the red blood cells proved to be highly reproducible. This separation took ~14 minutes.

Finally the first paper demonstrating the successful separation of microbes using capillary electrophoresis was published in 1993²⁰¹. In these experiments, the bacterium *Enterococcus faecalis*, *Streptococcus pyrogenes*, *Streptococcus Agalactiae*, *Streptococcus pneumonia*, and *Staphylococcus aureus* were isolated into discrete bands. Although this proved the separation was possible, the separation took nearly 90 minutes. Despite this long separation time, it was encouraging that a significant portion (90%) of the bacteria was thought to remain viable after the separation.

Over the next few decades microorganism separation via CE has sparked widespread interest. From these experiments we have learned that different sizes and charges of bacteria facilitate their separation and can serve as a factor in characterizing bacteria²⁰². Although we have gained knowledge that electrophoretic separation of large molecules contributes to more detailed cell characterization;²⁰³ the exact manner in which the surface groups affect migration are still not fully understood²⁰⁴. Furthermore, separations with massive molecules are not comparable to that of smaller molecules, and the separations can be very lengthy taking several hours^{205,206}.

4.2.4 CE and Mitochondria Separations

Much work has been done on CE separation of mitochondrial components and catabolic substances, including mitochondrial DNA²⁰⁷, cardiolipin²⁰⁸, thioredoxins²⁰⁹, L-carnitine²¹⁰, and glutathione²¹¹. However, CE work on intact mitochondria has been limited to a single group²¹². CE separations have suggested that several factors including pH, mitochondria source, surface proteins, surface charge distribution, and disruption technique have all affected mitochondria electrophoretic mobility^{176, 213}. Mitochondria migration is very complex, and thought to be a function of the electrical charge on the particles surface, its morphology, and less significantly its size.

Strack *et al.* developed a capillary electrophoresis assay to detect individual mitochondria²¹². This technique requires a home built CE instrument in which dual laser detection is possible by two PMT boxes for post capillary detection. This system allows labeled mitochondria to be detected along with mitochondrial components or molecules with affinity for mitochondria simultaneously. The fast separation and acquisition rate

allows individual mitochondria spikes to be observed allowing individual mitochondria and its unique electrophoretic mobility to be analyzed.

Intact mitochondrial separations on CE are more challenging than bacterial separations because they are limited to isotonic separation buffers and low electric fields to conserve the integrity of the mitochondria. Additionally, coated capillaries that prevent wall interactions are highly recommended which can make charge separations difficult²¹⁴. Furthermore, only intact mitochondria can be observed through labeling which eliminates detection of mitochondrial fragments and contaminants in the sample.

4.2.5 CE-SELEX Selections of Bacteria and Mitochondria

Most selections are performed on specific cell and organelle components such as surface proteins, lipids, or envelopes. Only recently was whole cell SELEX introduced for the identification of individual cancer cell types^{101, 215}. The idea of cell SELEX has become widely popular²¹⁶⁻²¹⁸. However, original work on whole cell SELEX was performed on mammalian cancer cells which tend to have high homogeneity. Furthermore, it took 20 selection rounds to obtain aptamers with moderate affinity¹⁰¹. Further challenges are presented when working with large biomolecules such as bacteria or mitochondria in which the sample is not homogeneous.

Very recently the first report of aptamers that bind bacteria was published²¹⁹. These aptamers bound to the whole, live gram positive bacterium *Lactobacillus acidophilus*. In these experiments, the partitioning method to separate bound and free sequences in each cycle was centrifugation. This is consistent with earlier whole cell

SELEX protocols¹⁰¹. Aptamers were identified in 6-8 rounds of with an impressive dissociation constant of 13 ± 3 nM. However, aptamer specificity was not discussed.

The previous work on bacteria and mitochondria CE separations suggested that once proper considerations were observed to maintain the integrity of the organelle/cell, CE would be a possible partitioning method of these SELEX experiments. In addition, separations have been studied extensively and optimized which provided information on separation criteria for these targets. In combination with successful CE separations of bacteria, the successful history of highly selective aptamer identification via CE-SELEX makes it a logical protocol for identification of specific aptamers that bind bacteria.

4.2.6 Aptamers for Bacteria and Mitochondria

Aptamers for non uniform samples such as mitochondria and bacteria would be advantageous because of the current limitations in mitochondrial and bacteria diagnostics materials and methods. More specifically, bacterial aptamers that can distinguish between different species of bacteria would be a significant improvement from the current Gram testing method. This would allow doctors to provide bacteria specific treatment depending on the bacterial strain. An additional benefit of aptamer technology is the likelihood that the diagnostic agent would also work in therapeutics. Many bacteria strains become pathogenic when they are able to adhere to normal body parts. Aptamers that not only bind the bacteria, but also inhibit adhesion to surfaces could be used for diagnosis and treatment.

Mitochondrial aptamers would greatly alleviate the complicated, time consuming process of diagnosing of mitochondrial diseases. Furthermore, aptamers could be used to

answer other mitochondrial questions such as quantitation in various cells, and identification of other mitochondrial phenomenon such as giant mitochondria. Because of the crucial role of mitochondria in various biological functions, mitochondria is also a large therapeutic target because of its role in many diseases²²⁰. The well rounded nature of aptamers gives them potential in all these areas.

4.3 Experimental Section

4.3.1 Materials

Unless otherwise noted, all samples and buffers were prepared in deionized water obtained from a Milli-Q water purification system (Millipore Corp. Bedford, MA). The ssDNA library consisted of a 40 base random region flanked by two 20 base primer regions 5'-FAM-AGC AGC ACA GAG GTC AGA TG (40 random bases) TTC AGC GTA GCA CGC ATA GG-3'. The DNA library and PCR primers were obtained from Integrated DNA Technologies, Inc (Coralville, IA). *Escherichia coli* JM109 was obtained from New England Biolabs (Ipswich, MA). *Bacillus subtilis* was obtained from ATCC (Manassas, VA). Liquid LB broth and LB agar was obtained from Invitrogen (Carlsbad, CA). All other chemicals were obtained from Sigma-Aldrich (St. Louis, MO) and were of the best grade available. The selection buffer for *E. coli* and *B. subtilis* consisted of 5 mM tris, pH 8.0. The selection buffer for mitochondria was 250 mM sucrose, 10 mM HEPES, pH 7.0 (adjusted with KOH).

4.3.2 *Escherichia coli* and *Bacillus subtilis* Culturing

Escherichia coli JM109 was grown in liquid LB broth directly from the glycerol stock. 1 μ L bacteria stock was put in 5 mL LB broth containing 10 μ g/mL streptomycin.

The solution was incubated while shaking at 37°C, 250 rpm overnight. A control in the absence of bacteria was performed to confirm the cells were not contaminated by naturally occurring bacteria. The resulting cells were put in 5 mM tris buffer by performing the following procedure 5 times: Centrifuge 1 mL bacteria culture 14,000 rpm for 2 minutes. Extract liquid leaving the DNA pellet. Add 1 mL of 5 mM tris, sonicate, and mix completely. The final solution was diluted in 100 µL buffer and quantitated by UV absorbance on capillary electrophoresis. The capillary electrophoresis conditions were as follows: 40.2 cm, 150 µm i.d., 360 µm o.d. bare fused silica capillary, 200 nm detection, ambient temperature. The capillary was rinsed with 15 psi for 1 minute with the bacteria stock solution. The absorbance at 0.8 minutes was used to calculate the concentration from a calibration curve. *Bacillus subtilis* was prepared the same was except the antibiotic was nalidixic acid.

4.3.3 Bacteria Viability

The viability of freshly prepared bacteria was determined by counting the cells on a microscope and comparing that to the number of colonies grown. To stain the cells they were diluted to a concentration of approximately 5 cells/µL. 10 µL was placed on a glass slide and quickly heated to firmly mount the bacteria on the slide. Crystal violet dye was added to the *B. subtilis* which stained the gram positive cells blue. These cells were counted on the microscope. Since the gram negative *E. coli* cells do not uptake the crystal violet dye, they were washed with ethanol to disrupt the bacterial wall. These cells were treated with safranin dye and stained red for easy counting under a microscope. In both cases, the number of cells observed under the microscope was

compared to the number of colonies from the same stock grown overnight on a LB agar plate with 10 µg/mL antibiotic.

4.3.4 Nuclease Activity Determination

To check the bacteria for nuclease activity, 1 µM ssDNA library was heated to 72°C for 1 minute and allowed to cool to room temperature. This ssDNA was distributed into several tubes. Approximately 10^6 bacteria cells were added to each DNA sample. The tubes were allowed to incubate for defined intervals (0-60 minutes) at 37°C. Following incubation, the samples were heated to 94°C for 2 minutes to denature the bacteria. 5 µL of each sample was added to 5 µL, 2X blue-orange dye and loaded on a 2% agarose gel with ethidium bromide staining for 200 V, 60 minutes. The concentration of DNA was quantitated and the gel was examined for smaller DNA fragments.

4.3.5 Mitochondria Isolation

Purified mitochondria was the kind gift of Edgar Arriaga (University of Minnesota, Minneapolis, MN). Briefly, DsRed2 labeled mitochondria was isolated from a 143B cell culture by the following method. Approximately 10^6 cells were centrifuged 600 x g for 5 minutes and the supernatant was removed. The cells were rinsed twice by suspending in mitochondria isolation buffer (210 mM mannitol, 70 mM sucrose, 5 mM HEPES, 5 mM EDTA, pH 7.4 adjusted by KOH) and centrifuging 600 x g for 5 minutes. 10 µL of 1 mg/mL digitonin was added and at least 75% cells were disrupted. The mitochondria was purified from other cell fragments by partitioning centrifugation. The cell debris and nuclei were separated using 600 x g for 10 minutes. The supernatant containing the mitochondria was collected and pelleted at 12,000 x g for 10 minutes.

This pellet was re-dissolved in the CE separation buffer. “Treated” mitochondria was prepared the same way except an additional incubation with 1 % trypsin overnight to remove the cytoskeleton and surface proteins.

4.3.6 Capillary Electrophoresis Selection

4.3.6.1 Escherichia coli and Bacillus subtilis

Selections were performed on a P\ACE MDQ capillary electrophoresis instrument with 32 Karat software (Beckman Coulter, Inc., Fullerton, CA). A 50.2 cm, 75 μm i.d., 360 μm o.d. bare fused silica capillary (Polymicro Technologies, Phoenix, AZ) was used for CE-SELEX selections. The capillary was regenerated daily by rinsing with the following series 0.5 M NaOH for 2 minutes, water for 5 minutes, and buffer for 5 minutes. Samples were injected on the capillary by applying 1 psi, 4 second pressure to the inlet of the capillary. The bound and free sequences were separated by applying a 30 kV voltage, normal polarity at 25°C. The separation of the bound and free fluorescently labeled library was monitored using LIF detection ($\lambda_{\text{ex}} = 488$, $\lambda_{\text{em}} = 520$). CE fractions migrating at least 30 seconds before the free DNA peak were collected into a sample vial containing 48 μL buffer. This vial was distributed evenly into 8 PCR tubes while the remaining unbound sequences on the capillary were washed to waste using a pressure rinse.

4.3.6.2 Mitochondria

Mitochondria selections were performed on a P\ACE MDQ capillary electrophoresis instrument (Beckman Coulter, Fullerton, CA). The separation was performed on a 50 μm i.d., 360 μm o.d. N-CHO coated capillary (Beckman Coulter,

Fullerton, CA). Pressure injections of 1 psi, 4 seconds introduced approximately 10^{13} sequences in the initial selection round. The bound and free fractions were separated under a 15 KV, reverse polarity voltage. The free aptamer peak was visible using LIF detection ($\lambda_{\text{ex}} = 488$, $\lambda_{\text{em}} = 520$). At least 30 seconds after the free library peak migrated off the capillary, the bound fraction was rinsed into a clean collection vial with pressure (50 psi, 10 min). This vial was distributed evenly into 8 PCR tubes.

4.3.7 Centrifugal Selection

B. subtilis selections were also performed using centrifugal partitioning to compare the results of a traditional based assay and the CE-SELEX procedure. In these experiments, approximately 10,000 cells were incubated with the 200 μM library at ambient temperature for 20 minutes. The cells were centrifuged 500 RCF for 10 minutes and the liquid containing the unbound sequences was removed. The bacteria pellet containing the bound sequences was re-dissolved in 1 mL buffer and the process was repeated 10 times. After the final wash step, the *B. subtilis* was dissolved in 48 μL buffer and distributed evenly into 8 PCR tubes for PCR amplification.

4.3.8 PCR Amplification

PCR reagent mix containing the following was added to each sample to a final volume of 100 μL : 1 mM of each dNTP, 1.5 μM primer 1 (5'-FAM\ AGC AGC ACA GAG GTC AGA TG), 1.5 μM primer 2 (5'-\biotin\ TTC AGC GTA GCA CGC ATA GG-3'), 0.15 U/ μL taq polymerase, and 7.5 mM MgCl_2 . The PCR cycling conditions were as follows for 18 cycles 94°C for 30 seconds, 53°C for 30 seconds, and 72°C for 30 seconds except the final extension was extended to 5 minutes. Careful controls were

performed with all of the PCR reagents except the DNA. The PCR was analyzed by taking aliquots and running on a 2% agarose gel with ethidium bromide staining.

4.3.9 Purification

PCR products were made single stranded by using a streptavidin-agarose column (Pierce Biotechnology, Rockford, IL). The column was equilibrated with streptavidin binding buffer (10 mM tris, 50 mM NaCl, and 1 mM EDTA, pH 7.5) by washing for 5 minutes. The PCR products and 500 μ L streptavidin binding buffer was added to the streptavidin beads and allowed to incubate for 30 minutes, shaking periodically. Extra PCR products and target fragments were discarded by washing the column with 500 μ L aliquots of streptavidin buffer for 30 minutes. 200 μ L of 0.5 M NaOH was added to the column and incubated at 37°C for 15 minutes to disrupt the hydrogen bonds between the dsDNA retained on the column by the strong biotin-streptavidin interaction. The ssDNA sequence was washed into a collection vial containing 200 μ L of 0.5 M acetic acid and 1 mL ice cold ethanol. The desired ssDNA was concentrated by ethanol precipitation and re dissolved into 30 μ L buffer. Further selection rounds were performed by mixing 10 μ L of this ssDNA pool and 1.1 μ L of the target.

4.3.10 *E. coli* and *B. subtilis* Binding Measurements

The progress of the bacteria selections was monitored using single color flow cytometry. Because of the large volume requirement for flow cytometry, only 2 concentrations of DNA were tested to determine % bound instead of dissociation constants. The DNA was heated to 72°C for 2 minutes and cooled to room temperature to allow the stable room temperature conformations to fold. The bacteria was added and

the samples were incubated at ambient temperature for 20 minutes. The resulting mixtures were analyzed using flow cytometry. Since the ssDNA was labeled ($\lambda_{em} = 488$ nm, $\lambda_{ex} = 520$ nm), signals that had the light scattering profile of the bacteria and the fluorescence of the DNA were counted as the bound fraction. Free fractions of the unbound bacteria were determined by bacteria scatter in the absence of a fluorescent signal. The flow cytometry parameters are described in Table 4.1.

Parameter	Channel	Voltage	Scale	Threshold
P1	Forward Scatter	E00	Linear	20
P2	Side Scatter	326	Linear	0
P3	Fluorescence in channel 1 (488 nm)	617	Log	52

Table 4.1: Flow cytometry parameters.

No gating was necessary and 10,000 events were counted on slow flow for each sample. To account for daily variations in cell growth and expression, all samples were compared to the affinity of the original library had for the bacterium.

4.3.11 Mitochondria Binding Measurements

Dissociation constants were estimated on a homebuilt CE instrument (Figure 4.2). A high voltage CZE1000R power supply was used to perform injections and separate the bound and free fractions. A 15 kV, 5 second electrokinetic injection was used to introduce the sample to the capillary. The samples were separated on a 30 cm, AAP coated capillary with 15 kV reverse polarity voltage. Post column detection was made possible via a single 488 nm argon ion laser line. Dual emissions were detected through PMTs which allowed the simultaneous detection of the sdRed2 labeled mitochondria (λ_{ex}

=543 nm, λ_{em} =560 nm) and carboxyfluorescein labeled DNA (λ_{ex} = 488 nm, λ_{em} = 520nm). The output was analyzed using a LabView program. The concentration of the mitochondria was held constant and titrated with increasing concentrations of ssDNA library. Bound fractions were determined by observing fluorescence in the DNA and mitochondria channels simultaneously.

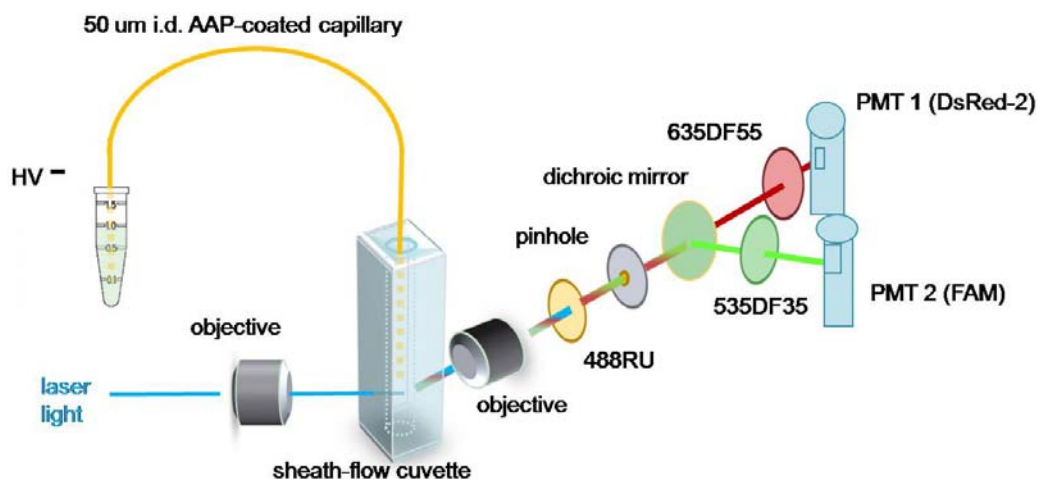


Figure 4.2: Schematic of homebuilt CE instrument with dual wavelength detection. Image adopted with permission from Vratislav Kostal and Edgar Arriaga, University of Minnesota.

4.4 Results and Discussion

4.4.1 Bacteria

Initial bacteria experiments involved testing the different properties of Gram negative bacteria *E. coli* and the Gram positive bacteria *B. subtilis*. Because of the myriad of features on the surface of bacteria, it was speculated that the initial library might have considerable non specific affinity for the bacteria. Initial dissociation constants were measured using flow cytometry (Figure 4.3). Although some initial affinity was observed (22 ± 300 nM and 1200 ± 1000 nM respectively) selections were

performed because we believed the affinity would become more specific for particular surface features after several selection rounds.

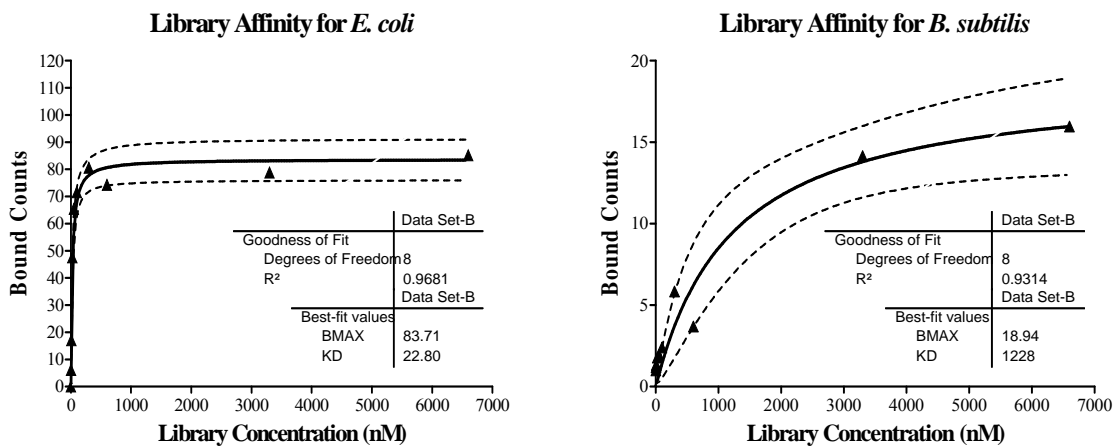


Figure 4.3: Dissociation constants of library for *E. coli* (left) and *B. subtilis* (right) measured using flow cytometry. A constant library concentration was titrated with increasing concentrations of cells. The bound fraction was identified by the detection of fluorescence where the cells scatter.

Bacteria often possess nuclease activity which would be detrimental to nucleic acid aptamers. To test the nuclease activity, an experiment was performed in which a constant concentration of ssDNA aptamer was incubated for various times with the bacteria. Nuclease activity would have been observed by degradation of the ssDNA over time. No nuclease activity was observed over the 2 hour time frame tested (Figure 4.4). This suggested that bacterial nucleases would not degrade the ssDNA over the time course of the selections and binding experiments.



Figure 4.4: Gel image describing nuclease activity of *E. coli* and *B. subtilis*. Lane 1-8 were *E. coli* controls, lane 8 and 18 were a 25 bp DNA ladder, and lane 9-17 were the *B. subtilis* controls. Length of incubation time increased from left to right.

It was believed it may be challenging to elute bacteria in a single, sharp peak because the variable surface features that contribute to the overall migration are may not be consistent within a sample. Initial *E. coli* studies were plagued by aggregates which caused capillary clogging and varying migration times on the electropherogram. Increasing the inner diameter of the capillary eliminated clogging problems. Further optimization involved sonicating cells during sample preparation to dissociate aggregates. Careful controls were performed to ensure that the cells were not disrupted by the sample preparation procedure. Although sonication drastically improved aggregate formation, we were unable to completely eliminate aggregates which caused sequences with affinity for aggregates to be included in collections (Figure 4.5). The library migrated at approximately 1.5-2 minutes yielding an adequate separation between the *E. coli* cells and the library.

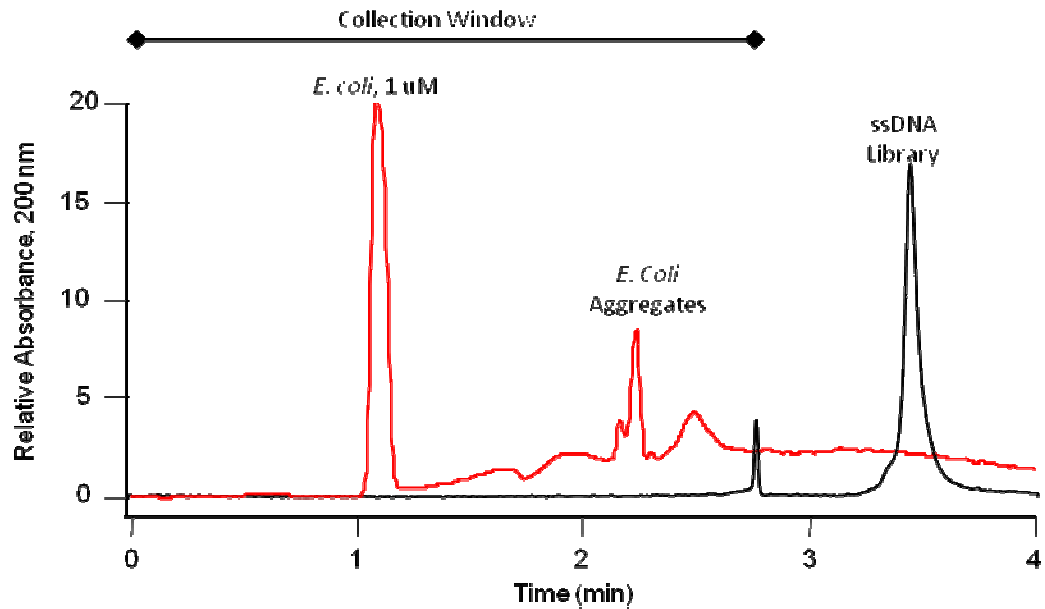


Figure 4.5: Electropherogram demonstrating separation of *E. coli*. Separation conditions: 50.2 cm, 75 μm i.d., 350 μm o.d. bare fused silica capillary, 1 psi, 4 second injection, 30 KV separation normal polarity. Cell aggregates could be observed which was minimized by sonicating the cells prior to separation.

Bacterial selections were performed for both the gram negative bacteria *E. coli* and the gram positive bacteria *B. subtilis*. Initial studies binding studies for the library and *B. subtilis* were carried out (Figure 4.6). The large shift to the right when library was added to *B. subtilis* indicated that a high fluorescent signal was present with the bacteria. This suggested that several sequences in the library had affinity for *B. subtilis*. Interestingly, this peak shift was not observed when selected library was added to the *B. subtilis* sample, indicating a decrease in affinity of the selected library for *B. subtilis* (Figure 4.6). Similar results were found for the *E. coli* selections (data not shown). This was not surprising since the surface of bacteria is constantly changing. The constantly changing surface of bacteria suggests two explanations for this observation. First, the surface features of the bacteria could have changed to adapt to environmental conditions.

Any changes to the bacteria surface may affect binding affinity of the ssDNA to the target. More likely the ssDNA still had affinity for surface features, but they were present at such a low abundance that binding could not be observed.

Since bacterial cells are constantly changing, aptamers must identify a feature on the surface of the bacteria that is consistent even in varying environmental conditions. If selective aptamers are desired, affinity for features that are conserved among other bacterial strains and species must also be avoided. This greatly decreases the possible binding sites on the bacteria. Having a minimal amount of binding sites makes binding characterization difficult. Since the cells are held at a constant concentration in these binding experiments, the number of binding sites is limited. No further increase in binding will be detected once all of the binding sites are already occupied. This trend has a greater impact when a low number of binding sites are present. In these cases, it is possible to have all binding sites occupied at a concentration that is below the limit of detection of the ligand, or within error of the measurement. Ultimately this can cause an inaccurate nonbinding result.

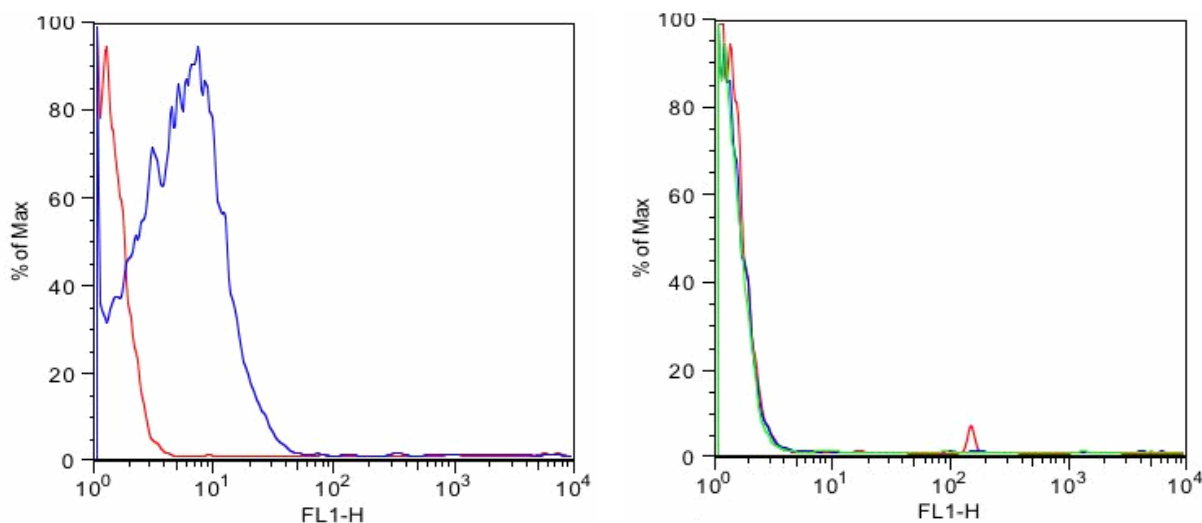


Figure 4.6: Histograms of *B. subtilis* binding using flow cytometry. Left: Bacteria control (red) and 25 nM library (blue). Right: After collection 7 bacteria control (red), 25 nM collection #7 (blue), and 25 nM library (green). The significant shift for the library indicated initial affinity that was not observed after collections.

In addition to CE-SELEX selections, traditional SELEX protocols were also used to identify aptamers for the bacterium *B. subtilis*. These experiments used centrifugation to separate the bound and free fraction. Because of previous results comparing SELEX and CE-SELEX (Chapter 1), it was expected that more rounds would be required for traditional selections as opposed to CE-SELEX. A total of 17 cycles were performed using the centrifugation method. Binding enrichment was determined by monitoring the fluorescent signal where a bacterium scatters using flow cytometry. An increase in fluorescent signal suggested that more ssDNA was binding to the bacteria. Consistent with the CE-SELEX results, the initial library demonstrated affinity which was not observed in later selection rounds when using centrifugation as the partitioning method. The lack of observed binding is attributed to ssDNA enrichment for species on the bacterial surface that are not very abundant.

4.4.2 Mitochondria

The separation between the mitochondria and the library was difficult to achieve because they are both negatively charged and the selections were performed in the absence of EOF (Figure 4.7). There were several spikes of mitochondria observed after the bulk peak in the untreated mitochondrial samples suggesting that surface proteins can play a critical role in the varying migration times of mitochondrial species in a sample of mitochondria.

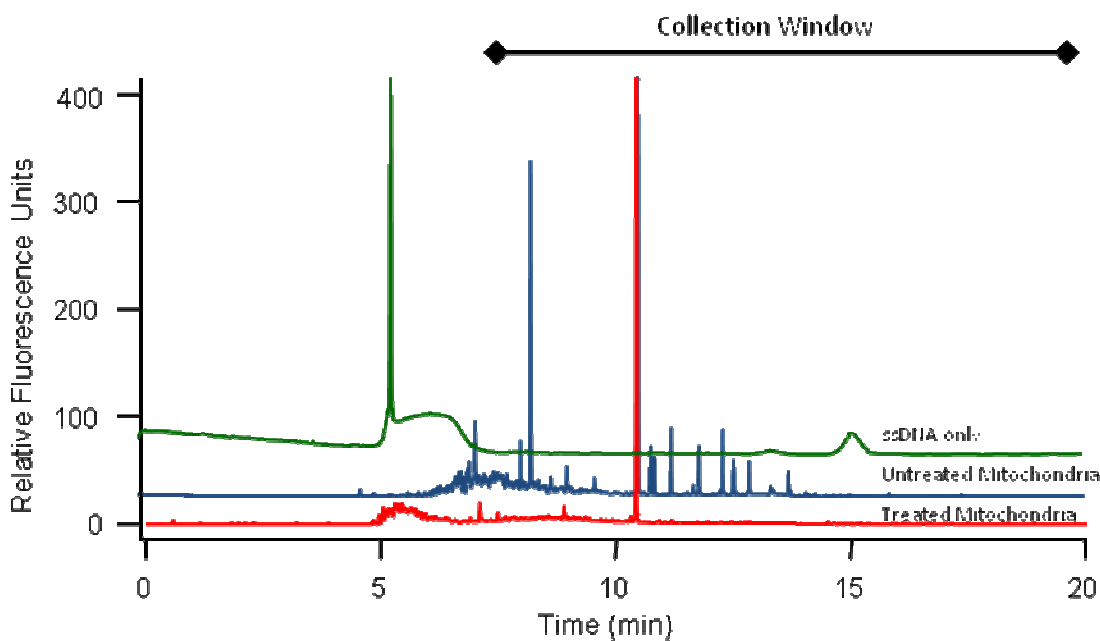


Figure 4.7: Electropherograms of mitochondria and DNA migration under selection conditions. Top trace is DNA only, middle trace is untreated mitochondria and bottom trace is trypsin treated mitochondria. Selection conditions: 50.2 cm 50 μm i.d., 360 μm o.d. N-CHO coated capillary, 15 kV separation reverse polarity, 1 psi, 4 second injection.

As expected, these spikes were not observed for the mitochondrion that was treated with trypsin demonstrating the effective removal of surface proteins. Untreated mitochondria was chosen for collections because of the separation between the later eluting mitochondrial peaks and the library. Additionally, these later eluting peaks must have

different surface properties than the mitochondria that migrates in the bulk peak which makes them of interest for further characterization. The major drawback in using untreated mitochondria for selections is the presence of surface proteins and cytoskeletal material which aptamers may bind to instead of the mitochondria itself. However, the benefits of aptamer identification for these mitochondria outweighed the specificity issues.

Initial experiments aimed to identify binding affinity of the initial library for mitochondria. These experiments were performed by incubating the mitochondria with increasing concentrations of ssDNA library. An obvious increase in ssDNA spikes was discovered as the concentration of library increased, suggesting that the library had some initial nonspecific affinity for the mitochondria (Figure 4.8). This was not surprising since the mitochondria sample was untreated, meaning there is a myriad of proteins on the surface which could act as binding sites. In addition, mitochondria samples are difficult to purify and may contain other components such as lysozymes and cytoskeletal material. The library may have affinity for any of these sample components.

To achieve a more accurate impression of what the ssDNA library has affinity for, the number of spikes in each channel was compared to the coincident spikes that appeared in both channels simultaneously (Table 4.2). Since only mitochondria that is intact and viable will contain the red dye, coincident spikes indicate library binding to intact mitochondria. Spikes only in the mitochondria channel represent unbound intact mitochondria. Spikes only in the ssDNA channel represent ssDNA that is bound to other

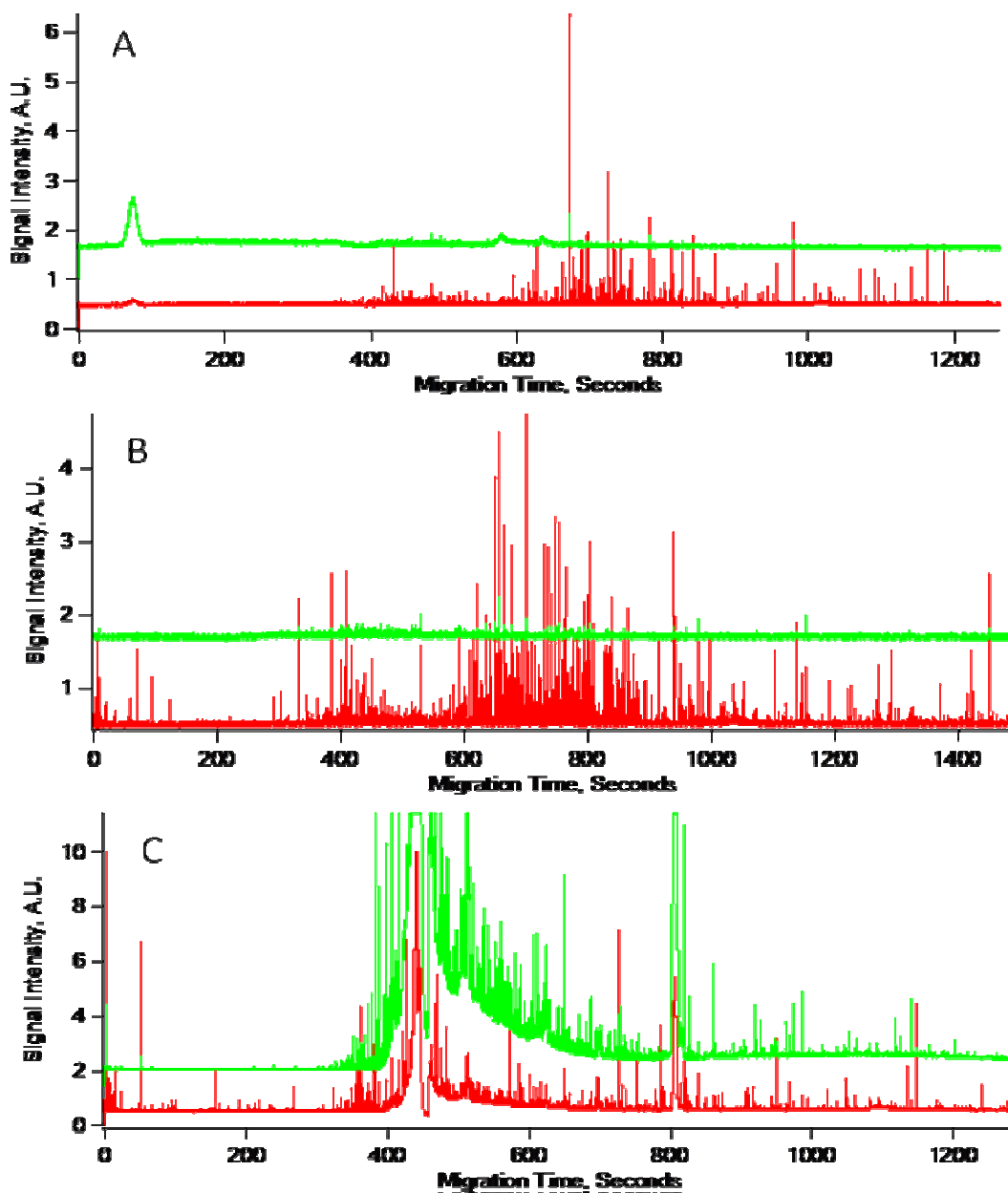


Figure 4.8: Example electropherograms of dual detection capillary electrophoresis. A) sample in the absence of DNA. B) sample with mitochondria and 2 nM DNA. C) sample with mitochondria and 20 nM DNA. Top (green) trace is the ssDNA and the bottom trace (red) is the mitochondria. Spikes that appeared in both channels were attributed to bound DNA. CE conditions: 15 kV reverse polarity separation, 15 kV, 5 second electrokinetic injection, 30 cm AAP coated capillary. Post column detection with dual PMT boxes for mitochondria ($\lambda_{\text{ex}} = 543 \text{ nm}$, $\lambda_{\text{em}} = 560 \text{ nm}$) and carboxyfluorescein labeled DNA ($\lambda_{\text{ex}} = 488 \text{ nm}$, $\lambda_{\text{em}} = 520 \text{ nm}$).

components in the sample which may include mitochondrial fragments, cytoskeletal material, and lysozymes. Table 4.2 indicates that the ssDNA has affinity for the mitochondria itself and for other components in the sample.

These preliminary experiments suggest that, it is necessary to not only look at enrichment in binding, but also what component the aptamers are actually binding to. It is feasible that increased affinity for the mitochondria as a whole will not be observed. Instead, binding may become more selective toward a specific sample component. We did not try these experiments; however, they would have been performed by centrifuging the mitochondria samples into several fractions containing different sample components and determining the affinity of the DNA for each fraction.

Sample	Total Mitochondria Counts	Total DNA Counts	Coincident Events
Mitochondria Only	582	45	21
Mito + 2 nM DNA library	1555	168	101
Mito + 20 nM DNA library	1489	3119	623

Table 4.2: Number of events from each channel and coincident events.

4.5 Concluding Remarks

Although detection of small, pure samples such as proteins has become much more sensitive and accurate, detection of large, whole molecules such as bacteria and mitochondria remains challenging. Aptamers are known to be highly selective for their targets. Therefore it can be difficult to identify an aptamer that has affinity for a specific species of bacteria or mitochondria unless it has affinity for a specific component that is unique to the species of interest. Our data suggests that an overall increase in affinity was not found for these large targets despite the number of cycles performed. However,

our data indicates that binding may have become more selective for specific features on the molecule or components in the sample. These aptamers may be extremely useful for the identification of cellular or subcellular components that make bacterial and mitochondrial species unique. These components may be used to accurately and specifically identify these large molecules in the future.

Chapter 5: Significance and Future Directions

5.1 Summary of Research

Several factors make an analytical technique successful. Two major factors for the widespread adaptation of a viable method are time and efficiency. Although SELEX technology has been around since 1990, the technique did not flourish until newer protocols that minimized laborious procedures and increased the performance of aptamers were introduced. Among these modifications were techniques utilizing different partitioning methods to separate bound from free sequences. These methods included filter binding assays, panning separations, and magnets. Although these methods decreased the time requirement of the process, several cycles (8-12) were still required. In addition, negative selections to eliminate sequences binding to linker molecules and filters biased the output. It wasn't until CE-SELEX was introduced with capillary electrophoresis as the partitioning method that aptamers could efficiently be obtained without bias.

The work in Chapter 2 and 3 described the use of capillary electrophoresis-SELEX as a selection protocol for aptamers. As described in these chapters CE-SELEX has alleviated many of the limitations that plagued traditional SELEX selections including the efficiency and time requirement of the process. Fewer cycles were required while still conserving the integrity of the process. In fact, 100% of the aptamers in later CE-SELEX selection rounds demonstrated considerable affinity for the target even though there was no sequence or structure conservation observed. Despite the tight binding (180-500 pM) observed for our HIVRT aptamers, no inhibition was

demonstrated. It is likely that the aptamers bind a region separate from the active site on the enzyme; though experiments to identify this location were not performed.

The introduction of CE-SELEX has spawned widespread interest in aptamer technologies. Since aptamers have become easier to isolate, aptamer technologies have branched into a variety of areas of analytical chemistry. These aptamers have found success for both diagnostic and therapeutic applications. Despite prevalent interest in aptamers, little work has been done on aptamers of non-uniform samples. Although there is a great analytical need for aptamers that can be selected for targets that adapt with the environment or cannot be purified, this challenge has yet to be overcome.

Chapter 4 described CE-SELEX selections of non-uniform targets.

Unfortunately, aptamer isolation of non uniform analytes still remains challenging. After several cycles of bacteria and mitochondria targets, no increase in affinity was observed. A likely explanation is that each CE-SELEX cycle refined the ssDNA pool to bind to specific sample components or consistent surface features on the target.

5.2 Future Directions

5.2.1 Aptamers for Specific Binding Regions

As aptamers enter the world of therapeutics, it is becoming important to drive selections toward specific binding regions. There are two main ways this can be done (Figure 5.1). In the first method, a separate molecule can shield the entire target except the active region. Positive selections can then be performed to selectively identify aptamers that bind the active region. After selections, the shielding molecule can be

removed. This method is more difficult because aptamers that have non specific affinity for previously shielded regions on the target may be retained if they also have affinity for the active region. Furthermore, the shielding molecule must be carefully selected so that the library does not have non specific affinity for it which would result in conservation of aptamers that do not bind the region of interest. Shielding molecules can be selected by first identifying molecules that have shield the desired region without compromising the binding region. Molecules that promote nonspecific ssDNA binding such as positively charged molecules should be avoided. Finally, the affinity for proposed molecules can be determined. Molecules with little to no affinity for the library can be used.

In the second method, a positive selection can be performed for the target itself which will result in collection of *all* aptamers that bind the target. The selection can be refined for aptamers that bind a specific region on the target by performing a negative selection (Section 5.2.2). The negative selection is performed against the target bound to some other molecule or a molecule similar to the original target, but without the binding region of interest. In negative selections, aptamers that bind the target-molecule complex or modified target are discarded. Nonbinding sequences are used in the next selection. The result is an aptamer that binds the target only in the specific region of interest. This is the proposed method of our experiments.

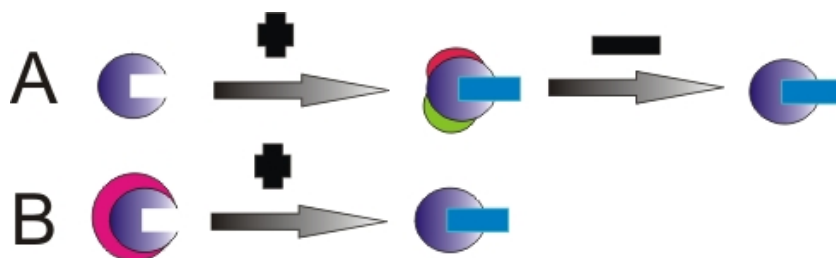


Figure 5.1: Selection procedure for driving the selection toward a binding pocket. A) Overall outcome of first doing a positive selection to obtain all aptamers and then do a negative selection to eliminate sequences that do not bind to the desired location. B) Selection schematic of blocking all of the regions on the target except the desired binding region.

5.2.2 Negative Selections

Negative selections are performed in a similar fashion to positive selections (Figure 5.2). In this case, the target-molecule complex or modified target molecule will be incubated with the library. This effectively shields the active region of interest. This complex is incubated with the refined library from a positive selection. The bound and free fractions are separated using capillary electrophoresis. Since the goal is to eliminate sequences that bind regions other than the active site, the unbound fraction in these separations will be collected. This fraction is PCR amplified, made single stranded, and purified. The result is a refined library which has affinity for only the active site of the protein. Two notable considerations when performing negative selections is that 1) the library should be a very low concentration with respect to the target so that even sequences with moderate affinity for the non-desired target are discarded 2) negative selections should be performed in conjunction with positive selections, usually every other selection.

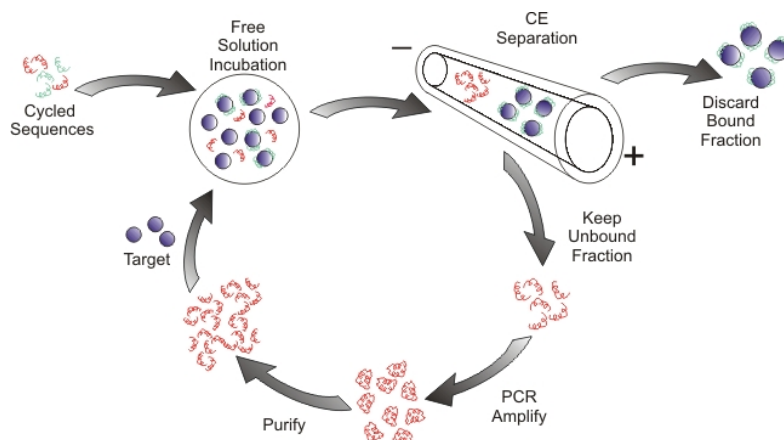


Figure 5.2: Schematic of a negative selection: A refined library from a positive selection is incubated with the modified target that you do not desire affinity to. The bound and free fractions are separated using capillary electrophoresis. The unbound fraction is collected, PCR amplified, made single stranded, and purified. The result is a refined library that can be used in the next positive selection.

5.2.3 The Model

Capsid is an HIV replication protein. The role of capsid in HIV infection has been described in a number of reviews²²¹⁻²²³. Briefly, during HIV replication the HIV protease cleaves Gag into the mature p17 matrix, p24 capsid, p7 nucleocapsid, and p6 proteins. All of these play a role in HIV replication. The capsid protein specifically makes up the conical core by condensing to form a shell around the viral RNA/nucleocapsid complex. This core plays an important role in the infectivity of HIV.

Structural analysis using NMR spectroscopy²²⁴ and x-ray crystallography²²⁵ have provided detailed structural information of the N and C terminal domains of capsid. These studies in conjunction with extensive mutational analysis suggest that the C terminal domain of capsid is largely responsible for viral packaging and assembly. In fact, small point mutations in the C terminal domain virtually eliminate viral assembly altogether²²⁶.

Another feature of the capsid protein is the major homology region, a highly conserved stretch of 20 residues found in all retroviruses^{84, 227-229}. It is believed that this region plays a critical role in protein-protein interactions²³⁰ such as capsid-capsid dimerization and capsid-lys RS interactions. Disruption of these interactions significantly affects viral pathogenicity and replication.

The role of capsid in HIV replication and infectivity makes it a major pharmacological target for the treatment of HIV/AIDS. Previous work demonstrated that disrupting several regions of capsid halts viral replication. One of these regions is the capsid-[lys-RS] interaction that occurs between viral capsid and human Lys-RS. Upsetting this interaction may lead to highly effective HIV therapies. Since aptamers have gained increased interest for these types of therapeutic applications, they would be an ideal mode of disruption of this complex. However, the aptamer must specifically bind to capsid in the region that binds Lys-RS in order to be effective.

5.2.4 Preliminary Results

Experimental Conditions

5.2.4.1 Materials

Unless otherwise noted, all samples and buffers were prepared in deionized water obtained from a Milli-Q water purification system (Millipore Corp., Bedford, MA). The ssDNA library consisted of a 40 base random region flanked by two 20 base primer regions (5'-AGC AGC ACA GAG GTC AGA TG (40 random bases) TTC AGC GTA GCA CGC ATA GG-3'). All DNA libraries, PCR primers, and aptamers were obtained from Integrated DNA Technologies, Inc (Coralville, IA). Capsid was the kind gift of Karin Musier-Forsyth (Ohio State University, Columbus, OH). All other chemicals were

obtained from Sigma-Aldrich (St. Louis, MO) and were the best grade available. CE separation buffer consisted of 25 mM tris, 192 mM glycine, and 5 mM KH_2PO_4 (TGK) at pH 8.3.

5.2.4.2 Capillary Electrophoresis Selection

Prior to the selection the library was diluted in separation buffer, heated to 72°C and cooled to room temperature. Capsid was added to the library yielding a final concentration of 2.5 mM ssDNA library and 10 nM Capsid. This mixture was incubated at room temperature for 20 minutes prior to CE selection.

Capillary electrophoresis separations were performed on a P/ACE MDQ capillary electrophoresis system (Beckman Coulter, Inc., Fullerton, CA). A 50.2 cm long, 50 μm inner diameter, 360 μm outer diameter uncoated fused silica separation capillary (Polymicro Technologies, Phoenix, AZ) was used. Samples were injected using 1 psi pressure for 5 seconds. The separation was performed under the following conditions: 30 kV voltage (normal polarity), UV detection at 254 nm, and ambient temperature. All sequences migrating more than 30 seconds earlier than the unbound sequences were collected into 48 μL of separation buffer at the capillary outlet. The exact time that the unbound sequences would reach the outlet of the capillary were calculated for each separation since detection takes place 10 cm from the end of the capillary (see Chapter 1). After the bound fraction migrated off the capillary, the separation voltage was turned off and the unbound sequences remaining on the capillary were flushed to waste using a high pressure rinse.

5.2.4.3 PCR Amplification

The 48 μL fraction containing the bound sequences obtained using CE selection were distributed evenly into 8 PCR tubes. PCR buffer was added to these fractions so

that the final concentrations were as follows: 1.5 μM forward primer (5'-AGC AGC ACA GAG GTC AGA TG-3'), 1.5 μM reverse primer (5'-/biotin/-TTC ACG GTA GCA CGC ATA GG-3'), 0.15 unit/ μL taq polymerase, and 7.5 mM MgCl_2 . The final volume in each PCR tube was 100 μL . The above samples and a control with no added DNA were placed in a thermal cycler and heated to 94°C for 5 minutes to ensure complete denaturation and dissociation of bound sequences from HIVRT. A total of 18 cycles of denaturing, annealing, and extension were then carried out for 30 seconds at 94°C, 30 seconds at 53°C, and 20 seconds at 72°C, respectively. At completion, a final 5 minute extension was carried out at 72°C. The presence of DNA following PCR was confirmed by electrophoresis on a 2% agarose gel (60 minutes at 200 V with ethidium bromide staining).

5.2.4.4 Purification

The double stranded PCR products were purified and made single stranded using a streptavidin agarose column (Pierce Biotechnology, Rockford, IL). The column was washed with streptavidin binding buffer (10 mM tris, 50 mM NaCl, and 1 mM EDTA, pH 7.5) for 5 minutes. A 500 μL sample of streptavidin buffer was then added to the column with the amplified PCR products and allowed to incubate with periodic shaking for 30 minutes at room temperature. The column was then rinsed with streptavidin binding buffer for 15 minutes, to remove extra PCR components. 200 μL of 0.15 M NaOH was added to the column at 37°C to disrupt the hydrogen bonds between the DNA sequences. The eluted ssDNA was concentrated by ethanol precipitation and redissolved in 20 μL of separation buffer, providing a new nucleic acid pool for further rounds of CE selection. To perform subsequent rounds of selection, 1.1 μL of capsid was added to 10 μL of the refined ssDNA pool to give a solution containing 10 nM capsid.

5.2.4.5 Affinity Measurements

Selection progress was determined by calculating % bound at 22 μM after each collection. The ssDNA sequences were labeled with a 5',6'-carboxyfluorescein label to facilitate these measurements. To label the ssDNA, a 0.5 μL aliquot of the ssDNA pool was PCR amplified using the conditions described above for eight cycles in the presence of 5',6-carboxyfluorescein labeled forward primer. Sequences were purified and made single stranded using the procedure described above. An aliquot of ssDNA was analyzed using CE in the absence of capsid and in the presence of 22 μM capsid. CE conditions were the same as those used for selection except that laser induced fluorescence (LIF) was used for detection ($\lambda_{\text{ex}} = 488 \text{ nm}$, $\lambda_{\text{em}} = 520 \text{ nm}$). % bound was determined by the following equation:

$$\frac{I_B}{I_o} \times 100 \quad \text{Equation 5.1}$$

Where I_B is the peak intensity of the unbound ssDNA in the presence of 22 M capsid, and I_o is the peak intensity in the absence of capsid.

5.2.5 Preliminary Results and Discussion

Initial experiments involved optimizing separation conditions to achieve a separation between the target and the free ssDNA. This was determined by finding the mobility of the capsid and ssDNA separately. The migration time of capsid was confirmed by injecting different volumes on the capillary. In most cases the aptamer-target complex will migrate between the free target and free aptamer (see Chapter 1). Under our conditions, there is approximately a 2 minute separation, leaving ample time for the collection (Figure 5.3).

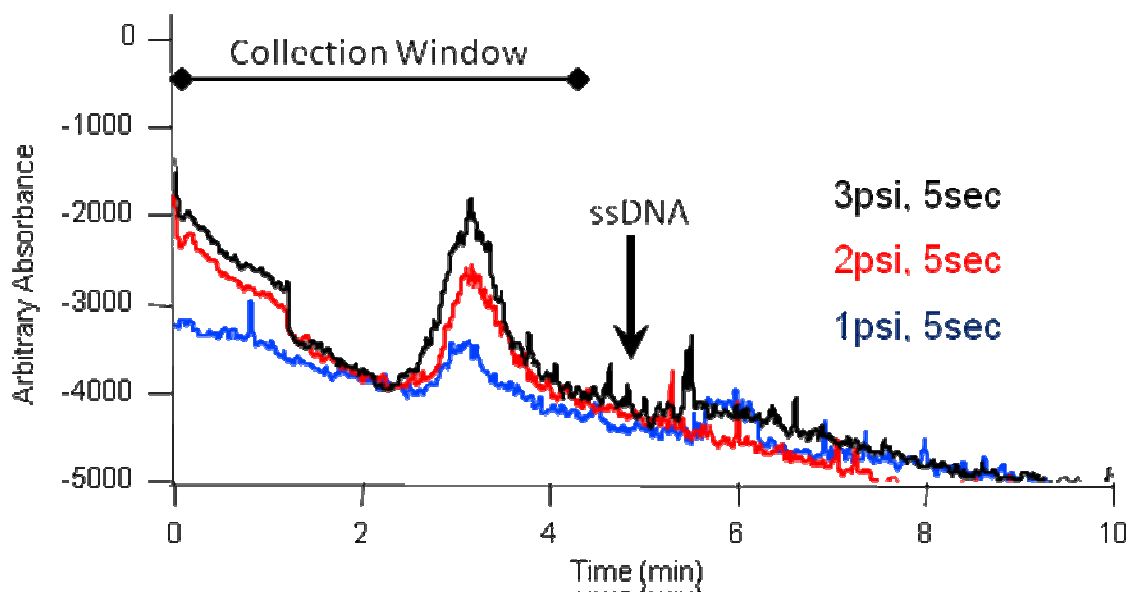


Figure 5.3: Migration time of 22 μm capsid confirmed by varying the injection volume. (top) 3 psi, 5 sec, (middle) 2 psi, 5 sec, (bottom) 1 psi, 5 sec. Selection conditions: TGK separation buffer, 50.2 cm, 50 μm i.d., 360 μm o.d. bare fused silica capillary, 30 KV separation, 200 nm UV detection. The ssDNA library migrates at approximately 5 minutes indicated by the arrow.

The affinity after each cycle was monitored by calculating the % bound at 22 μM .

Full dissociation constants could not be measured due to limited capsid concentrations.

After 3 selection rounds, 50% of the sequences were bound at 22 μM . Surprisingly, no affinity was observed in subsequent rounds (Table 5.1).

Cycle	% bound at 22 μM
Lib	0
1	35
2	20
3	50
4-10	0

Table 5.1: Affinity of library for capsid after each collection cycle. Affinity measured by % bound at 22 μM . CE conditions: 30 kV normal polarity separation, 1 psi, 4 sec injection, 50 μm i.d., 360 μm o.d., 50.2 cm capillary, TGK separation buffer, 1/5 PBS incubation buffer.

There are several explanations for the observed decrease in affinity. Capsid dimerization is the driving force of virus assembly²³¹⁻²³⁴. This happens at a concentration of $18 \pm 1 \mu\text{M}$ ²³⁵. This means during affinity determinations, the majority of capsid is dimerized. However, since selections are performed with minimal concentrations of capsid, aptamers are selected for capsid in the monomeric form. In earlier rounds, affinity could apparently increase since the pool is not yet refined and may contain sequences that have affinity for many parts of the protein. However, during later rounds, the aptamers may become more selective for a specific region on capsid, presumably the region involved in dimerization. If capsid has more affinity for itself than the aptamer, affinity will not be observed.

5.3 Future Experiments

5.3.1 Further Capsid Experiments

Data suggests that dimerization of capsid is retarded at basic pH²³⁶. Although this can indicate that the capsid does not fold in its native form in some buffers, it raises the possibility that buffers can be used to control capsid dimerization. Further experiments should be carried out in a buffer in which capsid dimerization is significantly retarded, assuming capsid still folds in its native state. Other experiments could include kinetic studies to determine if the aptamers disrupt capsid dimerization in addition to the previously planned experiment to disrupt the interaction between capsid and Lys-RS.

5.3.2 Selection Optimization

Aptamer technology has been around since 1990. Since then, modifications of the partitioning method for aptamer selection have been studied extensively. Although

aptamers are becoming easier to obtain and new processes are increasingly efficient; selection protocols have yet to be optimized. This is likely because the characterization process is very time consuming and labor intensive. However, optimization of selections will further increase efficiency and provide more specific parameters for starting selections.

5.3.2.1 Library length

The length of the random region in current aptamer selections is between 40-80 bases long². This number is completely arbitrary. It was previously thought that longer libraries would be beneficial because they increase the randomization of the pool. Longer random regions also increase the positions along the library at which structural motifs can be located. However, longer libraries are difficult to synthesize, and obtaining them with high purity can be costly. In addition, the large mass requirements of creating such libraries is unrealistic. This poses a question of the minimal random region on a library. Future experiments aim to identify the optimal library length. These experiments would involve performing selections with everything constant except the library length and the evaluating each cycle for enrichment efficiency and the end result for final aptamer affinity/specificity.

5.3.2.2 Library Concentration

It was previously thought that the concentration of the library should be large with respect to the target. Higher concentrations increase the number of sequences in the pool as well as competition for binding sites on the surface of the target. Traditional selections introduced approximately 10^{15} sequences into the initial starting pool. This is greatly

reduced during CE-SELEX selections (10^{13}) due to resolution limited injections⁴²⁻⁴⁴. Despite this limitation, comparable, and sometimes even better aptamers are identified using CE-SELEX. Since higher concentrations present separation challenges and require expensive mass production, performing selections using lower concentrations are perceivably beneficial. The concentration of the library will probably not affect the efficiency of the process, since after the first cycle the same amount of aptamers is collected each time (defined by the concentration of the target and how many binding sequence are present). However, larger libraries may effect the highest affinity aptamer possible in the final collection rounds.

5.3.2.3 Buffer Selection

Buffers for aptamer selection are usually chosen based on compatibility with the final desired application of the aptamer. Final aptamer characterization suggests that buffer selection plays a critical role in DNA performance. It is no far stretch that it must also play a role in identifying aptamers. Some buffer additives are known to promote certain kinds of folding. For example, magnesium and potassium are known to promote and stabilize g-quartet formations²³⁷. Without these additives it is unlikely these structures will be formed. In addition to buffer components, the ionic strength of buffers should be considered. Salt is known to promote and stabilize DNA folding^{238, 239}. However, largely ionic buffers will likely shield electrostatic DNA-target interactions, decreasing overall affinity.

Buffer characterization is a little more obscure. Selections for the same target should first be performed in the presence and absence of buffer components that are

known to aid special folding. In addition, selections should be performed in buffers with the same components, but differing ionic strengths to determine the role on buffer ions with overall aptamer identification.

5.3.2.4 Library Modifications

In many cases, aptamers are modified with fluorescent or radioactive tags to provide more sensitive detection. Other modifications include the addition of non natural bases or the molecules such as carbohydrates which increase solubility and the half life of DNA *in vivo*^{240, 241}. These modifications tend to be large in comparison to a DNA base, meaning it is possible their addition could cause the aptamer to fold into a different structure than that of the original selection. This is especially true for shorter sequences. Identifying appropriate tags that perform the desired function while conserving the integrity of the original aptamer will dramatically improve the development of aptamers into therapeutics and diagnostic agents²⁴².

5.4 Conclusions

As the therapeutic and diagnostic potential of aptamers is realized, they are becoming increasingly popular for a number of applications. Significant progress has been made to make the selection process more efficient, reducing the time requirement and cost associated with aptamer identification. As the process becomes more standardized for specific applications, aptamer technology will continue to grow exponentially. Undoubtedly aptamers will make their way into therapeutics and diagnostics for years to come.

References

- (1) Ellington, A. D.; Szostak, J. W. *Nature* **1990**, *346*, 818-822.
- (2) Kulbachinskiy, A. V. *Biochemistry* **2006**, *72*, 1505-1518.
- (3) Conrad, R. C.; Giver, L.; Tian, Y.; Ellington, A. D. *Methods on Enzymology* **1996**, *267*, 336-367.
- (4) Patel, D. J. *Current Opinion in Chemical Biology* **1997**, *1*, 32-46.
- (5) Eaton, B. E.; Gold, L.; Zichi, D. A. *Chemical Biology* **1995**, *2*, 633-638.
- (6) Kruger, K.; Grabowski, P. J.; Zaung, A. J.; Sands, J.; Gottschling, D. E.; Cech, T. R. *Cell* **1982**, *31*, 147-157.
- (7) al, J. M. e. *EMBO* **1985**, *4*, 1609-1614.
- (8) Napoli, C.; Lemieux, C.; Jorgensen, R. *Plant Cell* **1990**, *2*, 279.
- (9) Brenner, S. A.; Burgstaller, P.; Battersby, T. R.; Jurczyk, S. *Did the RNA World Exploit and Expanded Genetic Alphabet?*, Second ed.; Cold Spring Harbor Press, 1999.
- (10) Spiegelman, S. Q. *Reviews in Biophysics* **1971**, *4*, 213-253.
- (11) Klussman, S. In *The Aptamer Handbook*; Klussman, S., Ed.; Wiley VCH, 2005.
- (12) Kruger, K.; Grabowski, P. J.; Zaung, A. J.; Sands, J.; Gottschling, D. E.; Cech, T. R. *Cell* **1982**, *31*, 147-157.
- (13) Gardiner, K.; Pace, N. R. *Journal of Biological Chemistry* **1980**, *255*, 7507-7509.
- (14) Carothers, J. M.; Szostak, J. W. In *The Aptamer Handbook*; Klussman, S., Ed.; Wiley-VCH, 2005, pp 3-28.
- (15) Been, M. D.; Cech, T. R. *Science* **1988**, *238*, 1412-1416.
- (16) Waugh, D. S.; Green, C. J.; Pace, N. R. *Science* **1989**, *244*, 1569-1571.
- (17) Tuerk, C.; Gold, L. *Science* **1990**, *249*, 505-510.
- (18) Joyce, G. F. *Gene* **1989**, *82*, 83-87.
- (19) Bunka, D. H. J.; Stockley, P. G. *National Reviews in Microbiology* **2006**, *4*.
- (20) Klug, S. J.; Famulok, M. *Molecular Biology Reports* **1994**, *20*, 97-107.
- (21) Famulok, M.; Mayer, G.; Blind, M. *Accounts of Chemical Research* **2000**, *33*, 591-599.
- (22) Osborne, S. E.; Ellington, A. D. *Chemical Reviews* **1997**, *97*, 349-370.
- (23) Forst, C. V. *Journal of Biotechnology* **1998**, *64*, 101-118.
- (24) Sekiya, S.; Noda, K.; Mishikawa, F.; Nishikawa, T.; Kumar, P.; Nishikawa, S. *Journal of Biological Chemistry* **2006**, *139*, 383-390.
- (25) Gopinath, S.; Misono, T.; Kawasaki, K.; Mizuno, T.; Imai, M.; Odagiri, T.; Kumar, P. *Journal of General Virology* **2006**, *87*, 479-487.
- (26) Gopinath, S.; Yuriko, S.; Kazunori, K.; Kumar, P. *Journal of Biochemistry* **2006**, *139*, 837-846.
- (27) Homann, M.; Goring, H. U. *Nucleic Acids Research* **1999**, *27*, 2006-2014.
- (28) Zhang, F.; Anderson, D. *The Journal of biological chemistry* **1998**, *273*, 2947-2953.
- (29) Homann, M.; Goring, U. *Nucleic Acids Research* **1999**, *27*, 2006-2014.
- (30) Blank, M.; Weinschenk, T.; Priemer, M.; Schluesener, H. *Journal of Biological Chemistry* **2001**, *276*, 16464-16468.
- (31) Misono, T.; Kumar, P. *Analytical Biochemistry* **2005**, *342*, 312-317.
- (32) Liang, X.; Nazarenus, T. J.; Stone, J. M. *Biochemistry* **2008**, *47*, 3645-3653.
- (33) Smith, D.; Kirschenheuter, G. P.; Charlton, J.; Guidot, D. M.; Repine, J. E. *Journal of Chemical Biology* **1995**, *2*, 741-750.

- (34) Smith, D.; Kirschenheuter, G.; Charlton, J.; Guidot, D.; Repine, J. *Chemical Biology* **1995**, *2*, 741-750.
- (35) Goodman, S. D.; Velten, N. J.; Gao, Q.; Robinson, S.; Segall, A. M. *Journal of Bacteriology* **1999**, *181*, 3246-3255.
- (36) Bruno, J. G.; Kiel, J. L. *Biosensors and Bioelectronics* **1999**, *14*, 457-464.
- (37) Nieuwlandt, D.; Wecker, M.; Gold, L. *Biochemistry* **1995**, *34*, 5651-5659.
- (38) Stoltenburg, R.; Reinemann, C.; Strehlitz, B. *Analytical and Bioanalytical Chemistry* **2005**, *383*, 83-91.
- (39) Dobbelstein, M.; Shenk, T. *Journal of Virology* **1995**, *69*, 8027-8034.
- (40) Weiss, S.; Proske, D.; Neumann, M.; Groschup, M.; Kretzschmar, H.; Famulok, M.; Winnacker, E. *Journal of Virology* **1997**, *71*, 8790-8797.
- (41) Takagaki, Y.; Manley, J. L. *Molecular and Cellular Biology* **1997**, *17*, 3907-3914.
- (42) Mendonsa, S. D.; Bowser, M. T. *J. Amer. Chem. Soc.* **2004**, *126*, 20-21.
- (43) Mendonsa, S. D.; Bowser, M. T. *Analytical Chemistry* **2004**, *76*, 5387-5392.
- (44) Mendonsa, S. D.; Bowser, M. T. *Journal of the American Chemical Society* **2005**, *127*, 9382-9383.
- (45) Mosing, R. K.; Mendonsa, S. D.; Bowser, M. T. *Analytical Chemistry* **2005**, *77*, 6107-6112.
- (46) Eulberg, D.; Klussman, S. *ChemBioChem Reviews* **2003**, *4*, 979-983.
- (47) Jensen, K. B.; Atkinson, B. L.; Willis, M. C.; Koch, T. H.; Gold, L. *Proceedings of the National Academy of Sciences* **1995**, 12220-12224.
- (48) Michaelis, L. *Biochemische Zeitschrift* **1909**, *17*, 231-234.
- (49) Skoog, D. A.; Holler, F. J.; Nieman, T. A. In *Principles of Instrumental Analysis*; Saunders College Publishing, 1998, pp 778-795.
- (50) Weinberger, R. *Practicle Capillary Electrophoresis*, Second ed.; Academic Press, 2000.
- (51) Landers, J. P. In *Capillary and Microchip Electrophoresis and Associated Microtechniques*; Landers, J. P., Ed.; CRC press, 2008, pp 3-75.
- (52) Helmholtz, H. Z. *Ann. Phys. Chem.* **1879**, *7*, 337.
- (53) Ghosal, S. *journal of Fluid Mechanics* **2003**, *491*, 285-300.
- (54) Watzig, H.; Kaupp, S.; Graf, M. *Trends in Analytical Chemistry* **2003**, *22*, 588-604.
- (55) Buchanan, D. D.; Jameson, E. E.; Perlette, J.; Malik, A.; Kennedy, R. T. *Electrophoresis* **2003**, *24*, 1375-1382.
- (56) Chu, Y.-H.; Avila, L.; Biebuyck, H. A.; Whitesides, G. M. *Journal of the American Chemical Society* **1992**, *35*, 2915-2917.
- (57) Nielsen, R. G.; Rickard, E. C.; Santa, P. F.; Sharknas, D. A.; Sittampalam, G. S. *Journal of Chromatography A* **1991**, *539*, 177-185.
- (58) Kraak, J. C.; Busch, S.; Poppe, H. *Journal of Chromatography A* **1992**, *608*, 257-264.
- (59) Avila, L.; Chu, Y. H.; Blossey, E. C.; Whitesides, G. M. *Journal of Medicinal Chemistry* **1993**, *36*, 126-133.
- (60) Zhang, H.; Li, X.-F.; le, X. C. *Journal of the American Chemical Society* **2008**, *130*, 34-35.
- (61) Heegaard, N. H. H.; Kennedy, R. T. *Electrophoresis* **1999**, *20*, 3122-3133.
- (62) Heegaard, N. H. H.; Kennedy, R. T. *Journal of Chromatography B* **2002**, *768*, 93-103.
- (63) Monning, C. A.; Kennedy, R. T. *Analytical Chemistry* **1994**, *66*, 280R-314R.
- (64) Heegaard, N. H.; Robey, F. A. *American Laboratory* **1994**, *26*, 28T-28X.
- (65) Haupt, K.; Roy, F.; Vijayalakshmi, M. A. *Analytical Biochemistry* **1996**, *234*, 149-154.
- (66) Rasmussen, B. W.; Bjerrum, M. J. *Journal of Inorganic Biochemistry* **2003**, *95*, 113-123.

- (67) Muncha, P.; Szyk, A.; Rekowski, P.; Guenther, R.; Agris, F. *RNA* **2002**, *8*, 298-704.
- (68) Foulds, G. J.; Eitzkorn, F. A. *Nucleic Acids Research* **1998**, *26*, 4304-4305.
- (69) Foulds, G. J.; Eitzkorn, F. A. *Journal of Chromatography A* **1999**, *862*, 231-236.
- (70) Mucha, P.; Szyk, A.; rekowski, P.; Barciszewski, J. *Journal of Chromatography A* **2002**, *968*, 211-220.
- (71) Kennedy, R. T. *Analytica Chimica Acta* **1999**, *400*, 163-180.
- (72) Cho, E. J.; Rajendran, M.; Ellington, A. D. *Topics in Fluorescence Spectroscopy* **2005**, *10*, 127-155.
- (73) German, I.; Buchanan, D. D.; Kennedy, R. T. *Analytical Chemistry* **1998**, *70*.
- (74) Haes, A. J.; Giordano, B. C.; Collins, G. E. *Analytical Chemistry* **2006**, *78*, 3758-3764.
- (75) Pavski, V.; Le, X. C. *Analytical Chemistry* **2001**, *73*, 6070-6076.
- (76) Zhang, H.; Wang, Z.; Li, X. F.; Le, X. C. *Angew. Chem. Int. Ed.* **2006**, *45*, 1576-1580.
- (77) Okhonin, V.; Krylova, S. M.; Krylov, S. *Analytical Chemistry* **2004**, *76*.
- (78) Petrenko, V. A.; Sorokulova, I. B. *Journal of Microbiological Methods* **2004**, *58*, 147-168.
- (79) Berezovski, M.; Krylov, S. N. *Journal of the American Chemical Society* **2002**, *124*, 13764-13765.
- (80) Berezovski, M.; Nutiu, R.; Li, Y.; Krylov, S. N. *Analytical Chemistry* **2003**, *77*, 1526-1529.
- (81) Krylova, S. M.; Musheev, M.; Nutiu, R.; Li, Y.; Krylov, S. N. *FEBS Letters* **2005**, *579*, 1371-1375.
- (82) Yang, P.; Whelan, R. J.; Jameson, E. E.; Kurzer, J. H.; Argetsinger, L. S.; Carter-Su, C.; A, K.; Malik, A.; Kennedy, R. T. *Analytical Chemistry* **2005**, *77*, 2482-2489.
- (83) Mosing, R. K.; Bowser, M. T. In *Handbook of Capillary Electrophoresis and Associated Microtechniques*; Landers, J. P., Ed., 2008, pp 797-811.
- (84) Swanstrom, R.; Wills, J. W. In *Retroviruses*; Cold Spring Harbor Laboratory Press: Cold Spring Harbor, 1997, pp 263-334.
- (85) Chenna, R.; Sugawara, H.; Koike, T.; Lopez, R.; Gibson, T. J.; Higgins, D. G.; Thompson, J. D. *Nucleic Acids Research* **2003**, *31*, 3497-3500.
- (86) Zuker, M. *Nucleic Acids Research* **2003**, *31*, 3406-3415.
- (87) Berezovski, M.; Drabovich, A.; Krylova, S. M.; Musheev, M.; Okhonin, V.; Petrov, A.; Krylov, S. N. *Journal of the American Chemical Society* **2005**, *127*, 3165-3171.
- (88) Drabovich, A. P.; Berezovski, M.; Okhonin, V.; Krylov, S. N. *Analytical Chemistry* **2006**, *78*.
- (89) Wiegand, T. W.; Williams, P. B.; Dreskin, S. C.; Jouvin, M. H.; Kinet, J. P.; Tasset, D. *Journal of Immunology* **1996**, *157*, 221-230.
- (90) Schneider, D. J.; Feigon, J.; Hostomsky, Z.; Gold, L. *Biochemistry* **1995**, *1995*, 9599-9610.
- (91) Proske, D.; Hofliger, M.; Soll, R. M.; Beck-Sickinger, A. G.; Famulok, M. *Journal of Biological Chemistry* **2002**, *277*, 11416-11422.
- (92) Drabovich, A.; Berezovski, M.; Krylov, S. N. *Journal of the American Chemical Society* **2005**, *127*, 11224-11225.
- (93) Mallikaratchy, P.; Stahelin, R. V.; Cao, Z.; Tan, W. *Chemical Communications* **2006**, 3229-3231.
- (94) Hesselberth, J.; Robertson, M. P.; Jhaveri, S.; Ellington, A. D. *Reviews in Molecular Biotechnology* **2000**, *74*, 15-25.
- (95) Lin, L.; Hom, D.; Lindsay, S. M.; Chaput, J. C. *Journal of the American Chemical Society* **2007**, *129*, 14568-14569.
- (96) Tang, J.; Xie, J.; Shao, N.; Yan, Y. *Electrophoresis* **2006**, *27*, 1303-1311.

- (97) Berezovski, M.; Musheev, M.; Drabovich, A.; Krylov, S. N. *Journal of the American Chemical Society* **2006**, *128*, 1410-1411.
- (98) Fickert, H.; Fransson, I. G.; Hahn, U. In *The Aptamer Handbook*; Klussman, S., Ed.; Wiley VCH: Weinheim, 2006, pp 95-115.
- (99) Nimjee, S. M.; Rusconi, C. P.; Sullenger, B. A. In *The Aptamer Handbook*; Klussman, S., Ed.; Wiley-VCH: Weinheim, 2006, pp 131-166.
- (100) Herr, J. K.; Smith, J. E.; Medlay, C. D.; Shangguan, D.; Tan, W. *Analytical Chemistry* **2006**, *78*, 2918-2924.
- (101) Shangguan, D.; Li, Y.; Tang, Z.; Cao, Z. C.; Chen, H. W.; Mallikaratchy, P.; Sefah, K.; Tang, C. J.; Tan, W. *PNAS* **2006**, *103*, 11838-11843.
- (102) Kaur, G.; Roy, I. *Expert Opinion in Investigational Drugs* **2008**, *17*, 43-60.
- (103) Wochner, A.; Menger, M.; Rimmel, M. *Expert Opinion in Drug Discovery* **2007**, *2*, 1205-1224.
- (104) Eckstein, F. *Expert Opinion on Biological Therapy* **2007**, *7*, 1021-1034.
- (105) Jayasena, S. D. *Clinical Chemistry* **1999**, *45*, 1628-1650.
- (106) Mosing, R. K.; Bowser, M. T. *Journal of Separation Science* **2007**, *30*, 1420-1246.
- (107) Tombelli, S.; Minunni, M.; Mascini, M. *Biosensors and Bioelectronics* **2005**, *20*, 2424-2434.
- (108) Siddiqui, M. A. A.; Keating, G. M. *Drugs* **2005**, *65*, 1571-1577.
- (109) Lee, J.-H.; Canny, M. D.; Erkenez, A. D.; Krilleke, D.; Ng, Y.-S.; Shima, D. T.; Pardi, A.; Jucker, F. *Proceedings of the National Academy of Sciences of the United States of America* **2005**, *102*, 18902-18907.
- (110) Ravelet, C.; Grosset, C.; Peyrin, E. *Journal of Chromatography A* **2006**, *1117*, 1-10.
- (111) Collett, J. R.; Cho, E. J.; Ellington, A. D. *Methods* **2005**, *37*, 4-15.
- (112) Cho, E. J.; Collett, J. R.; Szafranska, A. E.; Ellington, A. D. *Analytica Chimica Acta* **2006**, *564*, 82-90.
- (113) Bock, C.; Coleman, M.; Collins, B.; Davis, J.; Foulds, G.; Gold, L.; Greef, C.; Heil, J.; Heilig, J. S.; Hicke, B.; Hurst, M. N.; Husar, G. M.; Miller, D.; Ostroff, R.; Petrach, H.; Scneider, D.; Vant-Hull, B.; Waugh, S.; Weiss, A.; Wilcox, S. K.; Zichi, D. *Proteomics* **2004**, *4*, 609-618.
- (114) Petach, H.; Gold, L. *Current Opinion in Biotechnology* **2002**, *13*, 309-314.
- (115) Golden, M. C.; Collins, B. D.; Willis, M. C.; Koch, T. H. *Journal of Biotechnology* **2000**, *81*, 167-178.
- (116) Kotia, R. B.; Li, L.; McGown, L. B. *Analytical Chemistry* **2000**, *72*, 827-831.
- (117) Vo, T. U.; McGown, L. B. *Electrophoresis* **2004**, *25*, 1230-1236.
- (118) Vo, T. U.; McGown, L. B. *Electrophoresis* **2006**, *27*, 749-756.
- (119) Muchaud, M.; Jourdan, E.; Ravelet, C.; Villet, A.; Ravel, A.; Grosset, C.; Peyrin, E. *Analytical Chemistry* **2004**, *76*, 1015-1020.
- (120) Muchaud, M.; Jourdan, E.; Ravelet, C.; Ravel, A.; Grosset, C.; Peyrin, E. *Journal of the American Chemical Society* **2003**, *125*, 8672-8679.
- (121) Brumbt, A.; Ravelet, C.; Grosset, C.; Ravel, A.; Villet, A.; Peyrin, E. *Analytical Chemistry* **2005**, *77*, 1993-1998.
- (122) Ravelet, C.; Boukdedid, R.; Ravel, A.; Grosset, C.; Villet, A.; Fize, J.; Peyrin, E. *Journal of Chromatography A* **2005**, *1076*, 62-70.
- (123) Charles, J. A. M.; McGown, L. B. *Electrophoresis* **2002**, *23*, 1599-1604.
- (124) Rehder-Silinski, M. A.; McGown, L. B. *Journal of Chromatography A* **2003**, *1008*, 233.

- (125) Rehder, M. A.; McGown, L. M. *Electrophoresis* **2001**, *22*, 3759-3764.
- (126) Connor, A. C.; McGown, L. B. *Journal of Chromatography A* **2006**, *1111*, 115-119.
- (127) Deng, Q.; German, I.; Buchanan, D.; Kennedy, R. T. *Analytical Chemistry* **2001**, *73*, 5415-5421.
- (128) Deng, Q.; Watson, C. J.; Kennedy, R. T. *Journal of Chromatography A* **2003**, *1005*, 123-130.
- (129) Cox, J. C.; Hayhurst, A.; Hesselberth, J.; Bayer, T. S.; Georgiou, G.; Ellington, A. D. *Nucleic Acids Research* **2002**, *30*, e108.
- (130) Cox, J. C.; Rudolph, P.; Ellington, A. D. *Biotechnology Progress* **1998**, *14*, 845-850.
- (131) Hybarger, G.; Bynum, J.; Williams, R. F.; Valdes, J. J.; Chambers, J. P. *Analytical and Bioanalytical Chemistry* **2006**, *384*, 191-198.
- (132) Tan, G. T.; Wickramasinghe, A.; Verma, S.; Singh, R.; Hughes, S. H.; Pezzuto, J. M.; Baba, M.; Mohan, P. *Journal of Medicinal Chemistry* **1992**, *35*, 4846-4853.
- (133) Kensch, O.; Connolly, B. A.; Steinhoff, H. J.; McGregors, A.; Goody, R. S.; Restle, T. *Journal of Biological Chemistry* **2000**, *275*, 18271-18278.
- (134) Freeman, G. A.; Andrews, C. W.; Hopkins, A. L.; Lowell, G. S.; Schaller, L. T.; Cowan, J. R.; Gonzales, S. S.; Koszalka, G. W.; Hazen, R. J.; Boone, L. R.; Ferris, R. G.; Creech, K. L.; Roberts, G. B.; Short, S. A.; Weaver, K.; Reynolds, D. J.; Milton, J.; Ren, J.; Stuart, D. I.; Stammers, D. K.; Chan, J. *Journal of Medicinal Chemistry* **2004**, *47*, 5923-5936.
- (135) Tuerk, C.; MacDougall, S.; Gold, L. *Proceedings of the National Academy of Sciences of the United States of America* **1992**, *89*, 6988-6992.
- (136) Kopylov, A. M.; Spiridonova, V. A. *Molecular Biology Reports* **2000**, *34*, 1097-1113.
- (137) Bowser, M. T. *Analyst* **2005**, *130*, 128-130.
- (138) White, R. R.; Sullenger, B. A.; Rusconi, C. P. *The Journal of Clinical Investigation* **2000**, *106*, 929-934.
- (139) Hicke, B. J.; Stephens, A. W. *Journal of Clinical Investigation* **2000**, *106*, 923-928.
- (140) Homann, M.; Goring, H. U. *Bioorganic and Medicinal Chemistry* **2001**, *9*, 2571-2580.
- (141) Rimmele, M. *ChemBioChem* **2003**, *4*, 963-971.
- (142) Devare, S. G. *Journal of Medical Virology* **2007**, *79*, s11-s15.
- (143) Pilcher, C. D.; Jr., J. J. E.; Galvin, S.; Gay, C.; Cohen, M. S. *The Journal of Clinical Investigation* **2004**, *113*, 937-945.
- (144) Tsongalis, G. J. *Microbiology and Infectious Disease* **2006**, *126*, 448-453.
- (145) Isaguliant, M. G.; Belikov, S. V.; Starodubova, E. S.; Gizatullin, R. Z.; Rollman, E.; Zuber, B.; Zuber, A. K.; (Grischenko), O. I. A.; Rytting, A.-S.; Kallander, C. F. R.; Kochetkov, S. N.; Karpov, V. L.; Wahren, B. *AIDS Research and Human Retroviruses* **2004**, *20*, 191-201.
- (146) Warnke, D.; Barreto, J.; Temesgen, Z. *Journal of Clinical Pharmacology* **2007**, *47*, 1570-1579.
- (147) Lee, L. H.; Wu, C. L.; Lee, B. R.; Lee, C.-J. *Clinical Trials of Drugs and Biopharmaceuticals* **2006**, 391-399.
- (148) Rizza, S. A.; Badley, A. D. *Medicinal Chemistry* **2008**, *4*, 75-79.
- (149) Louis, J. M.; Ishima, R.; Torchia, D. A.; Weber, I. T. In *Advances in Pharmacology*: San Diego, 2007, pp 261-298.
- (150) Root, M. J.; Kay, M. S.; Kim, S. *Science* **2001**, *291*, 884-888.
- (151) Kilby, J. M.; Hopkins, S.; Venetta, T. *National Medicine* **1998**, *4*, 1302-1307.
- (152) Chantry, D. *Expert Opinion on Emerging Drugs* **2004**, *9*, 1-7.

- (153) Haes, A. J.; Giordano, B. C.; Collins, G. E. *Analytical Chemistry* **2006**, *78*, 3758-3764.
- (154) Baltimore, D. *Nature* **1970**, *226*, 1209-1211.
- (155) Temin, H. M.; Mizutani, S. *Nature* **1970**, *226*, 1211-1213.
- (156) Jin, J.; Kaushik, N.; Singh, K.; Modak, M. J. *Journal of Biological Chemistry* **1999**, *274*, 20861-20868.
- (157) Kaushik, N.; Chowdhury, K.; Pandey, V. N.; Modak, M. J. *Biochemistry* **2000**, *39*, 5155-5165.
- (158) Shi, Q.; Singh, K.; Srivastava, A.; Kaushik, N.; Modak, M. J. *Biochemistry* **2002**, *41*, 14831-14842.
- (159) Pan, W.; Craven, R. C.; Qiu, Q.; Wilson, C. B.; Wills, J. W.; Golovine, S.; Wang, J. F. *Proceedings of the National Academy of Sciences* **1995**, *92*, 11509-11513.
- (160) Gopinath, S. C.; Misono, T. S.; Kawasaki, K.; Mizuno, T.; Imai, M.; Odagiri, T.; Kumar, P. K. *Journal of General Virology* **2006**, *87*, 479-487.
- (161) Xiao, Z.; Shangguan, D.; Cao, Z.; Fang, X.; Tan, W. *Chemistry--A European Journal* **2008**, *14*, 1769-1775.
- (162) Shamah, S. M.; Healy, J. M.; Clod, S. T. *Accounts of Chemical Research* **2008**, *41*, 130-138.
- (163) Cox, J. S.; Smith, D. S.; Warren, L. A.; Ferris, F. G. *Environmental Science and Technology* **1999**, *33*, 4514-4521.
- (164) Borrok, D.; Fein, J. B.; Tischler, M.; E.O'Loughlin; Meyer, H.; Liss, M.; Kemmer, K. M. *Chemical Geology* **2004**, *209*, 107-119.
- (165) Samuelson, P.; Gunneriusson, E.; Nygren, P.-A.; Stahl, S. *Journal of Biotechnology* **2002**, *96*, 129-154.
- (166) Desai, M. J.; Armstrong, D. W. *Microbiology and Molecular Biology Reviews* **2003**, *67*, 38-51.
- (167) Mozes, N.; Handley, P. S.; Busscher, H. J.; Rouxhet, P. G. *Microbial Cell Surface Analysis; Structural and Physicochemical Methods*; VCH Publishers: New York, 1991.
- (168) Baron, S.; Peake, R. C.; James, D. A.; Susman, M.; Kennedy, C. A.; Singleton, M. J. D.; Schuenke, S. *Medical Microbiology*, 4th ed.; University of Texas Medical Branch: Galveston, 1996.
- (169) Madigan, M. T.; Martinko, J. M.; Dunlap, P. V.; Clark, D. P. *Brock Biology of Microorganisms*; Prentice Hall, 2008.
- (170) Beveridge, T. J.; Davies, J. A. *Journal of Bacteriology* **1983**, *156*, 846-858.
- (171) Call, D. R.; Borucki, M. K.; Loge, F. J. *Journal of Microbiological Methods* **2003**, *53*, 235-243.
- (172) Jenkins, A. T. A.; Ffrench-Constant, R.; Buckling, A.; Clarke, D. J.; Jarvis, K. *Biotechnology Progress* **2004**, *20*, 1233-1236.
- (173) Deisingh, A. K.; Thompson, M. *Canadian Journal of Microbiology* **2004**, *50*, 69-77.
- (174) Hofler, G. *Journal of Pathology* **1994**, *78*, 104-110.
- (175) Sheratt, H. S. *Revue Neurologique* **1991**, *147*, 417-30.
- (176) Ahmadzadeh, H.; Andreyev, D.; Arriaga, E.; Thompson, L. V. *Journal of Gerontology* **2006**, *61A*, 1211-1218.
- (177) Sims, N. R.; Anderson, M. F. *Nature Protocols* **2008**, *3*, 1228-1239.
- (178) Millar, A. H.; Liddell, A.; Leaver, C. J. *Methods in Cell Biology* **2007**, *80*, 65-90.
- (179) Boldogh, I. R.; Pon, L. A. *Methods in Cell Biology* **2007**, *80*, 45-64.

- (180) Petit, P. X.; Susin, S. A.; Zamzami, N.; Mignotte, B.; Kroemer, G. *FEBS Letters* **1996**, *396*, 7-13.
- (181) Parone, P. A.; James, D.; Martinou, J. C. *Biochimie* **2002**, *84*, 105-111.
- (182) Rizzuto, R.; Pinton, P.; Carrington, W.; Fay, F. S.; Fogarty, K. E.; Lifschitz, L. M.; Tuft, R. A.; Pozzan, T. *Science* **1998**, *280*, 1763-1766.
- (183) Rutter, G. A.; Rizzuto, R. *Cell Motil Cytoskeleton* **2000**, *25*, 215-221.
- (184) Scheffler, I. E. *Mitochondrion* **2001**, *1*, 3-31.
- (185) Saraste, M. *Science* **1999**, *283*, 1488-1493.
- (186) Wallace, D. C. *Science* **1999**, *283*, 1482-1488.
- (187) Mazat, J. P.; Rossignol, R.; Malgat, M.; Rocher, C.; Faustin, B.; Letellier, T. *Biochim Biophys Acta* **2001**, *1504*, 20-30.
- (188) Challa, S.; Kanikannan, M. A.; Jagarlapudi, M. M. K.; Bhoompally, V. R.; Surath, M. *Neurology India* **2004**, *52*, 353-358.
- (189) Collins, T. J.; Berridge, M. J.; Lipp, P.; Bootman, M. D. *EMBO* **2002**, *21*, 1616-1627.
- (190) Jacobson, J.; Duchen, M. R. *Journal of Cell Science* **2002**, *115*, 1175-1188.
- (191) Pivovarov, N. B.; Hongpaisan, J.; Andrews, S. B.; Friel, D. D. *Journal of Neuroscience* **1999**, *19*, 6372-6384.
- (192) Faa, G.; Terlizzo, M.; Gerosa, C.; Congiu, T.; Angelucci, E. *Haematologica* **2002**, *87*, 479-484.
- (193) Tsai, Y. L.; Sasaki, S.; Nakagaki, I.; Tsujita, J.; Hori, S.; Hori, K. *Japanese Journal of Physiology* **2001**, *51*, 531-537.
- (194) Ashkin, A.; Schutze, K.; Dziedzic, J. M.; Euteneuer, U.; Schliwa, M. *Nature* **1990**, *348*, 346-348.
- (195) Jonas, E. A.; Buchanan, J.; Kaczmarek, L. K. *Science* **1999**, *286*, 1347-1350.
- (196) Bertoni-Freddari, C.; Fattoretti, P.; Casoli, T.; DiStefano, G.; Solazzi, M.; Gracciotti, N.; Pompei, P. *Journal of Histochem Cytochem* **2001**, *49*, 1191-1192.
- (197) Marti, A.; Larrarte, E.; Novo, F. J.; Garcia, M.; Martinez, J. A. *International Journal of Obesity* **2001**, *25*, 68-74.
- (198) Duffy, C. F.; Fuller, K. M.; Malvey, M. W.; O'Kennedy, R.; Arriaga, E. A. *Analytical Chemistry* **2002**, *74*, 171-176.
- (199) Hjertan, S.; Elenbring, K.; Kilar, F.; Liao, J. L.; Chen, A. J.; Siebert, C. J.; Zhu, M. D. *Journal of Chromatography A* **1987**, *403*, 47-61.
- (200) Zhu, A.; Chen, Y. *Journal of Chromatography A* **1989**, *470*, 251-260.
- (201) Ebersole, R. C.; McCormick, R. M. *Bio/Technology* **1993**, *11*, 1278-1282.
- (202) Buszewski, B.; Szumski, M.; Klodzinska, E.; Dahm, H. *Journal of Separation Science* **2003**, *26*, 1045-1049.
- (203) Pfetsch, A.; Welsch, T. *Fresenius Journal of Analytical Chemistry* **1997**, *359*, 198-201.
- (204) Budde, A.; Knippel, E.; Grummer, G.; Nitzche, R. *Electrophoresis* **1994**, *15*, 577-579.
- (205) Armstrong, D. W.; Schulte, G.; Schneiderheinze, J. M.; Westenberg, D. J. *Analytical Chemistry* **1999**, *71*, 5465-6469.
- (206) Stinson, S. *Chemical and Engineering News* **1999**, *77*, 52.
- (207) Wirtz, M.; Schumann, C. A.; Schellentrager, M.; Gab, S.; Brocke, J. V.; Podeschwa, M. A.; Altenbach, H.-J.; Oscier, D.; Schmitz, O. J. *Electrophoresis* **2005**, *26*, 2599-2607.
- (208) Qi, L.; Danielson, N. D.; Dai, Q.; Lee, R. M. *Electrophoresis* **2003**, *24*, 1680-1686.

- (209) Bunik, V.; Shoubnikova, A.; Bisswanger, H.; Follmann, H. *Electrophoresis* **1997**, *18*, 762-766.
- (210) Prokoratova, V.; Kvasnicka, F.; Sevcik, R.; Voldrich, M. *Journal of Chromatography A* **2005**, *1081*, 60-64.
- (211) Muscari, C.; Pappagallo, M.; Ferrari, D.; Giordano, E.; Capanni, C.; Caldarera, C. M.; Guirnieri, C. *Journal of Chromatography B* **1998**, *707*, 301-307.
- (212) Strack, A.; Duffy, C. F.; Malvey, M.; Arriaga, E. *Analytical Biochemistry* **2001**, *294*, 141-147.
- (213) Fuller, K.; Arriaga, E. *Journal of Chromatography B* **2004**, *806*, 151-159.
- (214) Whiting, C. E.; Arriaga, E. *Electrophoresis* **2006**, *27*, 4523-4531.
- (215) Shangquan, D.; Meng, L.; Cao, Z. C.; Xiao, S.; Fang, X.; Li, Y.; Cardona, D.; Witek, R. P.; Liu, C.; Tan, W. *Analytical Chemistry* **2008**, *80*, 721-728.
- (216) Cerchia, L.; Duconge, F.; Pestourie, C.; Boulay, J.; Aissouni, Y.; Gombert, K.; Tavitian, B.; Franciscis, V. d.; Libri, D. *PLoS Biol.* **2005**, *3*, e123.
- (217) Chen, F.; Zhou, J.; Luo, F.; Mohommed, A.-B.; Zhang, Z.-L. *Biochemical and Biophysical Research Communications* **2007**, *357*, 743-748.
- (218) Daniels, D. A.; Chen, H.; Hicke, B. J.; Swiderek, K. M.; Gold, L. *Proceedings of the National Academy of Sciences* **2003**, *100*, 15416-15421.
- (219) Hamula, C. L. A.; Zhang, H.; Guan, L. L.; Li, X. F.; Le, X. C. *Analytical Chemistry* **2008**, ASAP.
- (220) Armstrong, J. S. *Antioxidants and Redox Signaling* **2008**, *10*, 575-578.
- (221) Adamson, C. S.; Jones, I. M. *Reviews in Medical Virology* **2004**, *14*, 107-121.
- (222) Freed, E. O. *Somatic Cell and Molecular Genetics* **2001**, *26*, 13-33.
- (223) Ganser-Pornillos, B. K.; Yeager, M.; Sundquist, W. I. *Current Opinion in Structural Biology* **2008**, *18*, 203-217.
- (224) Gitti, R. K.; Walker, B. M.; Summers, M. F.; Yoo, S.; Sundquist, W. I. *Science* **1996**, *273*, 231-235.
- (225) Gamble, T. R.; Yoo, S.; Vajdos, F. F.; VonSchwedler, U. K.; Worthylake, D. K.; Wang, H.; McCutcheon, J. P.; Sundquist, W. I.; Hill, C. P. *Science* **1996**, *278*, 849-853.
- (226) Liang, C.; Hu, J.; Whitney, J. B.; Kleiman, L.; Wainberg, M. A. *Journal of Virology* **2003**, *77*, 1772-1783.
- (227) Hunter, E. *Semin. Virology* **1994**, *5*, 71-83.
- (228) Wills, J. W.; Craven, R. C. *AIDS* **1991**, *5*, 639-654.
- (229) Freed, E. O. *Virology* **1998**, *251*, 1-15.
- (230) Provitera, P.; Goff, A.; Harenberg, A.; Bouamr, F.; Carter, C.; Scarlata, S. *Biochemistry* **2001**, *40*, 5565-5572.
- (231) Ganser, B. K.; Li, S.; Kliskho, V. Y.; Finch, J. T.; Sundquist, W. I. *Science* **1999**, *283*, 80-83.
- (232) Li, S.; Hill, C. P.; Sundquist, W. I.; Finch, J. T. *Nature* **2000**, *407*, 409-413.
- (233) Borsetti, A.; Ohagen, A.; Gottlinger, H. G. *Journal of Virology* **1998**, *72*, 9313-9317.
- (234) Wang, C. T.; Barklis, E. *Journal of Virology* **1993**, *67*, 4264-4273.
- (235) Gamble, T. R.; Yoo, S.; Vados, F. F.; Schwedler, U. K. V.; Worthylake, D. K.; Wang, H.; McCutcheon, J. P.; Sundquist, W. I.; Hill, C. P. *Science* **1997**, *278*, 849-853.
- (236) Lidon-Moya, M. C.; Francisco N., B.; Bueno, M.; Perez-Jimenez, P.; Sancho, J.; Mateu, M. G.; Niera, J. L. *Science* **2005**, *14*, 2387-2404.
- (237) Sugimoto, N.; Ochmichi, T.; Sasaki, M. *Nucleosides and Nucleotides* **1996**, *15*, 559-67.
- (238) Tan, Z.-J.; Chen, S.-J. *Biophysical Journal* **2006**, *90*, 1175-1190.

- (239) Tan, Z.-J.; Chen, S.-J. *Biophysical Journal* **2008**, *95*, 738-752.
- (240) Kool, E. T.; Morales, J. C.; Guckian, K. M. *Angewandte Chemie International Edition* **2000**, *39*, 990-1009.
- (241) Luo, D.; Saltzman, W. M. *Nature Biotechnology* **2000**, *18*, 33-37.
- (242) Ng, E. W. M.; Shima, D. T.; Calias, P.; Jr., E. T. C.; Guyer, D. R.; Adamis, A. P. *Nature Reviews Drug Discovery* **2006**, *5*, 123-132.